

LARGE-SCALE KERNEL METHODS
AND APPLICATIONS TO LIFELONG ROBOT
LEARNING

Raffaello Camoriano



UNIVERSITÀ
DEGLI STUDI
DI GENOVA



LARGE-SCALE KERNEL METHODS
AND APPLICATIONS TO LIFELONG
ROBOT LEARNING

by

Raffaello Camoriano

A thesis submitted in partial fulfillment of the
requirements for the degree of

DOCTOR OF PHILOSOPHY

Doctoral Course in Bioengineering and Robotics
XXIX Cycle
Curriculum in Humanoid Robotics

Advisors:

Prof. Giorgio Metta
Prof. Lorenzo Rosasco

iCub Facility
Istituto Italiano di Tecnologia (IIT)

Laboratory for Computational and Statistical Learning
Istituto Italiano di Tecnologia (IIT)

Dipartimento di Informatica, Bioingegneria, Robotica e
Ingegneria dei Sistemi (DIBRIS)
Università degli Studi di Genova (UNIGE)

March 2017

© 2014–2017 Raffaello Camoriano

Abstract

In the last few decades, the digital revolution has produced an unparalleled abundance of data in many fields. The capability of automatically identifying recurring patterns and extracting information from data has acquired a prominent role in the value creation chain of today's economy and in the advancement of science. As the size and richness of available datasets grow larger, the opportunities for solving increasingly challenging problems with algorithms learning directly from data grow at the same pace. Notable examples of learning problems are visual object recognition, speech recognition, and lifelong robot learning, empowering robotic agents to learn continuously from experience in dynamic environments. Consequently, the capability of learning algorithms to work with large amounts of data has become a crucial scientific and technological challenge for their practical applicability. Hence, it is no surprise that large-scale learning is currently drawing plenty of research effort in the machine learning research community. In this thesis, we focus on kernel methods, a theoretically sound and effective class of learning algorithms yielding nonparametric estimators. Kernel methods, in their classical formulations, are accurate and efficient on datasets of limited size, but do not scale up in a cost-effective manner. Recent research has shown that approximate learning algorithms, for instance random subsampling methods like Nyström and random features, with time-memory-accuracy trade-off mechanisms are more scalable alternatives. In this thesis, we provide analyses of the generalization properties and computational requirements of several types of such approximation schemes. In particular, we expose the tight relationship between statistics and computations, with the goal of tailoring the accuracy of the learning process to the available computational resources. Our results are supported by experimental evidence on large-scale datasets and numerical simulations. We also study how large-scale learning can be applied to enable accurate, efficient, and reactive lifelong learning for robotics. In particular, we propose algorithms allowing robots to learn continuously from experience and adapt to changes in their operational environment. The proposed methods are validated on the iCub humanoid robot in addition to other benchmarks.

Acknowledgments

The fruitful path of my doctoral studies would not have been possible without the help, the support, and the invaluable insights of a number of extraordinary and open-minded people. I start by thanking my advisors, Giorgio Metta and Lorenzo Rosasco, whose guidance and consideration inspired me to grow as a scientist, and also, I hope, as a person. My deep (or shallow, as they may prefer) gratitude also goes to Alessandro Rudi, with whom I have had the privilege to closely and extensively work in these years on exciting projects, and Giulia Pasquale, who has always been available to discuss about any matter regarding our shared experience as Ph. D. students and friends. I would also like to warmly thank all my other co-authors: Tomás Angles, Alessandro Chiuso, Carlo Ciliberto, Junhong Lin, Diego Romeres, Lorenzo Natale, Francesco Nori, Silvio Traversaro, and Mattia Zorzi. I have been lucky enough to be part of three unique research groups: iCub Facility (IIT), the Laboratory for Computational and Statistical Learning (LCSL, IIT-MIT), and the Slipguru group (DIBRIS, University of Genoa). It would take too long to name all the exceptional people with whom I have had the privilege and pleasure to discuss about scientific and more worldly topics throughout these years. I will only mention some of them in random order, aware of the fact that I am probably forgetting too many (in this case, I beg your pardon!): Silvia Villa, Bang Công Vu, Guillaume Garrigos, Saverio Salzo, Alessandro Verri, Matteo Barbieri, Samuele Fiorini, Gian Maria Marconi, Elisa Maiettini, Fabio Anselmi, Gemma Roig, Luigi Carratino, Enrico Cecini, Andrea Tacchetti, Matteo Santoro, Benoît Dancoisne, Georgios Evangelopoulos, Maximilian Nickel, Ugo Pattacini, Vadim Tikhanoﬀ, Alessandro Roncone, Francesco Romano, Tanis Mar, Matej Hoffmann, Massimo Regoli, Anand Suresh, Andrea Schiappacasse, Francesca Odone, Ernesto De Vito, Annalisa Barla, Fabio Solari, Manuela Chessa, Nicoletta Noceti, Alessia Vignolo, Damiano Malafrente, Federico Tomasi, Sriram Kumar, Prabhu Kumar, Stefano Saliceti, Ali Paikan, Daniele Pucci, Elena Ceseracciu, Sean Ryan Fanello, and Arjan Gijsberts. I am also very thankful to the reviewers of this thesis, Alessandro Chiuso and Alessandro Lazaric, for their patience and useful comments, and to all the reviewers of the works I submitted to the attention of the scientific community. On a more personal level, I am and will

always be wholeheartedly grateful to my parents, Carla and Gian Pietro, my grandmother Gaby, my entire family, my girlfriend Sara and her family, and my best friends Antonio, Claire, Edoardo, Enrico, Francesco, Ilaria, and all of those who decisively helped me to complete this extremely challenging and arduous path.

This journey has definitely been the best time of my life, and I feel honored to have shared it with every single one of you.

Notation

\mathbb{N}	natural numbers
\mathbb{R}	real numbers
\mathbb{R}_+	positive real numbers
z	column vector (if not differently specified)
Z	matrix
z^\top, Z^\top	transpose of vector z or matrix Z
$x \in \mathcal{X}$	input sample and input space
X	input matrix (each row is a sample x^\top)
$y \in \mathcal{Y}$	output label (or vector) and output space
Y	output matrix (each row is an output label — or vector — y^\top)
$\mathcal{Z} = \mathcal{X} \times \mathcal{Y}$	data space
$n \in \mathbb{N}$	number of training samples
$d \in \mathbb{N}$	dimensionality of the input space \mathcal{X}
$T \in \mathbb{N}$	dimensionality of the output space \mathcal{Y}
S_n	set of n input-output pairs $\{x_i, y_i\}_{i=1}^n$
$\langle \cdot, \cdot \rangle_{\mathcal{H}}$	inner product in space \mathcal{H}
$\ \cdot \ _p$	p -norm, with $p = 2$ if not specified
$f(\cdot) \in \mathcal{F}$	function belonging to a space of functions
$K(\cdot, \cdot)$	kernel function
K_n	empirical kernel matrix of size $n \times n$ associated to K
\mathcal{H}_K	reproducing kernel Hilbert space (RKHS) associated to K
$\Phi(\cdot)$	feature map
I_n	$n \times n$ identity matrix
$\mathbf{0}$	zero vector
\hat{y}	predicted output
$\ell(\cdot, \cdot)$	loss function
$\rho(\cdot)$	probability distribution
$\mathcal{N}(\mu, \sigma^2)$	Gaussian distribution with mean μ and variance σ^2
$\mathcal{U}(a, b)$	uniform distribution in the interval $[a, b]$
$\text{sign}(a)$	sign of a
$\text{rank}(Z)$	rank of Z
$\text{Tr}(Z)$	trace of Z
\mathbb{E}	expectation of a random variable

Acronyms

ALS	Approximate Leverage Scores
ERM	Empirical Risk Minimization
ES	Early Stopping
F/T	Force/Torque
FFT	Fast Fourier Transform
GPR	Gaussian Process Regression
i. i. d.	independent and identically distributed
KOLS	Kernel Ordinary Least Squares
KRLS	Kernel Regularized Least Squares
KRR	Kernel Ridge Regression
LGP	Local Gaussian Processes
LWPR	Locally Weighted Projection Regression
NKRLS	Nyström Kernel Regularized Least Squares
NP	Nonparametric
NYTRO	NYström iTerative RegularizatiOn
P	Parametric
PCA	Principal Component Analysis
PCR	Principal Component Regression
RBD	Rigid Body Dynamics
RBF	Radial Basis Function
RF	Random Features
RF-KRLS	Random Features Kernel Regularized Least Squares
RFRRLS	Random Features Recursive Regularized Least Squares
RKHS	Reproducing Kernel Hilbert Space
RLS(C)	Regularized Least Squares (for Classification)
(R)MSE	(Root) Mean Square Error
RRLS	Recursive Regularized Least Squares
SGD	Stochastic Gradient Descent
S(I)GM	Stochastic (Incremental) Gradient Method
SLT	Statistical Learning Theory
SP	Semiparametric
SVM	Support Vector Machine
(T)SVD	(Truncated) Singular Value Decomposition

List of Publications

Camoriano, R.*, Angles, T.*, Rudi, A., and Rosasco, L. (2016a). NYTRO: When Subsampling Meets Early Stopping. In *Proceedings of the 19th International Conference on Artificial Intelligence and Statistics (AISTATS)*, pages 1403–1411.

Camoriano, R.*, Pasquale, G.*, Ciliberto, C., Natale, L., Rosasco, L., and Metta, G. (2016b). Incremental Robot Learning of New Objects with Fixed Update Time. *arXiv preprint arXiv:1605.05045*.

Camoriano, R., Traversaro, S., Rosasco, L., Metta, G., and Nori, F. (2016c). Incremental semiparametric inverse dynamics learning. In *IEEE International Conference on Robotics and Automation (ICRA)*, pages 544–550. IEEE.

Camoriano, R.*, Pasquale, G.*, Ciliberto, C., Natale, L., Rosasco, L., and Metta, G. (2017). Incremental Robot Learning of New Objects with Fixed Update Time. To appear in *IEEE International Conference on Robotics and Automation (ICRA)*.

Lin, J., Camoriano, R., and Rosasco, L. (2016). Generalization Properties and Implicit Regularization for Multiple Passes SGM. In *International Conference on Machine Learning (ICML)*.

Romeres, D., Zorzi, M., Camoriano, R., and Chiuso, A. (2016). Online semiparametric learning for inverse dynamics modeling. In *Decision and Control (CDC), 2016 IEEE 55th Conference on*, pages 2945–2950. IEEE.

Rudi, A., Camoriano, R., and Rosasco, L. (2015). Less is More: Nyström Computational Regularization. In *Advances in Neural Information Processing Systems (NIPS) 28*, pages 1657–1665. Curran Associates, Inc.

Rudi, A., Camoriano, R., and Rosasco, L. (2016). Generalization Properties of Learning with Random Features. *ArXiv e-prints*.

* Equal contribution.

Contents

Introduction	17
I Mathematical Setting	23
1 Statistical Learning Theory	25
1.1 Supervised Learning	26
1.2 Data Space	28
1.3 Probabilistic Data Model	29
1.4 Loss Function	30
1.5 Expected Error	32
1.6 Generalization Error Bound	33
1.7 Overfitting and Regularization	34
1.8 Bias Variance Trade-off and Cross-validation	36
1.9 Empirical Risk Minimization & Hypotheses Space	36
1.10 Regularized Least Squares	37
1.10.1 Computations	38
2 Kernel Methods	39
2.1 Feature Maps	39
2.1.1 Beyond Linear Models	39
2.1.2 Computations	40
2.2 Representer Theorem	40
2.2.1 Representer Theorem for RLS	41
2.2.2 Representer Theorem Implications	41
2.3 Kernels	41
2.4 Kernel Regularized Least Squares	42
3 Spectral Regularization	45
3.1 Introduction	45
3.2 Tikhonov Regularization	46
3.2.1 Regularization Filters	47
3.3 Spectral Cut-off	48
3.4 Iterative Regularization via Early Stopping	49

3.4.1	Landweber Iteration	49
II	Kernel Methods for Large-scale Learning	51
4	Speeding up by Data-dependent Subsampling	53
4.1	Introduction	53
4.2	Less is More: Regularization by Subsampling	54
4.2.1	Setting	54
4.2.2	Supervised Learning with KRLS and Nyström	55
4.2.3	Theoretical Analysis	57
4.2.4	Incremental Updates and Experimental Analysis	62
4.3	NYTRO: Nyström Iterative Regularization	66
4.3.1	Setting	66
4.3.2	Learning and Regularization	67
4.3.3	Proposed Algorithm and Main Results	72
4.3.4	Experiments	77
5	Speeding up by Data-independent Subsampling	79
5.1	Setting	79
5.2	Background: Generalization Properties of KRLS	81
5.3	Regularized Learning with Random Features	83
5.3.1	Main Results	85
5.3.2	Comparison with Previous Works	88
5.4	Numerical results	90
III	Incremental Approaches and Lifelong Learning	93
6	Generalization Properties of SGM	95
6.1	Setting	95
6.2	Learning with SGM	97
6.3	Implicit Regularization for SGM	98
6.3.1	Convergence	98
6.3.2	Finite Sample Bounds for Smooth Loss Functions	99
6.3.3	Finite Sample Bounds for Non-smooth Loss Functions	102
6.3.4	Discussion and Proof Sketch	104
6.4	Numerical Simulations	106
6.4.1	Regularization in SGM and SIGM	107
6.4.2	Accuracy and Computational Time Comparison	108
7	Incremental Classification	111
7.1	Setting	111
7.2	Related Work	112
7.3	Classification Setting and Class Imbalance	114

7.3.1	Optimal Bayes Classifier and its Least Squares Surrogate	114
7.3.2	The Effect of Unbalanced Data	115
7.3.3	Rebalancing the Loss	116
7.3.4	Rebalancing and Recoding the Square Loss	117
7.3.5	Multiclass Rebalancing and Recoding	118
7.4	Incremental Multiclass Classification	119
7.4.1	Regularized Least Squares for Classification	119
7.4.2	Recursive Regularized Least Squares	120
7.5	Incremental Class Extension and Recoding	121
7.5.1	Class Extension	121
7.5.2	Incremental Recoding	121
7.6	Experiments	123
7.6.1	Experimental Protocol	123
7.6.2	Datasets	124
7.6.3	Model Selection	124
7.6.4	Results	126
8	Incremental Inverse Dynamics Learning	129
8.1	Setting	129
8.2	Background	132
8.2.1	Parametric Models of Robot Dynamics	132
8.2.2	Nonparametric Modeling with Kernel Methods	133
8.2.3	RLS for Parametric and Nonparametric Learning	135
8.2.4	Recursive RLS with Cholesky Update	135
8.3	Semiparametric Incremental Dynamics Learning	137
8.4	Experimental Results	138
8.4.1	Software	138
8.4.2	Robotic Platform	138
8.4.3	Validation	139
9	Conclusion	143
	Bibliography	157
	Appendices	159
A	Loss Functions and Target Functions	161
B	Linear Systems	163
C	Incremental Random Features	165
D	Incremental Algorithm for Nyström Computational Regularization	167

Introduction

Research in machine learning began in the 1950s within the field of artificial intelligence, at the intersection between statistics and computer science, with the objective of devising computer programs able to solve problems by learning from experience [Turing, 1950; Rosenblatt, 1958; Minsky and Papert, 1969; Crevier, 1993; Russell et al., 2003]. Many tasks in visual object recognition, speech recognition, and system identification and estimation, among others, can be framed in terms of learning the associated input-output mappings directly from examples. In other words, if a system solving the problem cannot be deterministically defined a-priori, it might be possible to find it by training a predictive model on data relevant to the task, made available by sensors and, possibly, a supervising agent. In recent years, the availability of large-scale datasets in many fields, such as robotics and computer vision, has posed an unprecedented opportunity towards the conception of novel learning systems enabling artificial agents to solve increasingly challenging problems without being explicitly pre-programmed. At the same time, a crucial scientific and technological challenge for the feasibility of a learning system is the scalability of the learning algorithm with respect to the number of training samples and their dimensionality. Among the numerous machine learning approaches available nowadays, we focus on kernel methods, a set of nonparametric methods with a firm theoretical grounding and the potential for high predictive accuracy. Exact kernel methods [Schölkopf and Smola, 2002; Shawe-Taylor and Cristianini, 2004; Hofmann et al., 2008], are effective and efficient on datasets of limited size, and cannot take full advantage of currently available large-scale datasets¹. Recent approximate algorithms with time-memory-accuracy trade-off mechanisms [Bottou and Bousquet, 2007] have proven to be flexible alternatives to exact kernel methods for learning nonlinear models over large datasets, representing a substantial step forward in the field (e. g. Random Features [Rahimi and Recht, 2007, 2008] and Nyström methods [Gittens and Mahoney, 2013]).

The main objective of this thesis is to present several types of scalable randomized large-scale learning algorithms, accompanied by rigorous analy-

¹For large-scale datasets, we mean datasets with a number of examples $n \gtrsim 10^5$

ses of their generalization properties in the statistical learning theory (SLT) framework [Cucker and Smale, 2002; Cucker and Zhou, 2007] and computational requirements, supported by experimental evidence on benchmark datasets and numerical simulations. We highlight the central role of the relationship between statistics and computations in our analyses, theoretically and empirically attesting that parameters affecting time and memory complexities can also control predictive accuracy. This results in very flexible and scalable learning algorithms which can be tailored to the statistical properties of a specific learning task and to the available computational resources. Moreover, we investigate the application of large-scale learning algorithms to robotics, in particular to lifelong robot learning [Thrun and Mitchell, 1995]. This allows for the continuous updating of the predictive models within a robotic system in an open-ended time span, based on an ever-growing amount of collected training samples, possibly with bounded time and memory complexities. We propose large-scale learning algorithms for lifelong learning tasks in visual object recognition for robotics and robot dynamics learning.

Large-scale Machine Learning

In their classical formulations, kernel methods rapidly become computationally intractable as the training set size increases. In the prominent case of Kernel Regularized Least Squares (KRLS) [Schölkopf and Smola, 2002], the computational complexity for training and testing strongly depends on the number of samples n composing the training set and the number of features d . In particular, training costs $O(n^2d + n^3)$ in time and $O(n^2)$ in memory complexity, while testing costs $O(n)$ in time. These computational complexities are overwhelming for current computer platforms if n is too large. The memory cost is the first bottleneck encountered in practical applications, since the kernel matrix cannot fit in the RAM memory and computationally intensive memory mapping techniques become necessary. On the other hand, linear learning algorithms such as Regularized Least Squares (RLS) [Rifkin, 2002] require the computation and storage of a covariance matrix of size $d \times d$ for training. This means that training a linear model does not suffer from a very large number of training samples. In fact, its training computational time, $O(d^3 + nd^2)$, is linear in n . Notably, testing only requires $O(d)$, which does not depend on n . However, in many learning problems the nonlinearity of the estimator is a fundamental property, and this is one of the main reasons supporting the choice of nonlinear learning algorithms like KRLS with respect to linear ones. For instance, the aforementioned inverse dynamics learning problem for robotics is a regression problem implying strongly nonlinear relations between the input features (joint positions, velocities and accelerations) and the predicted out-

puts (forces and torques), see [Rasmussen and Williams, 2006; Featherstone and Orin, 2008; Traversaro et al., 2013]. It is therefore clear that the ideal objective would be to devise kernelized learning algorithms, with their non-linear capabilities, while retaining, or at least not degrading too much, the advantageous computational properties of linear learning algorithms. To this aim, many computational strategies to scale up kernel methods have been recently proposed [Smola and Schölkopf, 2000; Williams and Seeger, 2000; Rahimi and Recht, 2007; Yang et al., 2014; Le et al., 2013; Si et al., 2014; Zhang et al., 2013]. In this thesis, we will focus on three types of randomized large-scale learning algorithms, namely:

- Data-independent subsampling schemes, including random features approaches.
- Data-dependent subsampling schemes, including Nyström methods.
- Stochastic gradient methods (SGM), in various formulations.

For these randomized approaches, we provide novel generalization analyses and experimental benchmarkings, as reported in [Rudi et al., 2015; Camoriano et al., 2016a; Rudi et al., 2016; Lin et al., 2016]. Now, we will briefly introduce these families of methods, which will be treated in greater detail in the corresponding chapters. Let us begin with random features (RF) [Rahimi and Recht, 2007], a subsampling scheme allowing to approximate kernel methods by means of features which are randomly generated in a data-independent fashion. These features can then be fed to a linear algorithm such as RLS, globally resulting in an approximated nonlinear learning algorithm (RF-RLS). The accuracy of RF-RLS can be made arbitrarily close to the one of KRLS by increasing the number of random features [Rudi et al., 2016]. The introduction of random features [Rahimi and Recht, 2007] has been an important step towards the application of classical kernel methods to large scale learning problems (see for example [Huang et al., 2014; Lu et al., 2014]). However, there are very few theoretical results about the statistical properties of RF-approximated kernel methods. We provide a statistical analysis of the accuracy of KRLS approximated by Random Features. In particular, we study the conditions under which it attains the same statistical properties of exact KRLS in terms of accuracy and analyze the implications on the computational complexity of the algorithm. Notably, we show that optimal learning rates can be achieved with a number of features smaller than the number of examples. As a byproduct, we also show that learning with random features can be seen as a way for controlling the statistical properties of the estimator, rather than only to speed up computations.

Another important class of large-scale algorithms are the Nyström methods [Williams and Seeger, 2000], based on a low-rank approximation of the kernel matrix. We present (as also reported in [Rudi et al., 2015]) new optimal

learning bounds for Nyström methods with generic subsampling schemes. Notably, we show that the amount of subsampling, besides computations, also affects accuracy. Leveraging on this, we propose a new efficient incremental version of Nyström KRLS with integrated model selection. We provide extensive experimental results supporting our findings.

Subsequently, we investigate the interplay between iterative regularization/early stopping learning algorithms [Engl et al., 1996; Zhang and Yu, 2005; Bauer et al., 2007; Yao et al., 2007; Caponnetto and Yao, 2010] and Nyström subsampling schemes. Iterative regularized learning algorithms, such as Landweber iteration or the ν -method [De Vito et al., 2006], are a family of methods which compute a sequence of solutions to the learning problem with increasingly high precision. They provide a valid alternative to Tikhonov regularization methods in terms of time complexity, especially in regimes in which the amount of noise in the data is large. Iterative methods are particularly efficient when used in combination with early stopping [Yao et al., 2007]. Still, in the dual formulation they require overwhelming amounts of memory for kernel matrix storage as the sample complexity increases. Following the idea of Nyström kernel approximation, widely applied to KRLS algorithm with Tikhonov regularization [Williams and Seeger, 2000; Rudi et al., 2015], we propose (as reported in [Camoriano et al., 2016a]) to combine Nyström subsampling techniques with early stopping in the kernelized iterative regularized learning context, in order to reduce memory and time requirements. The resulting learning algorithm, named NYTRO (NYström iTerative RegularizatiOn), is presented, together with the analysis of its generalization properties and extensive experiments.

Finally, we consider the stochastic gradient method (SGM), often called stochastic gradient descent. SGM is a widely used algorithm in machine learning, especially in large-scale settings, due to its simple formulation and reduced computational complexity [Bousquet and Bottou, 2008]. Despite being commonly used for solving practical learning problems, SGM's generalization properties have not been exhaustively investigated before. We study (as we also reported in [Lin et al., 2016]) the generalization properties of SGM for learning with convex loss functions and linearly parameterized functions. We show that, in the absence of penalizations or constraints, the stability and approximation properties of the algorithm can be controlled by tuning either the step-size or the number of passes over the training set. In this view, these parameters can be seen to control a form of implicit regularization. Numerical results complement our theoretical findings.

Lifelong Learning for Robotics

The iCub humanoid robot [Metta et al., 2010] is a suitable match for lifelong robot learning applications, due to its large variety and number of sensors and degrees of freedom (DOFs), the support for extended data generation processes with rich dynamics, an advanced visual system, and a number of open problems in perception and interaction in which learning can play a fundamental role. One of the goals of this thesis is to present the application of large-scale learning methods to lifelong visual object recognition in robotics. In particular, we propose (see also [Camoriano et al., 2016b, 2017]) a novel object recognition algorithm based on Regularized Least Squares for Classification (RLSC) [Rifkin et al., 2003], in which examples are presented incrementally in a real-world robot supervised learning scenario. The model learns incrementally to recognize classes of objects, taking into account the imbalancedness of the dataset at each step and adapting its statistical properties to changing sample complexity. New classes can be added on-the-fly to the model, with no need for retraining. Incoming labeled pictures are used for increasing the accuracy of the predictions and adapting them to changes in environmental conditions (e. g., lighting conditions).

Last, but not least, we present another robotics application of interest, that is inverse dynamics learning [Traversaro et al., 2013; Nguyen-Tuong and Peters, 2010; Gijssberts and Metta, 2011; Romeres et al., 2016]. We propose novel approaches for inverse dynamics learning applied to robotics, in particular to the iCub humanoid robot (for the scope of this work see [Camoriano et al., 2016c], and, for an alternative method, [Romerer et al., 2016]). Classical inverse dynamics estimators rely on rigid body dynamics (RBD) models of the kinematic chain of interest (e.g., a limb of the iCub). This modeling strategy enables good generalization performance in the robot workspace. Yet, it poses two issues: 1) The estimated inertial parameters of the RBD model might be inaccurate, especially after days of operation of the robot. The reasons include changes in the physical properties of the components, sensor drift, wear and tear, and thermal phenomena. 2) RBD models exclude the effects of limb and joint flexibility, and possibly others, on the inverse dynamics mapping. These dynamic effects can be substantial in real-world scenarios. On the other hand, machine learning approaches are capable of learning the input-output mapping directly from data, without the restrictions imposed by prior assumptions about the rigid physical structure of the system. We combine standard physics-based modeling techniques [Featherstone and Orin, 2008; Traversaro et al., 2013] with nonparametric modeling based on large-scale kernel methods based on random features [Gijssberts and Metta, 2011], in order to improve the model's predictive accuracy and interpretability. Unlike [Nguyen-Tuong and Peters, 2010], the proposed approach learns incrementally during robot

operation with fixed update complexity, making it suitable for real-time applications and lifelong robot learning tasks. The model can be adjusted in time via incremental updates, increasing the accuracy of its predictions and adapting to changes in physical conditions. The system has been implemented using the GURLS [Tacchetti et al., 2013] machine learning software library.

Organization

The thesis is organized as follows. Part I introduces essential machine learning concepts employed throughout the work. In particular, Chapter 1 provides an introduction to Statistical Learning Theory (SLT), Chapter 2 presents kernel methods, while Chapter 3 describes the fundamentals of spectral regularization. Subsequently, Part II focuses on scaling up kernel methods for large-scale learning applications, providing novel generalization analyses. Data-dependent subsampling schemes are treated in Chapter 4, with focuses on optimal learning bounds for Nyström KRLS in Section 4.2, and on the combination of early stopping and Nyström subsampling (the proposed NYTRO algorithm) in Section 4.3. Furthermore, data-independent subsampling schemes, in particular the optimal learning bounds for random features KRLS (RF-KRLS), are discussed in Chapter 5. Part III is concerned with iterative learning algorithms and lifelong learning, including specific applications to robotics. In particular, Chapter 6 presents the new statistical analysis of SGM, Chapter 7 describes our novel incremental multiclass classification algorithm with extension to new classes in constant time, and, finally, Chapter 8 deals with our recently proposed incremental semiparametric inverse dynamics learning method with constant update complexity. The thesis is concluded by final remarks in Chapter 9.

Part I

Mathematical Setting

Chapter 1

Statistical Learning Theory

The field of machine learning studies algorithms and systems capable of extrapolating information and learning predictive models from data, rather than being specifically programmed to solve a given task. These techniques are particularly useful for solving a wide range of tasks for which it is hard or unfeasible to define a comprehensive set of decision rules. Examples of use are widespread, and include visual object recognition, speech recognition, control policy learning, fraud detection, dynamic pricing, and product ranking. Machine learning tackles this kind of problems by learning from examples. It can be subdivided in the following sub-fields:

- **Supervised learning:** The algorithm learns the mapping between inputs and desired outputs, based on a set of input-output pairs associated with the task, provided by a supervising entity. A performance measure (e.g. a loss function) is required.
- **Unsupervised learning:** Data are made available to the learning algorithm, whose goal is to discover hidden structure in it. The provided examples do not include output labels. Main techniques falling in this definition include, among others: Clustering, feature learning, and dimensionality reduction techniques such as principal component analysis (PCA).
- **Reinforcement learning:** The learning system has access to a dynamic environment, in which it has to perform a goal for which no supervision is provided. The actions applied to the environment result in a reward signal to be maximized in order to achieve the goal. Application examples include autonomous driving and general game playing.

In this work, the focus will be on supervised learning, in particular in the large-scale context. In fact, when a significantly large number of data sam-

ples¹ is available, learning algorithms can become too computationally expensive for execution. This represents a relevant technological issue, hampering the way towards the applicability of machine learning methods. For this reason, it is necessary to design novel large-scale learning algorithms capable of taking full advantage of the remarkable volume of data available today. This unfolds many opportunities of scientific research, especially regarding the study of the interplay between the statistical and computational properties [Bottou, 2007] of these methods, and their generalization properties. Throughout this work, we will analyze the statistical properties of supervised learning algorithms in the Statistical Learning Theory (SLT) [Cucker and Smale, 2002] framework, introduced next.

1.1 Supervised Learning

Supervised learning assumes to have access to a set of n input-output pairs which are instances of the considered learning task. This finite set of examples is called *training set*:

$$S_n = \{(x_1, y_1), \dots, (x_n, y_n)\}.$$

The objective of a supervised learning algorithm is *learning from examples*, that is by computing an estimator f , based on the training set, mapping *previously unseen* inputs x_{new} into the corresponding outputs y_{new} (see Figure 1.1), as follows:

$$f : x_{\text{new}} \mapsto y_{\text{new}}.$$

The data are usually subject to *uncertainty* (e.g., due to noise). Statistical learning models this by assuming the existence of an underlying probabilistic model for the data, discussed in the following.

We will now more formally introduce the two fundamental concepts defining a learning task. First, examples are drawn from the *data space*, a probability space $\mathcal{X} \times \mathcal{Y}$ with measure ρ . \mathcal{X} is called *input space*, while \mathcal{Y} is called *output space* (see Figure 1.2). Secondly, a measurable *loss function*,

$$\ell : \mathcal{Y} \times \mathcal{Y} \rightarrow [0, \infty),$$

is defined to evaluate the quality of the predictions of the estimator.

On the basis of these key concepts, we can define the *expected error* (more details are reported in Section 1.5)

$$\mathcal{E}(f) = \int_{\mathcal{X} \times \mathcal{Y}} \ell(y, f(x)) d\rho(x, y).$$

¹We refer to input-output pairs as data points, samples or examples.

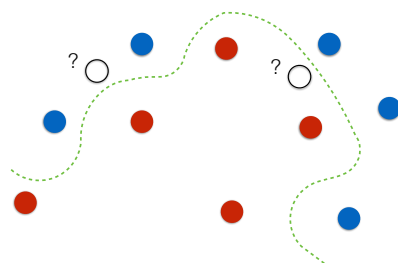


Figure 1.1: In binary classification, given examples (blue and red points) the problem is to learn a classifier (represented by the dashed line) correctly predicting the label of new input samples (white points).

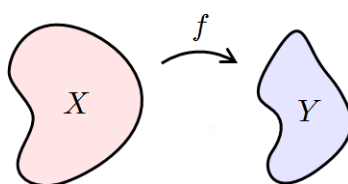


Figure 1.2: Input and outputs space related by a functional relationship.

The problem of learning is to find an estimator f minimizing the expected error, that is solving

$$\inf_{f \in \mathcal{F}} \mathcal{E}(f),$$

with ρ fixed and unknown. Here, \mathcal{F} is the set of functions $f : \mathcal{X} \rightarrow \mathcal{Y}$ such that the expected risk $\mathcal{E}(f)$ is well defined. Access to ρ is limited to a finite *training set* composed of samples identically and independently distributed (i. i. d.) according to ρ

$$S_n = \{(x_1, y_1), \dots, (x_n, y_n)\} \sim \rho^n.$$

Since ρ is known only via the training set S_n , finding an exact solution to the expected risk minimization is generally not possible. One way to overcome this problem is to define an *empirical error* measured on the available data to treat the learning problem in a computationally feasible way. We first discuss in greater detail the concepts introduced above.

1.2 Data Space

The input/output examples belong to the *data space* $\mathcal{Z} = \mathcal{X} \times \mathcal{Y}$. The *input space* \mathcal{X} can take several forms, depending on the specific learning problem. We report some of the most common cases:

- Linear spaces
 - Euclidean spaces: $\mathcal{X} \subseteq \mathbb{R}^d$, $d \in \mathbb{N}$.
 - Space of matrices: $\mathcal{X} \subseteq \mathbb{R}^{a \times b}$, $a, b \in \mathbb{N}$.
- Structured spaces
 - Probability distributions: Given a finite set Ω of dimension d , we can consider as input space the space of all possible probability distributions over Ω , which is $\mathcal{X} = \{x \in \mathbb{R}_+^d : \sum_{j=1}^d x^j = 1\}$, $d \in \mathbb{N}$. This also holds more in general for any set Ω , even if not finite.
 - Strings/Words: Consider an alphabet Σ of symbols. The input space can be the space of all possible words composed of $p \in \mathbb{N}$, as follows: $\mathcal{X} = \Sigma^p$.
 - \mathcal{X} is a space of graphs.

Similarly, the definition of output space \mathcal{Y} results in several different categories of learning problems, some of the most common of which are:

- Linear spaces
 - Regression: $\mathcal{Y} \subseteq \mathbb{R}$.
 - Multi-output (multivariate) regression: $\mathcal{Y} \subseteq \mathbb{R}^T$, $T > 1$.
 - Functional regression: Outputs are functions, \mathcal{Y} is a Hilbert space.
- Structured spaces
 - \mathcal{Y} is a space of probability distributions.
 - \mathcal{Y} is a space of strings.
 - \mathcal{Y} is a space graphs.
- Other spaces
 - Binary classification: $\mathcal{Y} = \{-1, 1\}$, or any pair of different numbers.
 - Multi-category (multiclass) classification: Each example belongs to one among T categories, $\mathcal{Y} = \{1, 2, \dots, T\}$, $T \in \mathbb{N}$.
 - Multilabel classification: Each example is associated to any subset of T output categories, $\mathcal{Y} = 2^{\{1, 2, \dots, T\}}$, $T \in \mathbb{N}$.

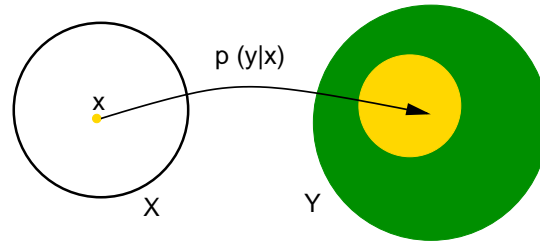


Figure 1.3: Given an input x , the yellow area is the support of its associated distribution of possible outputs $\rho(y|x)$. The green area represents the support of the distribution of all possible outputs $\rho(y)$.

Remark 1 (Multi-task Learning). *One of the most general supervised learning settings is called Multi-task Learning, for which $\mathcal{Z} = (\mathcal{X}_1, \mathcal{Y}_1) \times (\mathcal{X}_2, \mathcal{Y}_2) \times \dots \times (\mathcal{X}_T, \mathcal{Y}_T)$ and the training set S is composed of one training set S_i for each task i of the T tasks: $S = S_1, S_2, \dots, S_T, T \in \mathbb{N}$.*

1.3 Probabilistic Data Model

In supervised learning, in order to estimate an input/output relation, we assume that a model expressing this relationship exists. In SLT, the assumed model is probabilistic, in the sense that the data samples constituting the training and the test sets are assumed to be sampled independently from the same fixed and unknown data distribution $\rho(x, y)$ ² on the data space \mathcal{Z} . Thus, ρ encodes the uncertainty in the data, for instance caused by noise, partial information or quantization. By also assuming that $\rho(x, y)$ can be factorized as

$$\rho(x, y) = \rho_{\mathcal{X}}(x)\rho(y|x) \quad \forall (x, y) \in \mathcal{Z},$$

the various sources of uncertainty can be separated. In particular, the marginal distribution $\rho_{\mathcal{X}}(x)$ models the uncertainty in the sampling of the input points. Instead, $\rho(y|x)$ is the conditional distribution modeling the *non deterministic* input-output mapping, as shown in Figure 1.3. We now consider two instances of data model, associated with regression and classification.

Example 1 (Fixed and Random Design Regression). *In statistics, the commonly assumed data model for regression is the following,*

$$y_i = f^*(x_i) + \epsilon_i,$$

²In this case, we say that data samples are independent and identically distributed (i. i. d. assumption).

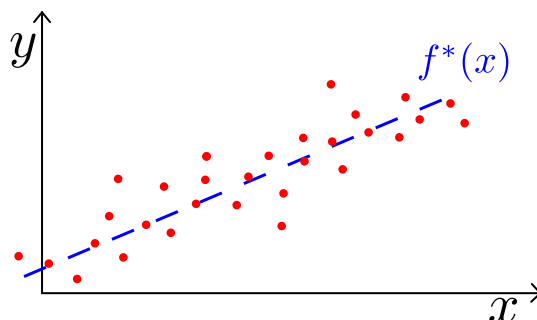


Figure 1.4: Fixed unknown linear function f^* and noisy examples sampled from the $y = f^*(x) + \epsilon$ model.

where $\mathcal{X} = \{x_1, x_2, \dots, x_n\}$ is a deterministic discrete set of inputs, f^* is a fixed unknown function and ϵ is random noise. For example, f^* could be a linear function $f^*(x) = x^\top w^*$ with $w^* \in \mathbb{R}^d$, and the ϵ component could be Gaussian noise, distributed according to $\mathcal{N}(0, \sigma)$, $\sigma \in [0, \infty)$. The aforementioned model is named fixed design regression, since \mathcal{X} is fixed and deterministic. By contrast, in SLT the so-called random design setting is often considered, according to which the training samples are not given a-priori, but according to a probability distribution $\rho_{\mathcal{X}}$ (for example, uniformly at random). See Figure 1.4 for an example.

Example 2 (Binary classification). In binary classification, input-output samples are sampled randomly according to a distribution ρ over $\mathcal{X} \times \{-1, 1\}$. In a simple example of binary classification problem, ρ is a mixture of two Gaussians, each corresponding to a class, $\rho(x, y) = \rho(x|y = -1) + \rho(x|y = 1)$, with

$$\rho(x|y = -1) = \frac{1}{c} \mathcal{N}(-1, \sigma_-), \quad \sigma_- \in [0, \infty)$$

$$\rho(x|y = 1) = \frac{1}{c} \mathcal{N}(+1, \sigma_+), \quad \sigma_+ \in [0, \infty)$$

where $c \in \mathbb{R}$ is a suitable normalization factor such that $\rho(x, y)$ is a probability distribution, that is s. t. $\int \rho(x, y) dx dy = 1$. An example dataset drawn according to the aforementioned $\rho(x, y)$ is shown in Figure 1.5

1.4 Loss Function

We have seen that the problem of learning an estimator amounts to finding a function f “best” approximating the underlying input-output relationship. To do so, we need a measure of the predictive accuracy of the learned

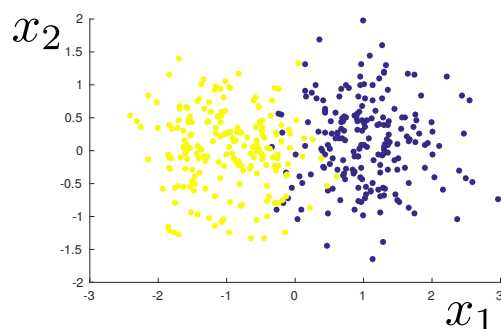


Figure 1.5: 2-D example of a dataset sampled from a mixed Gaussian distribution. Samples of the yellow class are realizations of a Gaussian centered at $(-1, 0)$, while samples of the blue class are realizations of a Gaussian centered at $(+1, 0)$. Both Gaussians have standard deviation $\sigma = 0.6$.

estimator with reference to the specific learning task in exam. In particular, the most natural way to do so is to define a point-wise *loss function*

$$\ell : \mathcal{Y} \times \mathcal{Y} \rightarrow [0, \infty),$$

measuring the loss $\ell(y, f(x))$ the learning system undergoes by predicting $f(x)$ instead of the actual output y . For instance, typical losses for regression problems differ from the ones used for classification. We will now recall some of the most usual ones.

Loss functions for regression usually depend on the deviation $y - a$ between the real output y and the predicted value $a = f(x)$.

- Square loss: It is the most commonly employed loss function for regression, defined as $\ell(y, a) = (y - a)^2$, with $a, b \in \mathcal{Y}$.
- Absolute loss: $\ell(y, a) = |y - a|$
- ϵ -insensitive loss: $\ell(y, a) = \max\{|y - a| - \epsilon, 0\}$, with $\epsilon \in (0, +\infty)$. It is used in Support Vector Machines (SVMs) for regression [Smola and Vapnik, 1997].

Loss functions for regression are shown in Figure 1.6.

Loss functions for classification: For the sake of simplicity, we consider the setting in which $\mathcal{Y} = \{+1, -1\}$.

- Misclassification loss (0-1 loss, counting loss): It is probably the most natural choice for measuring the accuracy of a classifier. It assigns a cost 1 if the predicted label is incorrect, and 0 otherwise. It can be defined as $\ell(y, a) = \mathbb{I}_{y \neq a}$, where $\mathbb{I}_{(\cdot)}$ is the indicator function, y is the

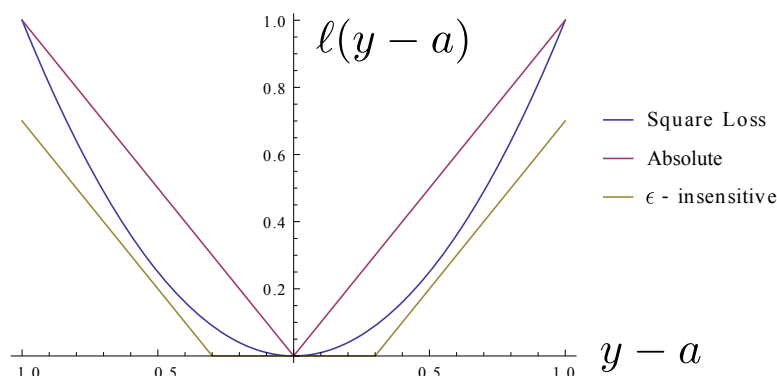


Figure 1.6: Loss functions for regression.

real output associated to the input x , and $a = \text{sign}(f(x))$ is the output label predicted by the learned estimator f .

- **Surrogate losses:** The 0-1 loss is non-convex and makes optimization very hard. To overcome this issue, convex *surrogate loss functions* acting as convex relaxations of the 0-1 loss are used. To introduce them, we consider the real-valued prediction $a = f(x)$, without taking the sign. Given a pair (x, y) and an estimator f , we define the quantity ya , called *margin*. Surrogate losses are often defined in terms of margin: $\ell(y, a) = \ell(ya)$. We report the most commonly used ones below:
 - **Hinge loss:** Used in Support Vector Machines (SVMs) for classification, it is defined as $\ell(y, a) = |1 - ya|_+ = \max\{1 - ya, 0\}$.
 - **Exponential loss:** $\ell(y, a) = e^{-ya}$, used in Boosting algorithms.
 - **Logistic loss:** $\ell(y, a) = \log(1 + e^{-ya})$, used in logistic regression.
 - **Square loss:** It can be used also for classification, and it can be written in terms of margin as $\ell(y, a) = (y - a)^2 = (1 - ya)^2$.

See Figure 1.7 for a pictorial representation of the aforementioned loss functions for classification.

1.5 Expected Error

The loss function ℓ , alone, is not enough for quantifying how well an estimator performs on any possible future data sample drawn from ρ . To this end, we define the *expected error* (also *expected risk* or *expected loss*) of an estimator f given a loss ℓ as

$$\mathcal{E}(f) = \int_{\mathcal{X} \times \mathcal{Y}} \ell(y, f(x)) d\rho(x, y), \quad (1.1)$$

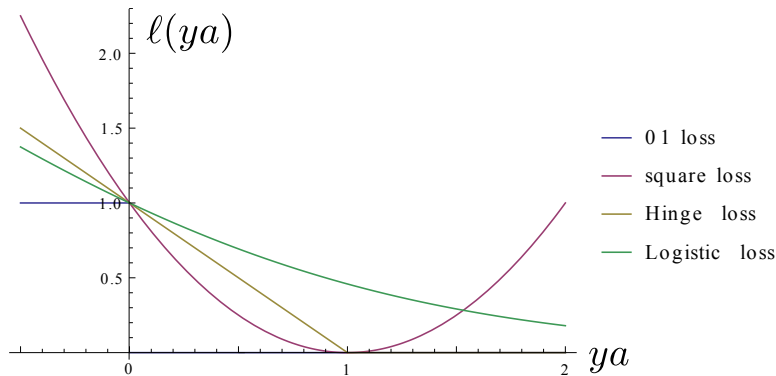


Figure 1.7: Margin-based loss functions for classification.

which expresses the average loss the estimator is expected to incur in on samples drawn from ρ . Hence, in the SLT framework the “best” possible estimator is the *target function* $f^* : \mathcal{X} \rightarrow \mathcal{Y}$ minimizing $\mathcal{E}(f)$,

$$\inf_{f \in \mathcal{F}} \mathcal{E}(f),$$

where \mathcal{F} is named *target space* and is the space of functions for which $\mathcal{E}(f)$ is well-defined. Notice that different loss functions yield different target functions, as reported in Appendix A. It is essential to note that this minimization cannot be computed in general, because the data distribution ρ is not available. The objective of a learning algorithm is to find an estimator f as close as possible to f^* and behaving well on unseen data, despite having access to just a finite realization $S_n \sim \rho^n$, the training set. An algorithm fulfilling this criterion is said to *generalize well*, which is the cornerstone concept of SLT and machine learning in general.

1.6 Generalization Error Bound

A learning algorithm \mathcal{A} can be thought of as a mapping $\mathcal{A} : S_n \mapsto \hat{f}$ from the the training set S_n to the associated estimator \hat{f} . To introduce the concepts of generalization and consistency, we assume that \mathcal{A} is deterministic, even if this assumption can be relaxed, as we will see in the following chapters. Here, the only source of uncertainty is therefore due to stochasticity in the data, modeled by ρ .

We have seen that the target function associated to a learning problem is the one minimizing the expected risk. A good learning algorithm is able to find an estimator \hat{f} yielding an expected error as close as possible to the one of the target function. However, to perform a more precise analysis of a learning algorithm we need to quantify this behavior, considering that the

learned estimator \hat{f} depends on the training set S_n . A widely studied property of learning algorithms is the *generalization error bound*, which describes a bound on the error with probability $1 - \delta$. More formally, given a distribution ρ , $\forall \delta \in [0, 1], n > 0$, there exists a function $\epsilon(\delta, n)$, called *learning rate* (or *learning error*), such that,

$$\mathbb{P} \left(\mathcal{E}(\hat{f}) - \inf_{f \in \mathcal{F}} \mathcal{E}(f) \leq \epsilon(\delta, n) \right) \geq 1 - \delta. \quad (1.2)$$

1.7 Overfitting and Regularization

Ideally, an estimator \hat{f} should *mimic* the target function f^* , in the sense that its expected error should get close to the one of f^* as $n \rightarrow \infty$. The latter requirement needs some care, since \hat{f} depends on the training set S_n and hence is random. As we have seen in (1.2), one possibility is to require an algorithm to have a good learning rate. Given a rich enough hypotheses space \mathcal{H} , a good learning algorithm should be able to describe well (fit) the data and at the same time disregard noise. Indeed, a key to ensure good generalization is to avoid *overfitting*, that characterizes estimators which are highly dependent on the training data. This can happen if \mathcal{H} is too rich, thus making the model “learn the noise” in the training data. In this case, the estimator is said to have high *variance*. On the other hand, if \mathcal{H} is too simple the estimator is less dependent on the training data and thus more robust to noise, but \mathcal{H} may not be rich enough to approximate well the target function f^* . *Regularization* is a general class of techniques that allow to restore stability and ensure generalization. It considers a sequence of hypotheses spaces \mathcal{H}_λ , parameterized by a *regularization parameter* λ , with

$$\lim_{\lambda \rightarrow 0} \mathcal{H}_\lambda = \mathcal{F}.$$

At this point, a natural question is whether an optimal regularization parameter in terms of learning algorithm performance exists, and, if so, how it can be found in practice. We next characterize the corresponding minimization problem to uncover one of the most fundamental aspects of machine learning. As we saw in the previous sections, the generalization performance of a learning algorithm is as much high as

$$\mathcal{E}(\hat{f}_\lambda) - \inf_{\mathcal{F}} \mathcal{E}(f) \quad (1.3)$$

is low. To get an insight on how to choose λ , we theoretically analyze how this choice influences performance. For a fixed λ , we can decompose (1.3) as

$$\mathcal{E}(\hat{f}_\lambda) - \inf_{\mathcal{F}} \mathcal{E}(f) = \underbrace{\mathcal{E}(\hat{f}_\lambda) - \inf_{\mathcal{H}_\lambda} \mathcal{E}(f)}_{\text{Variance}} + \underbrace{\inf_{\mathcal{H}_\lambda} \mathcal{E}(f) - \inf_{\mathcal{F}} \mathcal{E}(f)}_{\text{Bias}}. \quad (1.4)$$

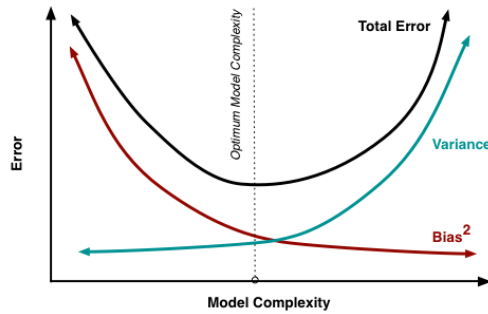


Figure 1.8: The Bias-variance trade-off. In Tikhonov regularization the parameter λ controls the model's complexity. A small λ yields high complexity, and vice-versa.

Indeed, on the one hand we introduce a *variance* term to control the complexity of the hypotheses space. On the other hand, we allow the class complexity to grow to reduce the *bias* term. The optimal λ^* is the one minimizing (1.4), the so-called bias variance trade off.

Specifically, by bias we mean the deviation

$$\inf_{\mathcal{H}_\lambda} \mathcal{E}(f) - \inf_{\mathcal{F}} \mathcal{E}(f).$$

This is often called the *approximation error* and does not depend on the data, but only on how well the class \mathcal{H}_λ "approximates" \mathcal{F} . There are many instances of the above setting in which it is possible to design regularization schemes so that the approximation error *decreases for decreasing* λ . In fact, in such schemes a small λ corresponds to a reduced penalization of rich function classes.

In contrast, the term

$$\mathcal{E}(\hat{f}_\lambda) - \inf_{\mathcal{H}_\lambda} \mathcal{E}(f)$$

is called *sample*, or *estimation error*, or simply the *variance* term. It is data dependent and stochastic, and measures the variability of the output of the algorithm, for a given complexity, with respect to an ideal algorithm having access to all the data. In most regularized learning algorithms a small λ corresponds to a complex model which is more sensitive to data stochasticity, thus leading to a larger variance term.

1.8 Bias Variance Trade-off and Cross-validation

We briefly discuss some practical considerations regarding the regularization parameter choice for regularized learning algorithms. As previously introduced, variance decreases with λ , while bias increases with it. A larger bias is preferred when training samples are few and/or noisy to achieve a better control of the variance, while it can be decreased for larger datasets. For any given training set, the best choice of λ would be the one guaranteeing the optimal trade-off between bias and variance (that is the value minimizing their sum), as shown in Figure 1.8. However, the theoretical analysis is not directly useful in practice since the data distribution, hence the expected loss, is not accessible. In practice, data driven procedures are used to find a proxy for the expected loss, the simplest of which is called *hold-out cross-validation*. Part of the training set is held-out and used to compute a (hold-out) error acting as a proxy of the expected error. An empirical bias variance trade-off is achieved choosing the value of λ with the minimum hold-out error. When data are scarce, the hold-out procedure, based on a simple "two ways split" of the training set, might be unstable. In this case, so called *V-fold cross validation* is preferred, which is based on multiple data splitting. More precisely, the data are divided in $V \in [2, \dots, n]$ (non overlapping) sets. Each set is held-out and used to compute a hold-out error, which is eventually averaged to obtain the final *V-fold cross-validation* error. The extreme case where $V = n$ is called *leave-one-out cross-validation*.

1.9 Empirical Risk Minimization & Hypotheses Space

A good learning algorithm is able to find an estimator f approximating the target function f^* . From the computational viewpoint, though, the minimization of the expected risk yielding f^* ,

$$\inf_{f \in \mathcal{F}} \mathcal{E}(f),$$

is unfeasible, since ρ is unknown and the algorithm can only access a finite training set S_n . An effective approach to learning algorithm design in this setting is to minimize the error on the finite training set instead of the whole distribution. To this end, given a loss ℓ we define the *empirical risk* (or *empirical error*)

$$\widehat{\mathcal{E}}(f) = \frac{1}{n} \sum_{i=1}^n \ell(y_i, f(x_i)),$$

acting as a proxy for the expected error defined in (1.1). In practice, to turn the above idea into an actual algorithm we need to select a suitable hypotheses space $\mathcal{H} \subset \mathcal{F}$ of candidate estimators, such that $\widehat{\mathcal{E}}(f)$ is well

defined $\forall f \in \mathcal{H}$. The hypotheses space should be such that computations are feasible and, at the same time, it should be *rich* enough to approximate f^* . To sum up, the ERM problem can be written as

$$\inf_{f \in \mathcal{H}} \widehat{\mathcal{E}}(f). \quad (1.5)$$

One possible method for controlling the size of the hypotheses space \mathcal{H} is *Tikhonov regularization* [Tikhonov, 1963]. This method adds a so-called *regularizer* to the empirical risk minimization problem in (1.5), which allows to control the size of $\mathcal{H} = \mathcal{H}_\lambda$ via the regularization parameter λ . A regularizer is a functional $R : \mathcal{H} \rightarrow [0, \infty)$ that penalizes estimators which are too “complex”. In this case, we could replace (1.5) by

$$\inf_{f \in \mathcal{H}} \widehat{\mathcal{E}}(f) + \lambda R(f), \quad (1.6)$$

for some *regularization parameter* $\lambda > 0$, with

$$\widehat{f}_\lambda = \arg \inf_{f \in \mathcal{H}} \widehat{\mathcal{E}}(f) + \lambda R(f).$$

In particular, we will use the squared norm in \mathcal{H} as a regularizer, obtaining

$$\widehat{f}_\lambda = \arg \inf_{f \in \mathcal{H}} \widehat{\mathcal{E}}(f) + \lambda \|f\|_{\mathcal{H}}^2, \quad (1.7)$$

with $\|f\|_{\mathcal{H}}^2 = \langle f, f \rangle_{\mathcal{H}}$.

1.10 Regularized Least Squares

In this section, we introduce Regularized Least Squares (RLS), a learning algorithm based on Tikhonov regularization employing the square loss. The learning algorithm is defined as

$$\min_{w \in \mathbb{R}^d} \frac{1}{n} \sum_{i=1}^n (y_i - w^\top x_i)^2 + \lambda w^\top w, \quad \lambda \geq 0, \quad (1.8)$$

considering as hypotheses space the class of linear functions, that is

$$\mathcal{H} = \{f : \mathbb{R}^d \rightarrow \mathbb{R} : \exists w \in \mathbb{R}^d \text{ such that } f(x) = x^\top w, \forall x \in \mathbb{R}^d\}. \quad (1.9)$$

Each function f is defined by a vector w , and we let $f_w(x) = x^\top w$. A motivation for considering the above scheme is to view the empirical risk

$$\widehat{\mathcal{E}}(f_w) = \frac{1}{n} \sum_{i=1}^n (y_i - w^\top x_i)^2,$$

with $f_w(x) = w^\top x$, as a proxy for the expected risk

$$\mathcal{E}(f_w) = \int \rho(x, y)(y - w^\top x)^2 dx dy,$$

which is not computable. Note that finding a function f_w reduces to finding the corresponding vector w . The term $w^\top w$ is the regularizer and helps preventing overfitting by controlling the stability of the solution. The parameter λ balances the empirical error term and the regularizer. As we will see in the following, this seemingly simple example will be the basis for much more complicated solutions.

1.10.1 Computations

It is convenient to introduce the input matrix $X \in \mathbb{R}^{n \times d}$, whose rows are the input samples, and the output vector $Y \in \mathbb{R}^n$ whose entries are the corresponding outputs³. With this notation, the empirical risk can be expressed as

$$\frac{1}{n} \sum_{i=1}^n (y_i - w^\top x_i)^2 = \frac{1}{n} \|Y - Xw\|^2.$$

A direct computation shows that the gradients with respect to w of the empirical risk and the regularizer are, respectively,

$$-\frac{2}{n} X^\top (Y - Xw), \quad \text{and} \quad 2w.$$

Then, setting the gradient to zero, we have that the solution of regularized least squares solves the linear system

$$(X^\top X + n\lambda I_d)w = X^\top Y,$$

where I_d is the $d \times d$ identity matrix. Several comments are in order. First, several methods can be used to solve the above linear system, Cholesky decomposition being the method of choice, since the matrix $X^\top X + n\lambda I_d$ is symmetric and positive definite. The complexity of the method is essentially $O(nd^2)$ for training and $O(d)$ for testing. The parameter λ controls the *invertibility* of the matrix $(X^\top X + n\lambda I_d)$.

³Note that in the 1-vs-all multiclass classification setting the output vector Y becomes an $n \times T$ matrix.

Chapter 2

Kernel Methods

In this section, we introduce the key concepts of *feature map* and *kernel*, that allow to generalize RLS to nonlinear models.

2.1 Feature Maps

A *feature map* is a map

$$\Phi : \mathcal{X} \mapsto \mathcal{V}$$

from the input space \mathcal{X} into a new space \mathcal{V} called *feature space*, endowed with a scalar product denoted by $\langle \cdot, \cdot \rangle_{\mathcal{V}}$. The feature space can be infinite dimensional.

2.1.1 Beyond Linear Models

The simplest case is when $\mathcal{V} = \mathbb{R}^p$, and we can view the entries $\Phi(x)^j$, $j = 1, \dots, p$ as novel measurements on the input points. For instance, consider $\mathcal{X} = \mathbb{R}^2$ and the feature map $x = (x_1, x_2) \mapsto \Phi(x) = (x_1^2, \sqrt{2}x_1x_2, x_2^2)$. With this choice, if we now consider

$$f_w(x) = w^\top \Phi(x) = \sum_{j=1}^p w^j \Phi(x)^j,$$

we effectively have that the function is no longer linear in the original input space \mathcal{X} , but it is a polynomial of degree 2. Clearly, the same reasoning holds for much more general choices of measurements (features), in fact *any* finite set of measurements. Although seemingly simple, the above observation allows to consider very general models. Figure 2.1 gives a geometric interpretation of the potential effect of considering a feature map. Points which are not easily classified by a linear model in the input space \mathcal{X} can be easily classified by a *linear model in the feature space* \mathcal{V} .

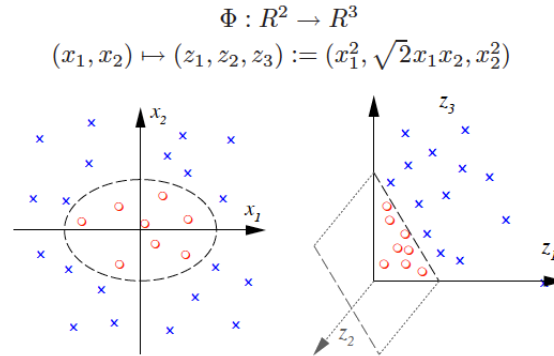


Figure 2.1: A pictorial representation of the potential effect of considering a feature map $\Phi : \mathbb{R}^2 \mapsto \mathbb{R}^3$ in a simple binary classification problem.

2.1.2 Computations

While feature maps allow to design nonlinear models, the computations are essentially the same as in the linear case. Indeed, it is easy to see that the computations considered for linear models, under different loss functions, remain unchanged, as long as we change $x \in \mathbb{R}^d$ into $\Phi(x) \in \mathbb{R}^p$. For example, for least squares we simply need to replace the $n \times d$ input matrix X with a new $n \times p$ feature matrix Φ_n , where each row is the image of an input point in the feature space, as defined by the feature map. Thus, the only changes in the time and memory complexities of the learning algorithms of choice lay in the replacement of d with p , and are noticeable only if $p \gg d$.

2.2 Representer Theorem

In this section we discuss how the above reasoning can be further generalized. The key result is that the solution of regularization problems of the form (1.7) can always be written as

$$\hat{w}^\top = \sum_{i=1}^n x_i^\top \alpha_i, \quad (2.1)$$

where x_1, \dots, x_n are the training inputs and $\alpha = (\alpha_1, \dots, \alpha_n)$ are a set of coefficients. The above result is an instance of the so-called representer theorem. We first discuss this result in the context of RLS.

2.2.1 Representer Theorem for RLS

The result follows by noting that the following equality holds,

$$(X^\top X + \lambda n I_d)^{-1} X^\top = X^\top (X X^\top + \lambda n I_n)^{-1}, \quad (2.2)$$

so that we have,

$$w = X^\top \underbrace{(X X^\top + \lambda n I_n)^{-1} Y}_c = \sum_{i=1}^n x_i^\top c_i.$$

Equation (2.2) follows from considering the singular value decomposition (SVD) of X , that is $X = U \Sigma V^\top$. Therefore, we have $X^\top = V \Sigma^\top U^\top$, so that

$$(X^\top X + \lambda n I_d)^{-1} X^\top = V (\Sigma^\top \Sigma + n \lambda I_d)^{-1} \Sigma^\top U^\top$$

and

$$X^\top (X X^\top + \lambda n I_n)^{-1} = V \Sigma^\top (\Sigma \Sigma^\top + n \lambda I_n)^{-1} U^\top.$$

Note that the equality

$$(\Sigma^\top \Sigma + n \lambda I_d)^{-1} \Sigma^\top = \Sigma^\top (\Sigma \Sigma^\top + n \lambda I_n)^{-1}$$

can be trivially verified.

2.2.2 Representer Theorem Implications

Using (2.1) and (2.2), it is possible to show how the vector α of coefficients can be computed considering different loss functions. In particular, for the square loss the vector of coefficients satisfies the following linear system

$$(K_n + \lambda n I_n) \alpha = Y \quad (2.3)$$

where $K_n \in \mathbb{R}^{n \times n}$ is a matrix with entries $(K_n)_{i,j} = x_i^\top x_j$. The matrix K_n is called the *kernel matrix* and is symmetric and positive semi-definite.

2.3 Kernels

Given an input space \mathcal{X} , a symmetric positive definite function $K : \mathcal{X} \times \mathcal{X} \rightarrow \mathbb{R}$ is a *kernel function* if there exists a feature map $\Phi : \mathcal{X} \mapsto \mathcal{H}$ for which

$$K(x, x') = \langle \Phi(x), \Phi(x') \rangle_{\mathcal{H}}, \quad \forall x, x' \in \mathcal{X},$$

where \mathcal{H} is the unique Hilbert space of functions from \mathcal{X} to \mathbb{R} defined by K as the completion of the linear span $\{K(\cdot, x) : x \in \mathcal{X}\}$ with respect to the inner product

$$\langle K(\cdot, x), K(\cdot, x') \rangle_{\mathcal{H}} = K(x, x'), \quad x, x' \in \mathcal{X},$$

see [Aronszajn, 1950]. The space \mathcal{H} is called the reproducing kernel Hilbert space (RKHS) associated to the reproducing kernel function K . The kernel matrix $(K_N)_{i,j} = K(x_i, x_j)$ associated to the positive definite kernel function K is positive semi-definite for all $x_1, \dots, x_N \in \mathcal{X}$, $N \in \mathbb{N}$. Moreover, the following two properties hold for K and \mathcal{H} :

1. For all $x \in \mathcal{X}$, $K_x(\cdot) = K(x, \cdot)$ belongs to \mathcal{H} .
2. The so called reproducing property holds: $f(x) = \langle f, K_x \rangle_{\mathcal{H}}$, for all $f \in \mathcal{H}$, $x \in \mathcal{X}$ [Steinwart and Christmann, 2008].

As we saw in the previous section, one of the main advantages for using the representer theorem is that the solution of the problem depends on the input points only through inner products $x^\top x'$. Kernel methods can be seen as replacing the inner product with a more general function $K(x, x')$. In this case, the representer theorem (2.1), that is $f_w(x) = w^\top x = \sum_{i=1}^n x_i^\top x \alpha_i$, becomes

$$\hat{f}(x) = \sum_{i=1}^n K(x_i, x) \alpha_i, \quad (2.4)$$

and in this way we can directly derive *kernelized* versions of many linear learning algorithms, including RLS, as we will see in the next section.

Popular examples of positive definite kernels include:

- Linear kernel $K(x, x') = x^\top x'$
- Polynomial kernel $K(x, x') = (x^\top x' + 1)^d$
- Gaussian kernel $K(x, x') = e^{-\frac{\|x-x'\|^2}{2\sigma^2}}$

The last two kernels have a tuning parameter, the degree d and Gaussian bandwidth σ , respectively.

2.4 Kernel Regularized Least Squares

We now analyze the kernelized version of RLS, namely Kernel Regularized Least Squares (KRLS) or Kernel Ridge Regression (KRR). Given data points

$$(x_1, y_1), \dots, (x_n, y_n) \in (\mathcal{X} \times \mathbb{R})^n,$$

and a kernel K , KRLS is defined by the minimization problem,

$$\hat{f}_\lambda = \arg \min_{f \in \mathcal{H}} \frac{1}{n} \sum_{i=1}^n (f(x_i) - y_i)^2 + \lambda \|f\|_{\mathcal{H}}^2, \quad \lambda > 0, \quad (2.5)$$

where $\|f\|_{\mathcal{H}}^2 = \langle f, f \rangle_{\mathcal{H}}$, for all $f \in \mathcal{H}$. The representer theorem [Kimeldorf and Wahba, 1970; Schölkopf et al., 2001] shows that, while the minimization

is taken over a possibly infinite dimensional space, the minimizer of the above problem is of the form,

$$\hat{f}_\lambda(x) = \sum_{i=1}^n \alpha_i K(x, x_i), \quad \alpha = (K_n + \lambda n I_n)^{-1} Y, \quad (2.6)$$

where $\alpha = (\alpha_1, \dots, \alpha_n)$, $K_n \in \mathbb{R}^{n \times n}$ with $(K_n)_{ij} = K(x_i, x_j)$ and $Y = (y_1, \dots, y_n)$.

In terms of computational complexity we can say that:

- Time complexity is $O(n^3 + n^2 d)$, where $n^2 d$ refers to the computation of K_n and n^3 to the inversion of the $n \times n$ matrix $(K_n + \lambda n I_n)$.
- Memory complexity is $O(n^2)$, due to the storage of the kernel matrix K_n .

In practice, KRLS's memory complexity is its main practical bottleneck, since state-of-the-art computers cannot trivially store in RAM full kernel matrices for $n > 10^5$. Consequently, in large-scale applications, in which n can be considerably larger, so-called "exact" kernel methods using the full kernel matrix, such as KRLS, are not a viable option. In Part II, we will see how kernel methods can be extended to large-scale settings and study their generalization properties.

Chapter 3

Spectral Regularization

In this section, we recall the concept of *spectral regularization*, a general formalism describing a large class of regularization methods giving rise to consistent kernel methods.

3.1 Introduction

Spectral regularization originates from the inverse problems literature, in particular from methods to invert matrices in a numerically stable way. The idea of applying spectral regularization to statistics [Wahba, 1990] and machine learning [Vapnik and Kotz, 1982; Poggio and Girosi, 1989; Schölkopf and Smola, 2002; De Vito et al., 2005b; Gerfo et al., 2008a] is based on the observation that the same principles allowing for numerically stable inversion can be shown to prevent overfitting in the SLT framework. Different spectral methods have a common derivation, but result in different regularized learning algorithms with specific computational complexities and statistical properties. As we saw in Chapter 1, a learning problem can be framed as the minimization of the expected risk on a suitable hypotheses space \mathcal{H} . The idea is that the solution satisfies

$$\inf_{f \in \mathcal{H}} \mathcal{E}(f).$$

In the following, we consider the square loss for simplicity. In practical algorithms, the empirical risk $\hat{\mathcal{E}}(f) = \frac{1}{n} \sum_{i=1}^n (y_i - f(x_i))^2$ is introduced as a proxy of the expected risk, and empirical risk minimization,

$$\inf_{f \in \mathcal{H}} \hat{\mathcal{E}}(f) = \inf_{f \in \mathcal{H}} \frac{1}{n} \sum_{i=1}^n (y_i - f(x_i))^2,$$

is performed. The unregularized solution to ERM (corresponding to the so called Kernel Ordinary Least Squares — KOLS — solution) can be written

as

$$\widehat{f}(x) = \sum_{i=1}^n \alpha_i K(x, x_i),$$

where K is a suitable kernel function and the coefficients vector $\alpha \in \mathbb{R}^n$ is the solution of the inverse problem

$$K_n \alpha = Y. \quad (3.1)$$

The solution can be subject to numerical instability caused by noise and sampling. For example, in the learning setting the kernel matrix can be decomposed as

$$K_n = Q \Sigma Q^\top,$$

where $\Sigma = \text{diag}(\sigma_1, \dots, \sigma_n)$ is the eigenvalues matrix, $\sigma_1 \geq \sigma_2 \geq \dots \sigma_n \geq 0$ are the eigenvalues in decreasing order, and q_1, \dots, q_n are the corresponding eigenvectors. Then,

$$\begin{aligned} \alpha &= K_n^{-1} Y \\ &= Q \Sigma^{-1} Q^\top Y \\ &= \sum_{i=1}^n \frac{1}{\sigma_i} \langle q_i, Y \rangle q_i, \end{aligned} \quad (3.2)$$

since $[\Sigma^{-1}]_{ii} = 1/\sigma_i$. It is therefore clear that in correspondence of small eigenvalues, small perturbations of the data due to sampling and noise can cause large changes in the solution. The spectral regularization literature includes a rich variety of methods allowing to invert linear operators with high condition number¹ in a stable way. In general, spectral regularization methods act on the eigenvalues of the matrix to stabilize its inversion. This is done by replacing the original unbounded operator with a *regularization operator* [Engl et al., 1996], which allows to control the condition number via a regularization parameter. We will see some examples of this in the following, starting from the case of Tikhonov regularization.

3.2 Tikhonov Regularization

In Tikhonov regularization [Tikhonov, 1963], an explicit penalization term R is added to the ERM objective function to enforce smoothness of the solution and prevent overfitting, as follows

$$\inf_{f \in \mathcal{H}} \widehat{\mathcal{E}}(f) + \lambda R(f) = \inf_{f \in \mathcal{H}} \frac{1}{n} \sum_{i=1}^n (y_i - f(x_i))^2 + \lambda \|f\|_{\mathcal{H}}^2. \quad (3.3)$$

¹The condition number of a normal matrix A is defined as $\kappa(A) = |\sigma_{\max}|/|\sigma_{\min}|$, where $\sigma_{\max}, \sigma_{\min}$ are the maximal and minimal eigenvalues of A respectively. Kernel matrices are normal.

We will now observe that Tikhonov regularization has an effect from a numerical point of view. In fact, it yields the linear system

$$(K_n + n\lambda I_n)\alpha = Y, \quad (3.4)$$

which stabilizes the possibly ill-conditioned matrix inversion problem of (3.1). In particular, by considering the eigendecomposition associated to the regularized problem in (3.4) we obtain that

$$\begin{aligned} \alpha &= (K_n + n\lambda I_n)^{-1}Y \\ &= Q(\Sigma + n\lambda I_n)^{-1}Q^\top Y \\ &= \sum_{i=1}^n \frac{1}{\sigma_i + n\lambda} \langle q_i, Y \rangle q_i. \end{aligned} \quad (3.5)$$

Regularization filters out the undesired components associated to small eigenvalues, increasing the condition number of the regularized linear operator. Eigenvalues are affected as follows:

- If $\sigma \gg \lambda n$, then $\frac{1}{\sigma_i + n\lambda} \approx \frac{1}{\sigma_i}$
- If $\sigma \ll \lambda n$, then $\frac{1}{\sigma_i + n\lambda} \approx \frac{1}{n\lambda}$

Consequently, the condition number is controlled as follows:

$$\kappa(K_n) = \frac{|\sigma_{\max}|}{|\sigma_{\min}|} \implies \kappa(K_n + n\lambda I_n) = \frac{|\sigma_{\max}|}{|n\lambda|}$$

A good range for the regularization parameter λ falls between the smallest and the largest eigenvalues of K_n .

3.2.1 Regularization Filters

We can generalize the notion of spectral regularization beyond the Tikhonov case by introducing the concept of *regularization filter* [Bertero and Boccacci, 1998] $G_\lambda : \mathbb{R}^{n \times n} \mapsto \mathbb{R}^{n \times n}$ acting on the eigenvalues of the kernel matrix, defined as

$$G_\lambda(K_n) = Q\bar{G}_\lambda(\Sigma)Q^\top,$$

with $\bar{G}_\lambda : \mathbb{R}^{n \times n} \mapsto \mathbb{R}^{n \times n}$. \bar{G}_λ , in turn, is defined in terms of the *scalar filter function* $g_\lambda : \mathbb{R} \mapsto \mathbb{R}$ as

$$[\bar{G}_\lambda(\Sigma)]_{ii} = g_\lambda(\sigma_i).$$

What g_λ does is simply to invert the eigenvalues in a controlled way to enforce smoothness of the solution. For instance, in the case of Tikhonov regularization filtering, we have that

$$g_\lambda(\sigma) = \frac{1}{\sigma + n\lambda}$$

is the corresponding scalar function. Thus, as seen in Equation (3.5), the coefficients vector can be computed as

$$\begin{aligned}\alpha &= G_\lambda(K_n) \\ &= \sum_{i=1}^n g_\lambda(\sigma_i) \langle q_i, Y \rangle q_i \\ &= \sum_{i=1}^n \frac{1}{\sigma_i + n\lambda} \langle q_i, Y \rangle q_i.\end{aligned}\tag{3.6}$$

As we will see in the following sections, this formalism is very flexible and can be used to characterize different regularized learning algorithms in a unified way. This class of algorithms is known collectively as spectral regularization. Each algorithm is defined by a suitable filter function G_λ , and is not necessarily based on penalized ERM. The notion of filter function was studied in machine learning and gave a connection between function approximation in signal processing and approximation theory.

Remark 2 (Filter function properties). *Not every scalar function defines a regularization scheme. Roughly speaking, a good filter function must have the following properties:*

- As λ goes to 0, $g_\lambda(\sigma) \rightarrow 1/\sigma$ so that $G_\lambda(K_n) \rightarrow K_n^{-1}$.
- λ controls the magnitude of the (smaller) eigenvalues of $G_\lambda(K_n)$.

3.3 Spectral Cut-off

This method is one of the oldest regularization techniques and is also known as Truncated Singular Value Decomposition (TSVD) and Principal Component Regression (PCR). Its nature is simple to explain: Given the eigendecomposition $K_n = Q\Sigma Q^\top$, a regularized inverse of the kernel matrix is built by discarding all the eigenvalues smaller than the prescribed threshold $n\lambda$. The associated regularization filter \bar{G}_λ is defined as

$$\bar{G}_\lambda(\Sigma) = \text{diag}(\sigma_1^{-1}, \dots, \sigma_m^{-1}, 0, \dots, 0),$$

where $m \in \mathbb{N}$ is the largest index for which $\sigma_i \geq n\lambda$, and corresponds to the scalar filter function

$$g_\lambda(\sigma) = \begin{cases} \frac{1}{\sigma} & \text{if } \sigma \geq n\lambda \\ 0 & \text{otherwise} \end{cases}.$$

Interestingly enough, one can show that spectral cut-off is equivalent to the following procedure:

- Unsupervised projection of the data using (kernel) PCA [Schölkopf et al., 1998].

- ERM on the projected data without explicit regularization.

Note that the only free parameter is the number of components m we retain for the projection, which depends on the threshold $n\lambda$. Therefore, we can say that in this algorithm the regularization operation coincides with the projection on the m largest eigencomponents.

3.4 Iterative Regularization via Early Stopping

In the previous sections, we have seen how explicit penalization (Tikhonov) and projection (spectral cut-off) can implement regularization mechanisms. Here, we outline another regularization strategy based on iterative regularization, whose driving principle is to recursively compute a sequence of solutions to the learning problem. The first few iterations yield simple solutions, while executing too many iterations may result in increasingly complex solutions, potentially leading to overfitting phenomena. Therefore, early termination of the iterations (early stopping) has a regularizing effect. We now describe this idea in greater detail by considering one of its most clear-cut instances, the Landweber iteration.

3.4.1 Landweber Iteration

The Landweber iteration (or iterative Landweber algorithm) can be seen as the minimization of the empirical risk

$$\hat{\mathcal{E}}(\hat{f}) = \frac{1}{n} \|Y - K_n c\|_2^2$$

via gradient descent. The Landweber iteration defines a sequence of solutions as follows:

$$\alpha_i = \alpha_{i-1} + \eta(Y - K_n \alpha_{i-1}), \quad (3.7)$$

with $\alpha_0 = 0$. If the largest eigenvalue of K_n is smaller than n , the above iteration converges if we choose the step size $\eta = 2/n$. It can be proven by induction that the solution at iteration t is

$$\alpha = \eta \sum_{i=0}^{t-1} (In - \eta K_n)^i Y.$$

Note that the well-known relation

$$\sum_{i=0}^{\infty} (1 - a)^i = a^{-1} \quad \forall a \in (0, 1)$$

also holds replacing a with a matrix. The resulting formula is called Neumann series,

$$\sum_{i=0}^{\infty} (I - A)^i = A^{-1},$$

and holds for any invertible matrix A such that $\|A\| < 1$. If we consider the kernel matrix (or rather $I_n - \eta K_n$), we obtain that an approximate inverse for it can be defined considering a truncated Neumann series, that is

$$K_n^{-1} = \eta \sum_{i=0}^{\infty} (I_n - \eta K_n)^i \approx \eta \sum_{i=0}^{t-1} (I_n - \eta K_n)^i = G_t(K_n). \quad (3.8)$$

The filter function $G_t(K_n)$ of the Landweber iteration corresponds to a truncated power expansion of K_n^{-1} , and the associated scalar filter function is

$$g_t(\sigma) = \eta \sum_{i=0}^{t-1} (I_n - n\sigma)^i.$$

The regularization parameter is the number of iterations t . Roughly speaking, $t \sim 1/\lambda$. In fact,

- Large values of t correspond to minimization of the empirical risk and tend to overfit.
- Small values of t tend to oversmooth (recall that $c_0 = 0$).

Early stopping of the iteration allows to find an optimal trade-off between oversmoothing and overfitting solutions, which corresponds to a regularization effect.

Part II

**Kernel Methods for Large-scale
Learning**

Chapter 4

Speeding up by Data-dependent Subsampling

4.1 Introduction

In Chapter 2, we have seen how kernel methods provide an elegant framework to develop nonparametric statistical approaches to learning [Schölkopf and Smola, 2002]. Prohibitive memory requirements of exact kernel methods, making these methods unfeasible when dealing with large datasets, have also been discussed. Indeed, this observation has motivated a variety of computational strategies to develop large-scale kernel methods [Smola and Schölkopf, 2000; Williams and Seeger, 2000; Rahimi and Recht, 2007; Yang et al., 2014; Le et al., 2013; Si et al., 2014; Zhang et al., 2013]. Approximation schemes based on generative probabilistic models have also been proposed in the Gaussian Processes literature (see for example [Quiñero-Candela and Rasmussen, 2005]), and are beyond the scope of this work.

In this chapter, we devote our attention to subsampling methods, that we broadly refer to as Nyström approaches. These methods replace the empirical kernel matrix, needed by standard kernel methods, with a smaller matrix obtained by column subsampling [Smola and Schölkopf, 2000; Williams and Seeger, 2000]. Such procedures are shown to often dramatically reduce memory/time requirements while preserving good practical performances [Kumar et al., 2009; Li et al., 2010; Zhang et al., 2008; Dai et al., 2014].

In Section 4.2 we study our recently proposed [Rudi et al., 2015] optimal learning bounds of subsampling schemes such as the Nyström method, while in Section 4.3 we investigate the generalization properties of NYTRO, a novel regularized learning algorithm combining subsampling and early stopping [Camoriano et al., 2016a].

4.2 Less is More: Regularization by Subsampling

4.2.1 Setting

The goal of this section is two-fold. First, and foremost, we aim at providing a theoretical characterization of the generalization properties of Nyström methods in a statistical learning setting. Second, we wish to understand the role played by the subsampling level both from a statistical and a computational point of view. As discussed in the following, this latter question leads to a natural variant of Kernel Regularized Least Squares (KRLS), where the subsampling level controls both regularization and computations.

From a theoretical perspective, the effect of Nyström approaches has been primarily characterized considering the discrepancy between a given empirical kernel matrix and its subsampled version [Drineas and Mahoney, 2005; Gittens and Mahoney, 2013; Wang and Zhang, 2013; Drineas et al., 2012; Cohen et al., 2015; Wang and Zhang, 2014; Kumar et al., 2012]. While interesting in their own right, these latter results do not directly yield information on the generalization properties of the obtained algorithm. Results in this direction, albeit suboptimal, were first derived in [Cortes et al., 2010] (see also [Jin et al., 2013; Yang et al., 2012]), and more recently in [Bach, 2013; Alaoui and Mahoney, 2014]. In these latter papers, sharp error analyses in expectation are derived in a fixed design regression setting for a form of Kernel Regularized Least Squares. In particular, in [Bach, 2013] a basic uniform sampling approach is studied, while in [Alaoui and Mahoney, 2014] a subsampling scheme based on the notion of leverage score is considered. The main technical contribution of our study is an extension of these latter results to the statistical learning setting, where the design is random and high probability estimates are considered. The more general setting makes the analysis considerably more complex. Our main result gives optimal finite sample bounds for both uniform and leverage score based subsampling strategies. These methods are shown to achieve the same (optimal) learning error as KRLS, recovered as a special case, while allowing substantial computational gains. Our analysis highlights the interplay between the Tikhonov regularization and subsampling parameters, suggesting that the latter can be used to control simultaneously regularization and computations. This strategy implements a form of *computational regularization* in the sense that the computational resources are tailored to the generalization properties in the data. This idea is developed considering an incremental strategy to efficiently compute learning solutions for different subsampling levels. The procedure thus obtained, which is a simple variant of classical Nyström Kernel Regularized Least Squares (NKRLS) with uniform sampling, allows for efficient model selection and achieves state of the art results on a variety of benchmark large-scale datasets.

The rest of the Section is organized as follows. In Subsection 4.2.2, we in-

roduce the setting and algorithms we consider. In Subsection 4.2.3, we present our main theoretical contributions. In Subsection 4.2.4, we discuss computational aspects and experimental results.

4.2.2 Supervised Learning with KRLS and Nyström

We consider a learning setting based on the one outlined in Chapter 1. Let $\mathcal{X} \times \mathbb{R}$ be a probability space with distribution ρ , where we view \mathcal{X} and \mathbb{R} as the input and output spaces, respectively. The learning goal is to minimize the *expected risk*,

$$\min_{f \in \mathcal{H}} \mathcal{E}(f), \quad \mathcal{E}(f) = \int_{\mathcal{X} \times \mathbb{R}} (f(x) - y)^2 d\rho(x, y), \quad (4.1)$$

provided ρ is known only through a training set. In the following, we consider kernel methods, as introduced in Section 2.3 in the case of random design regression, outlined in Section 1.3, in which

$$y_i = f_*(x_i) + \varepsilon_i, \quad i = 1, \dots, n, \quad (4.2)$$

with f_* a fixed *regression function*, $\varepsilon_1, \dots, \varepsilon_n$ a sequence of random variables seen as noise, and x_1, \dots, x_n random inputs. In Section 2.4, we have seen that a classical way to derive an empirical solution to problem (4.1) is to consider the KRLS learning algorithm, based on Tikhonov regularization,

$$\min_{f \in \mathcal{H}} \frac{1}{n} \sum_{i=1}^n (f(x_i) - y_i)^2 + \lambda \|f\|_{\mathcal{H}}^2, \quad \lambda > 0. \quad (4.3)$$

We recall that a solution \hat{f}_λ to problem (4.3) exists, it is unique and the representer theorem [Schölkopf and Smola, 2002] shows that it can be written as

$$\hat{f}_\lambda(x) = \sum_{i=1}^n \hat{\alpha}_i K(x_i, x) \quad \text{with} \quad \hat{\alpha} = (K_n + \lambda n I_n)^{-1} y, \quad (4.4)$$

where x_1, \dots, x_n are the training set points, $y = (y_1, \dots, y_n)$ and K_n is the empirical kernel matrix. Note that this result implies that we can restrict the minimization in (4.3) to the space,

$$\mathcal{H}_n = \left\{ f \in \mathcal{H} \mid f = \sum_{i=1}^n \alpha_i K(x_i, \cdot), \alpha_1, \dots, \alpha_n \in \mathbb{R} \right\}. \quad (4.5)$$

As already discussed, storing the kernel matrix K_n , and solving the linear system in (4.4), can become computationally unfeasible as n increases. In the following, we consider strategies to find more efficient solutions, based on the idea of replacing \mathcal{H}_n with

$$\mathcal{H}_m = \left\{ f \mid f = \sum_{i=1}^m \alpha_i K(\tilde{x}_i, \cdot), \alpha \in \mathbb{R}^m \right\},$$

where $m \leq n$ and $\{\tilde{x}_1, \dots, \tilde{x}_m\}$ is a subset of the input points in the training set. The solution $\hat{f}_{\lambda, m}$ of the corresponding minimization problem can now be written as,

$$\hat{f}_{\lambda, m}(x) = \sum_{i=1}^m \tilde{\alpha}_i K(\tilde{x}_i, x) \quad \text{with} \quad \tilde{\alpha} = (K_{nm}^\top K_{nm} + \lambda n K_{mm})^\dagger K_{nm}^\top y, \quad (4.6)$$

where A^\dagger denotes the Moore-Penrose pseudoinverse of a matrix A , and $(K_{nm})_{ij} = K(x_i, \tilde{x}_j)$, $(K_{mm})_{kj} = K(\tilde{x}_k, \tilde{x}_j)$ with $i \in \{1, \dots, n\}$ and $j, k \in \{1, \dots, m\}$ [Smola and Schölkopf, 2000]¹. The above approach is related to Nyström methods and different approximation strategies correspond to different ways to select the inputs subset. While our framework applies to a broader class of strategies, see Section C.1 of [Rudi et al., 2015], in the following we primarily consider two techniques.

- **Plain Nyström.** The points $\{\tilde{x}_1, \dots, \tilde{x}_m\}$ are sampled uniformly at random without replacement from the training set.
- **Approximate leverage scores (ALS) Nyström.** Recall that the *leverage scores* associated to the training set points x_1, \dots, x_n are

$$(l_i(t))_{i=1}^n, \quad l_i(t) = (K_n(K_n + tnI)^{-1})_{ii}, \quad i \in \{1, \dots, n\} \quad (4.7)$$

for any $t > 0$, where $(K_n)_{ij} = K(x_i, x_j)$. In practice, leverage scores are onerous to compute and approximations $(\hat{l}_i(t))_{i=1}^n$ can be considered [Drineas et al., 2012; Alaoui and Mahoney, 2014; Cohen et al., 2015]. In particular, in the following we are interested in suitable approximations defined as follows:

Definition 1 (T -approximate leverage scores). *Let $(l_i(t))_{i=1}^n$ be the leverage scores associated to the training set for a given t . Let $\delta > 0$, $t_0 > 0$ and $T \geq 1$. We say that $(\hat{l}_i(t))_{i=1}^n$ are T -approximate leverage scores with confidence δ , when with probability at least $1 - \delta$,*

$$\frac{1}{T} l_i(t) \leq \hat{l}_i(t) \leq T l_i(t) \quad \forall i \in \{1, \dots, n\}, t \geq t_0.$$

Given T -approximate leverage scores² for $t > \lambda_0$, $\{\tilde{x}_1, \dots, \tilde{x}_m\}$ are sampled from the training set independently with replacement, and with probability to be selected given by $P_t(i) = \hat{l}_i(t) / \sum_j \hat{l}_j(t)$.

In the next subsection, we state and discuss our main result showing that the KRLS formulation based on plain or approximate leverage scores Nyström provides optimal empirical solutions to problem (4.1).

¹Note that the estimator $\hat{f}_{\lambda, m}$ only depends on the m selected points, while if we used subsampling to first construct an approximation of the matrix K_n and then compute a vector $\alpha \in \mathbb{R}^n$ the estimator would be a combination of the kernel centered on all training points, thus less efficient.

²Algorithms for approximate leverage scores computation were proposed in [Drineas et al., 2012; Alaoui and Mahoney, 2014; Cohen et al., 2015].

4.2.3 Theoretical Analysis

We now state and discuss our main results, for which several assumptions are needed. The first basic assumption is that problem (4.1) admits at least a solution.

Assumption 1. *There exists an $f_{\mathcal{H}} \in \mathcal{H}$ such that*

$$\mathcal{E}(f_{\mathcal{H}}) = \min_{f \in \mathcal{H}} \mathcal{E}(f).$$

Note that, while the minimizer might not be unique, our results apply to the case in which $f_{\mathcal{H}}$ is the unique minimizer with minimal norm. Also, note that the above condition is weaker than assuming the regression function in (4.2) to belong to \mathcal{H} . Finally, we note that our study can be adapted to the case in which minimizers do not exist, but the analysis is considerably more involved and is therefore left to future work.

The second assumption is a basic condition on the probability distribution.

Assumption 2. *Let z_x be the random variable $z_x = y - f_{\mathcal{H}}(x)$, with $x \in \mathcal{X}$, and y distributed according to $\rho(y|x)$. Then, there exists $M, \sigma > 0$ such that $\mathbb{E}|z_x|^p \leq \frac{1}{2}p!M^{p-2}\sigma^2$ for any $p \geq 2$, almost everywhere on \mathcal{X} .*

The above assumption is needed to control random quantities and is related to a *noise* assumption in the regression model (4.2). It is clearly weaker than the often considered bounded output assumption [Steinwart and Christmann, 2008], and trivially verified in classification.

The last two assumptions describe the capacity (roughly speaking the “size”) of the hypothesis space induced by K with respect to ρ and the regularity of $f_{\mathcal{H}}$ with respect to K and ρ . To discuss them, we first need the following definition.

Definition 2 (Covariance operator and effective dimensions). *We define the covariance operator as*

$$C : \mathcal{H} \rightarrow \mathcal{H}, \quad \langle f, Cg \rangle_{\mathcal{H}} = \int_{\mathcal{X}} f(x)g(x)d\rho_{\mathcal{X}}(x) \quad , \quad \forall f, g \in \mathcal{H}.$$

Moreover, for $\lambda > 0$, we define the random variable

$$\mathcal{N}_x(\lambda) = \langle K_x, (C + \lambda I)^{-1} K_x \rangle_{\mathcal{H}},$$

with $x \in \mathcal{X}$ distributed according to $\rho_{\mathcal{X}}$, and let

$$\mathcal{N}(\lambda) = \mathbb{E}\mathcal{N}_x(\lambda), \quad \mathcal{N}_{\infty}(\lambda) = \sup_{x \in \mathcal{X}} \mathcal{N}_x(\lambda).$$

We add several comments. Note that C corresponds to the second moment operator, but we refer to it as the covariance operator with an abuse

of terminology. Moreover, note that $\mathcal{N}(\lambda) = \text{Tr}(C(C + \lambda I)^{-1})$, where “Tr” indicates the trace of a matrix (see [Caponnetto and De Vito, 2007]). This latter quantity, called effective dimension or degrees of freedom, can be seen as a measure of the capacity of the hypothesis space. The quantity $\mathcal{N}_\infty(\lambda)$ can be seen to provide a uniform bound on the leverage scores in (4.7). Clearly, $\mathcal{N}(\lambda) \leq \mathcal{N}_\infty(\lambda)$ for all $\lambda > 0$.

Assumption 3. *The kernel K is measurable, C is bounded. Moreover, for all $\lambda > 0$ and a $Q > 0$,*

$$\mathcal{N}_\infty(\lambda) < \infty, \quad (4.8)$$

$$\mathcal{N}(\lambda) \leq Q\lambda^{-\gamma}, \quad 0 < \gamma \leq 1. \quad (4.9)$$

Measurability of K and boundedness of C are minimal conditions to ensure that the covariance operator is a well defined linear, continuous, self-adjoint, positive operator [Steinwart and Christmann, 2008]. Condition (4.8) is satisfied if the kernel is bounded $\sup_{x \in \mathcal{X}} K(x, x) = \kappa^2 < \infty$, indeed in this case $\mathcal{N}_\infty(\lambda) \leq \kappa^2/\lambda$ for all $\lambda > 0$. Conversely, it can be seen that condition (4.8) together with boundedness of C imply that the kernel is bounded, indeed ³

$$\kappa^2 \leq 2 \|C\| \mathcal{N}_\infty(\|C\|).$$

Boundedness of the kernel implies in particular that the operator C is trace class and allows to use tools from spectral theory. Condition (4.9) quantifies the capacity assumption and is related to covering/entropy number conditions (see [Steinwart and Christmann, 2008] for further details). In particular, it is known that condition (4.9) is ensured if the eigenvalues $(\sigma_i)_i$ of C satisfy a polynomial decaying condition $\sigma_i \sim i^{-\frac{1}{\gamma}}$. Note that, since the operator C is trace class, Condition (4.9) always holds for $\gamma = 1$. Here, for space constraints and in the interest of clarity we restrict to such a polynomial condition, but the analysis directly applies to other conditions including exponential decay or a finite rank conditions [Caponnetto and De Vito, 2007]. Finally, we have the following regularity assumption.

Assumption 4. *There exists $s \geq 0$, $1 \leq R < \infty$, such that $\|C^{-s} f_{\mathcal{H}}\|_{\mathcal{H}} < R$.*

The above condition is fairly standard, and can be equivalently formulated in terms of classical concepts in approximation theory such as interpolation spaces [Steinwart and Christmann, 2008]. Intuitively, it quantifies the degree to which $f_{\mathcal{H}}$ can be well approximated by functions in the RKHS \mathcal{H} and allows to control the bias/approximation error of a learning solution. For $s = 0$, it is always satisfied. For larger s , we are assuming $f_{\mathcal{H}}$ to belong to subspaces of \mathcal{H} that are the images of the fractional compact

³If $\mathcal{N}_\infty(\lambda)$ is finite, then $\mathcal{N}_\infty(\|C\|) = \sup_{x \in \mathcal{X}} \|(C + \|C\| I)^{-1} K_x\|^2 \geq 1/2 \|C\|^{-1} \sup_{x \in \mathcal{X}} \|K_x\|^2$, therefore $K(x, x) \leq 2 \|C\| \mathcal{N}_\infty(\|C\|)$.

operators C^s . Such spaces contain functions which, expanded on a basis of eigenfunctions of C , have larger coefficients in correspondence to large eigenvalues. Such an assumption is natural in view of using techniques such as (4.4), which can be seen as a form of spectral filtering (see Chapter 3), that estimate stable solutions by discarding the contribution of small eigenvalues [Gerfo et al., 2008b]. In the next section, we are going to quantify the quality of empirical solutions of Problem (4.1) obtained by schemes of the form (4.6), in terms of the quantities in Assumptions 2, 3, 4.

Main results

In this section, we state and discuss our main results, starting with optimal finite sample error bounds for regularized least squares based on plain and approximate leverage score based Nyström subsampling.

Theorem 1. *Under Assumptions 1, 2, 3, and 4, let $\delta > 0$, $v = \min(s, 1/2)$, $p = 1 + 1/(2v + \gamma)$ and assume*

$$n \geq 1655\kappa^2 + 223\kappa^2 \log \frac{6\kappa^2}{\delta} + \left(\frac{38p}{\|C\|} \log \frac{114\kappa^2 p}{\|C\| \delta} \right)^p.$$

Then, the following inequality holds with probability at least $1 - \delta$,

$$\mathcal{E}(\hat{f}_{\lambda, m}) - \mathcal{E}(f_{\mathcal{H}}) \leq q^2 n^{-\frac{2v+1}{2v+\gamma+1}}, \quad (4.10)$$

with

$$q = 6R \left(2\|C\| + \frac{M\kappa}{\sqrt{\|C\|}} + \sqrt{\frac{Q\sigma^2}{\|C\|^\gamma}} \right) \log \frac{6}{\delta}, \quad (4.11)$$

with $\hat{f}_{\lambda, m}$ as in (4.6), $\lambda = \|C\| n^{-\frac{1}{2v+\gamma+1}}$ and

1. for plain Nyström

$$m \geq (67 \vee 5\mathcal{N}_\infty(\lambda)) \log \frac{12\kappa^2}{\lambda\delta};$$

2. for ALS Nyström and T -approximate leverage scores with subsampling probabilities P_λ , $t_0 \geq \frac{19\kappa^2}{n} \log \frac{12n}{\delta}$ and

$$m \geq (334 \vee 78T^2\mathcal{N}(\lambda)) \log \frac{48n}{\delta}.$$

We add several comments. First, the above results can be shown to be optimal in a minimax sense. Indeed, minimax lower bounds proved in [Caponnetto and De Vito, 2007; Steinwart et al., 2009] show that the learning rate in (4.10) is optimal under the considered assumptions (see

Theorems 2, 3 of [Caponnetto and De Vito, 2007], for a discussion on min-max lower bounds see Section 2 of [Caponnetto and De Vito, 2007]). Second, the obtained bounds can be compared to those obtained for other regularized learning techniques. Techniques known to achieve optimal error rates include Tikhonov regularization [Caponnetto and De Vito, 2007; Steinwart et al., 2009; Mendelson and Neeman, 2010], iterative regularization by early stopping [Bauer et al., 2007; Caponnetto and Yao, 2010], spectral cut-off regularization (a.k.a. principal component regression or truncated SVD) [Bauer et al., 2007; Caponnetto and Yao, 2010], as well as regularized stochastic gradient methods [Ying and Pontil, 2008]. All these techniques are essentially equivalent from a statistical point of view and differ only in the required computations. For example, iterative methods allow for a computation of solutions corresponding to different regularization levels which is more efficient than Tikhonov or SVD based approaches. The key observation is that all these methods have the same $O(n^2)$ memory requirement. In this view, our results show that randomized subsampling methods can break such a memory barrier, and consequently achieve much better time complexity, while preserving optimal learning guarantees. Finally, we can compare our results with previous analysis of randomized kernel methods. As already mentioned, results close to those in Theorem 1 are given in [Bach, 2013; Alaoui and Mahoney, 2014] in a fixed design setting. Our results extend and generalize the conclusions of these papers to a general statistical learning setting. Relevant results are given in [Zhang et al., 2013] for a different approach, based on averaging KRLS solutions obtained splitting the data in m groups (*divide and conquer* RLS). The analysis in [Zhang et al., 2013] is only in expectation, but considers random design and shows that the proposed method is indeed optimal provided the number of splits is chosen depending on the effective dimension $\mathcal{N}(\lambda)$. This is the only other work we are aware of establishing optimal learning rates for randomized kernel approaches in a statistical learning setting. In comparison with Nyström computational regularization the main disadvantage of the divide and conquer approach is computational and in the model selection phase where solutions corresponding to different regularization parameters and number of splits usually need to be computed. The proof of Theorem 1 is fairly technical and lengthy. It incorporates ideas from [Caponnetto and De Vito, 2007] and techniques developed to study spectral filtering regularization [Bauer et al., 2007; Rudi et al., 2013]. In the next section, we briefly sketch some main ideas and discuss how they suggest an interesting perspective on regularization techniques including subsampling.

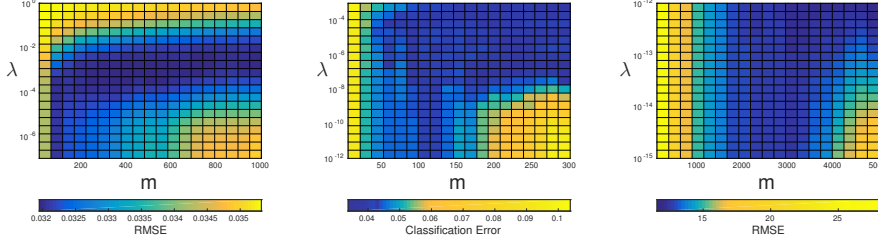


Figure 4.1: Validation errors associated to 20×20 grids of values for m (x axis) and λ (y axis) on `pumadyn32nh` (left), `breast cancer` (center) and `cpuSmall` (right).

Proof sketch and a computational regularization perspective

A key step in the proof of Theorem 1 is an error decomposition, and corresponding bound, for any fixed λ and m . Indeed, it is proved in Theorem 2 of [Rudi et al., 2015] and Proposition 2 of [Rudi et al., 2015] that, for $\delta > 0$, with probability at least $1 - \delta$,

$$\begin{aligned}
 & \left| \mathcal{E}(\hat{f}_{\lambda, m}) - \mathcal{E}(f_{\mathcal{H}}) \right|^{1/2} \lesssim \\
 & R \left(\frac{M \sqrt{\mathcal{N}_{\infty}(\lambda)}}{n} + \sqrt{\frac{\sigma^2 \mathcal{N}(\lambda)}{n}} \right) \log \frac{6}{\delta} + RC(m)^{1/2+v} + R\lambda^{1/2+v}. \quad (4.12)
 \end{aligned}$$

The first and last term in the right hand side of the above inequality can be seen as forms of *sample and approximation errors* [Steinwart and Christmann, 2008] and are studied in Lemma 4 of [Rudi et al., 2015] and Theorem 2 of [Rudi et al., 2015]. The mid term can be seen as a *computational error* and depends on the considered subsampling scheme. Indeed, it is shown in Proposition 2 of [Rudi et al., 2015] that $\mathcal{C}(m)$ can be taken as,

$$\mathcal{C}_{\text{pl}}(m) = \min \left\{ t > 0 \mid (67 \vee 5 \mathcal{N}_{\infty}(t)) \log \frac{12\kappa^2}{t\delta} \leq m \right\},$$

for the plain Nyström approach, and

$$\mathcal{C}_{\text{ALS}}(m) = \min \left\{ \frac{19\kappa^2}{n} \log \frac{12n}{\delta} \leq t \leq \|C\| \mid 78T^2 \mathcal{N}(t) \log \frac{48n}{\delta} \leq m \right\},$$

for the approximate leverage scores approach. The bounds in Theorem 1 follow by: 1) minimizing in λ the sum of the first and third term 2) choosing m so that the computational error is of the same order of the other terms. Computational resources and regularization are then tailored to the generalization properties of the data at hand. We add a few comments. First, note that the error bound in (4.12) holds for a large class of subsampling

schemes, as discussed in Section C.1 in the appendix of [Rudi et al., 2015]. Then specific error bounds can be derived developing computational error estimates. Second, the error bounds in Theorem 2 of [Rudi et al., 2015] and Proposition 2 of [Rudi et al., 2015], and hence in Theorem 1, easily generalize to a larger class of regularization schemes beyond Tikhonov approaches, namely spectral filtering [Bauer et al., 2007]. For space constraints, these extensions are deferred to a longer version of the paper. Third, we note that, in practice, optimal data driven parameter choices, e.g. based on hold-out estimates [Caponnetto and Yao, 2010], can be used to adaptively achieve optimal learning bounds.

Finally, we observe that a different perspective is derived starting from inequality (4.12), and noting that the role played by m and λ can also be exchanged. Letting m play the role of a regularization parameter, λ can be set as a function of m and m tuned adaptively. For example, in the case of a plain Nyström approach, if we set

$$\lambda = \frac{\log m}{m}, \quad \text{and} \quad m = 3n^{\frac{1}{2v+\gamma+1}} \log n,$$

then the obtained learning solution achieves the error bound in (4.10)⁴. As above, the subsampling level can also be chosen by cross-validation. Interestingly, in this case by tuning m we naturally control computational resources and regularization. An advantage of this latter parameterization is that, as described in the following, the solution corresponding to different subsampling levels is easy to update using Cholesky rank-one update formulas [Golub and Van Loan, 2012]. As discussed in the next section, in practice, a joint tuning over m and λ can be done starting from small m and appears to be advantageous both for error and computational performances.

4.2.4 Incremental Updates and Experimental Analysis

In this subsection, we first describe an incremental strategy to efficiently explore different subsampling levels and then perform extensive empirical tests aimed in particular at:

- Investigating the statistical and computational benefits of considering varying subsampling levels.
- Compare the performance of the algorithm with respect to state of the art solutions on several large-scale benchmark datasets.

⁴Note that in Theorem 1 the bound depends on λ and m . By optimizing these two parameters to minimize the upper bound we note that $m = \text{const}$ is sufficient for optimal bounds. Thus, we can simply write λ as a function of m .

Input: Dataset $(x_i, y_i)_{i=1}^n$, Subsampling $(\tilde{x}_j)_{j=1}^m$, Regularization Parameter λ .
Output: Nyström KRLS estimators $\{\tilde{\alpha}_1, \dots, \tilde{\alpha}_m\}$.
 Compute $\gamma_1; R_1 \leftarrow \sqrt{\gamma_1}$;
for $t \in \{2, \dots, m\}$ **do**
 Compute A_t, u_t, v_t ;
 $R_t \leftarrow \begin{pmatrix} R_{t-1} & 0 \\ 0 & 0 \end{pmatrix}$;
 $R_t \leftarrow \text{cholup}(R_t, u_t, '+')$;
 $R_t \leftarrow \text{cholup}(R_t, v_t, '-')$;
 $\tilde{\alpha}_t \leftarrow R_t^{-1}(R_t^{-\top}(A_t^\top Y))$;
end for

Algorithm 4.1: Incremental Nyström KRLS. `cholup` is the Cholesky rank-1 update routine.

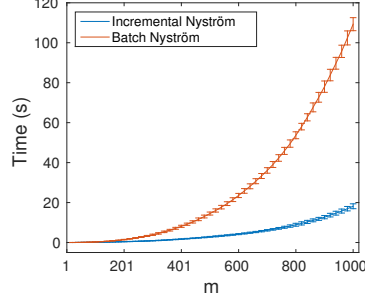


Figure 4.2: Model selection time on the `cpuSmall` dataset. $m \in [1, 1000]$ and $T = 50, 10$ repetitions.

We only consider a plain Nyström approach, deferring to future work the analysis of leverage scores based sampling techniques. Interestingly, we will see that such a basic approach can often provide state of the art performances.

Efficient incremental updates

Algorithm 4.1 efficiently computes solutions corresponding to different subsampling levels, by exploiting rank-one Cholesky updates [Golub and Van Loan, 2012]. The proposed procedure allows to efficiently compute a whole regularization path of solutions, and hence perform fast model selection⁵ (see Appendix D)⁶. In Algorithm 4.1, the function `cholup` is the Cholesky rank-one update formula available in many linear algebra libraries. The total cost of the algorithm is $O(nm^2 + m^3)$ time to compute $\tilde{\alpha}_2, \dots, \tilde{\alpha}_m$, while a naive non-incremental algorithm would require $O(nm^2M + m^3M)$ with M is the number of analyzed subsampling levels. The following are some quantities needed by the algorithm: $A_1 = a_1$ and $A_t = (A_{t-1} \ a_t) \in \mathbb{R}^{n \times t}$,

⁵The code for Algorithm 4.1 is available at [lcsl.github.io/NystromCoRe](https://github.com/lcsl/NystromCoRe).

⁶Note that Algorithm 4.1 allows to compute the regularization path incrementally in m for a fixed λ . In practice, the procedure can be easily parallelized over the candidate λ values to find the most convenient (λ, m) combination.

for any $2 \leq t \leq m$. Moreover, for any $1 \leq t \leq m$, $g_t = \sqrt{1 + \gamma_t}$ and

$$\begin{aligned} u_t &= (c_t/(1 + g_t), g_t), & a_t &= (K(\tilde{x}_t, x_1), \dots, K(\tilde{x}_t, x_n)), \\ v_t &= (c_t/(1 + g_t), -1), & b_t &= (K(\tilde{x}_t, \tilde{x}_1), \dots, K(\tilde{x}_t, \tilde{x}_{t-1})), \\ c_t &= A_{t-1}^\top a_t + \lambda n b_t, & \gamma_t &= a_t^\top a_t + \lambda n K(\tilde{x}_t, \tilde{x}_t). \end{aligned}$$

Experimental analysis

We empirically study the properties of Algorithm 4.1, considering a Gaussian kernel of width σ . The selected datasets are already divided in a training and a test part⁷. We randomly split the training part in a training set and a validation set (80% and 20% of the n training points, respectively) for parameter tuning via cross-validation. The m subsampled points for Nyström approximation are selected uniformly at random from the training set. We report the performance of the selected model on the fixed test set, repeating the process for several trials.

Interplay between λ and m . We begin with a set of results showing that incrementally exploring different subsampling levels can yield very good performance while substantially reducing the computational requirements. We consider the `pumadyn32nh` ($n = 8192$, $d = 32$), the `breast cancer` ($n = 569$, $d = 30$), and the `cpuSmall` ($n = 8192$, $d = 12$) datasets⁸. In Figure 4.1, we report the validation errors associated to a 20×20 grid of values for λ and m . The λ values are logarithmically spaced, while the m values are linearly spaced. The ranges and kernel bandwidths, chosen according to preliminary tests on the data, are $\sigma = 2.66$, $\lambda \in [10^{-7}, 1]$, $m \in [10, 1000]$ for `pumadyn32nh`, $\sigma = 0.9$, $\lambda \in [10^{-12}, 10^{-3}]$, $m \in [5, 300]$ for `breast cancer`, and $\sigma = 0.1$, $\lambda \in [10^{-15}, 10^{-12}]$, $m \in [100, 5000]$ for `cpuSmall`. The main observation that can be derived from this first series of tests is that a small m is sufficient to obtain the same results achieved with the largest m . For example, for `pumadyn32nh` it is sufficient to choose $m = 62$ and $\lambda = 10^{-7}$ to obtain an average test RMSE of 0.33 over 10 trials, which is the same as the one obtained using $m = 1000$ and $\lambda = 10^{-3}$, with a 3-fold speedup of the joint training and validation phase. Also, it is interesting to observe that for given values of λ , large values of m can decrease the performance. This observation is consistent with the results in Subsection 4.2.3, showing that m can play the role of a regularization parameter. Similar results are obtained for `breast cancer`, where for $\lambda = 4.28 \times 10^{-6}$ and $m = 300$ we obtain a 1.24% average classification error on the test set over 20 trials, while for $\lambda = 10^{-12}$ and $m = 67$ we obtain 1.86%. For `cpuSmall`, with $m = 5000$ and $\lambda = 10^{-12}$ the average test RMSE over 5 trials is 12.2,

⁷In the following we denote by n the total number of points and by d the number of dimensions.

⁸www.cs.toronto.edu/~delve and archive.ics.uci.edu/ml/datasets

Table 4.1: Test RMSE comparison for exact and approximated kernel methods. The results for KRLS, Batch Nyström, RF and Fastfood are the ones reported in [Le et al., 2013]. n_{tr} is the size of the training set.

Dataset	n_{tr}	d	Incremental Nyström RBF	KRLS RBF	Batch Nyström RBF	RF RBF	Fastfood RBF	Fastfood FFT	KRLS Matern	Fastfood Matern
Insurance Company	5822	85	$0.23180 \pm 4 \times 10^{-5}$	0.231	0.232	0.266	0.264	0.266	0.234	0.235
CPU	6554	21	2.8466 ± 0.0497	7.271	6.758	7.103	7.366	4.544	4.345	4.211
CT slices (axial)	42800	384	7.1106 ± 0.0772	NA	60.683	49.491	43.858	58.425	NA	14.868
Year Prediction MSD	463715	90	$0.10470 \pm 5 \times 10^{-5}$	NA	0.113	0.123	0.115	0.106	NA	0.116
Forest	522910	54	0.9638 ± 0.0186	NA	0.837	0.840	0.840	0.838	NA	0.976

while for $m = 2679$ and $\lambda = 10^{-15}$ it is only slightly higher, 13.3, but computing its associated solution requires less than half of the time and approximately half of the memory.

Regularization path computation. If the subsampling level m is used as a regularization parameter, the computation of a regularization path corresponding to different subsampling levels becomes crucial during the model selection phase. A naive approach, that consists in recomputing the solutions of (4.6) for each subsampling level, would require $O(m^2 n T + m^3 L T)$ computational time, where T is the number of solutions with different subsampling levels to be evaluated and L is the number of Tikhonov regularization parameters. On the other hand, by using the incremental Nyström algorithm the model selection time complexity is $O(m^2 n + m^3 L)$ for the whole regularization path. We experimentally verify this speedup on `cpuSmall1` with 10 repetitions, setting $m \in [1, 5000]$ and $T = 50$. The model selection times, measured on a server with $12 \times 2.10\text{GHz}$ Intel[®] Xeon[®] E5-2620 v2 CPUs and 132 GB of RAM, are reported in Figure 4.2. The result clearly confirms the beneficial effects of incremental Nyström model selection on the computational time.

Predictive performance comparison. Finally, we consider the performance of the algorithm on several large scale benchmark datasets considered in [Le et al., 2013], see Table 4.1. σ has been chosen on the basis of preliminary data analysis. m and λ have been chosen by cross-validation, starting from small subsampling values up to $m_{max} = 2048$, and considering $\lambda \in [10^{-12}, 1]$. After model selection, we retrain the best model on the entire training set and compute the RMSE on the test set. We consider 10 trials, reporting the performance mean and standard deviation. The results in Table 4.1 compare Nyström computational regularization with the following methods (as in [Le et al., 2013]):

- **Kernel Regularized Least Squares (KRLS):** Not compatible with large datasets.
- **Random Fourier features (RF):** As in [Rahimi and Recht, 2007], with

a number of random features $D = 2048$.

- **Fastfood RBF, FFT and Matern kernel:** As in [Le et al., 2013], with $D = 2048$ random features.
- **Batch Nyström:** Nyström method [Williams and Seeger, 2000] with uniform sampling and $m = 2048$.

The above results show that the proposed incremental Nyström approach behaves really well, matching state of the art predictive performances.

4.3 NYTRO: Nyström Iterative Regularization

4.3.1 Setting

A key feature towards scalability is being able to tailor computational requirements to the generalization properties/statistical accuracy allowed by the data. In other words, the precision with which computations need to be performed should be determined not only by the amount, but also by the quality of the available data.

Early stopping (see Section 3.4), known as iterative regularization in inverse problem theory [Engl et al., 1996; Zhang and Yu, 2005; Bauer et al., 2007; Yao et al., 2007; Caponnetto and Yao, 2010], provides a simple and sound implementation of this intuition. An empirical objective function is optimized in an iterative way with no explicit constraint or penalization and regularization is achieved by suitably stopping the iteration. Too many iterations might lead to overfitting, while stopping too early might result in oversmoothing [Zhang and Yu, 2005; Bauer et al., 2007; Yao et al., 2007; Caponnetto and Yao, 2010]. Then, the best stopping rule arises from a form of bias-variance trade-off [Hastie et al., 2001]. The key observation is that the number of iterations controls at the same time the computational complexity as well as the statistical properties of the obtained learning algorithm [Yao et al., 2007]. Training and model selection can hence be performed with often considerable gain in time complexity.

Despite these nice properties, early stopping procedures often share the same space complexity requirements, hence bottle necks, of other methods, such as those based on Tikhonov regularization (see [Tikhonov, 1963; Hoerl and Kennard, 1970]). As seen in previous sections, a natural way to tackle these issues is to consider randomized subsampling approaches. In this Section, we ask whether early stopping and subsampling methods can be fruitfully combined. With the context of kernel methods in mind, we propose and study NYTRO (NYström iTerative RegularizatiOn), a simple algorithm combining these two ideas. After recalling the properties and advantages of different regularization approaches in Subsection 4.3.2, in Subsection 4.3.3 we present in detail NYTRO and our main result, the charac-

terization of its generalization properties. In particular, we analyze the conditions under which it attains the same statistical properties of subsampling and early stopping. Indeed, our study shows that while both techniques share similar, optimal, statistical properties, they are computationally advantageous in different regimes and NYTRO outperforms early stopping in the appropriate regime, as discussed in Subsection 4.3.3. The theoretical results are validated empirically in Subsection 4.3.4, where NYTRO is shown to provide competitive results even at a fraction of the computational time, on a variety of benchmark datasets.

4.3.2 Learning and Regularization

In this section we introduce the problem of learning in the fixed design setting and discuss different regularized learning approaches, comparing their statistical and computational properties. This section is a survey that might be interesting in its own right, and reviews several results providing the context for the study in the paper.

The Learning Problem

We introduce the learning setting we consider in this section. Let $\mathcal{X} = \mathbb{R}^d$ be the input space and $\mathcal{Y} \subseteq \mathbb{R}$ the output space. Consider a *fixed design* setting [Bach, 2013], as introduced in Section 1.3, where the input points $x_1, \dots, x_n \in \mathcal{X}$ are fixed, while the outputs $y_1, \dots, y_n \in \mathcal{Y}$ are given by

$$y_i = f_*(x_i) + \epsilon_i, \quad \forall i \in \{1, \dots, n\}$$

where $f_* : \mathcal{X} \rightarrow \mathcal{Y}$ is a fixed function and $\epsilon_1, \dots, \epsilon_n$ are random variables. The latter can be seen as noise and are assumed to be independently and identically distributed according to a probability distribution ρ with zero mean and variance σ^2 . In this context, the goal is to minimize the *expected risk*, that is

$$\min_{f \in \mathcal{H}} \mathcal{E}(f), \quad \mathcal{E}(f) = \mathbb{E} \frac{1}{n} \sum_{i=1}^n (f(x_i) - y_i)^2, \quad \forall f \in \mathcal{H}, \quad (4.13)$$

on a hypotheses space \mathcal{H} . In a real applications, ρ and f_* are unknown and accessible only by means of a single realization $(x_1, y_1), \dots, (x_n, y_n)$ called *training set* and an approximate solution needs to be found. The quality of a solution f is measured by the *excess risk*, defined as

$$R(f) = \mathcal{E}(f) - \inf_{v \in \mathcal{H}} \mathcal{E}(v), \quad \forall f \in \mathcal{H}.$$

We next discuss estimation schemes to find a solution and compare their computational and statistical properties.

From (Kernel) Ordinary Least Square to Tikhonov Regularization

A classical approach to derive an empirical solution to Problem (4.13) is ERM, as seen in Section 1.9,

$$f_{\text{ols}} = \arg \min_{f \in \mathcal{H}} \frac{1}{n} \sum_{i=1}^n (f(x_i) - y_i)^2. \quad (4.14)$$

Here, we are interested in the case where \mathcal{H} is the RKHS induced by a positive definite kernel $K : \mathcal{X} \times \mathcal{X} \rightarrow \mathbb{R}$. In this case Problem (4.14) corresponds to Kernel Ordinary Least Squares (KOLS — see Section 3.1) and has the closed form solution

$$f_{\text{ols}}(x) = \sum_{i=1}^n \alpha_{\text{ols},i} K(x, x_i), \quad \alpha_{\text{ols}} = K_n^\dagger y, \quad (4.15)$$

for all $x \in \mathcal{X}$, where $(K_n)^\dagger$ denotes the pseudo-inverse of the $\in \mathbb{R}^{n \times n}$ empirical kernel matrix $[K_n]_{ij} = K(x_i, x_j)$ and $y = (y_1, \dots, y_n)$. The cost for computing the coefficients α_{ols} is $O(n^2)$ in memory and $O(n^3 + q(\mathcal{X})n^2)$ in time, where $q(\mathcal{X})n^2$ is the cost for computing K_n and n^3 the cost for obtaining its pseudo-inverse. Here, $q(\mathcal{X})$ is the cost of evaluating the kernel function. In the following, we are concerned with the dependence on n and hence view $q(\mathcal{X})$ as a constant.

The statistical properties of KOLS, and related methods, can be characterized by suitable notions of *dimension* that we recall next. The simplest is the *full dimension*, that is

$$d^* = \text{rank } K_n,$$

which measures the degrees of freedom of the kernel matrix. This latter quantity might not be stable when K_n is ill-conditioned. A more robust notion is provided by the *effective dimension*

$$d_{\text{eff}}(\lambda) = \text{Tr}(K_n(K_n + \lambda n I_n)^{-1}), \quad \lambda > 0.$$

Indeed, the above quantity can be shown to be related to the eigenvalue decay of K_n [Bach, 2013; Alaoui and Mahoney, 2014] and can be considerably smaller than d^* , as discussed in the following. Finally, consider

$$\tilde{d}(\lambda) = n \max_i (K_n(K_n + \lambda n I_n)^{-1})_{ii}, \quad \lambda > 0. \quad (4.16)$$

It is easy to see that the following inequalities hold,

$$d_{\text{eff}}(\lambda) \leq \tilde{d}(\lambda) \leq 1/\lambda, \quad d_{\text{eff}}(\lambda) \leq d^* \leq n, \quad \forall \lambda > 0.$$

Aside from the above notion of dimensionality, the statistical accuracy of empirical least squares solutions depends on a natural form of signal to

noise ratio defined next. Note that the function that minimizes the excess risk in \mathcal{H} is given by

$$\begin{aligned} f_{\text{opt}} &= \sum_{i=1}^n \alpha_{\text{opt},i} K(x, x_i), \quad \forall x \in \mathcal{X} \\ \alpha_{\text{opt}} &= K_n^\dagger \mu, \quad \text{with } \mu = \mathbb{E}y. \end{aligned}$$

Then, the signal to noise ratio is defined as

$$\text{SNR} = \frac{\|f_{\text{opt}}\|_{\mathcal{H}}^2}{\sigma^2}. \quad (4.17)$$

Provided with the above definitions, we can recall a first basic results characterizing the statistical accuracy of KOLS.

Theorem 2. *Under the assumptions of Section 4.3.2, the following equation holds,*

$$\mathbb{E}R(f_{\text{ols}}) = \frac{\sigma^2 d^*}{n}.$$

The above result shows that the excess risk of KOLS can be bounded in terms of the full dimension, the noise level and the number of points. However, in general ERM *does not* provide the best results and regularization is needed. We next recall this fact, considering first Tikhonov regularization, that is the KRLS algorithm (see Section 2.4) given by

$$\bar{f}_\lambda = \arg \min_{f \in \mathcal{H}} \frac{1}{n} \sum_{i=1}^n (f(x_i) - y_i)^2 + \lambda \|f\|_{\mathcal{H}}^2. \quad (4.18)$$

We recall that the solution of Problem (4.18) is

$$\bar{f}_\lambda(x) = \sum_{i=1}^n \bar{\alpha}_{\lambda,i} K(x, x_i), \quad \bar{\alpha}_\lambda = (K_n + \lambda n I_n)^{-1} Y, \quad (4.19)$$

for all $x \in \mathcal{X}$. The intuition that regularization can be beneficial is made precise by the following result comparing KOLS and KRLS.

Theorem 3. *Let $\lambda^* = \frac{1}{5NR}$. The following inequalities hold,*

$$\mathbb{E}R(\bar{f}_{\lambda^*}) \leq \frac{\sigma^2 d_{\text{eff}}(\lambda^*)}{n} \leq \frac{\sigma^2 d^*}{n} = \mathbb{E}R(f_{\text{ols}}).$$

We add a few comments. First, as announced, the above result quantifies the benefits of regularization. Indeed, it shows that there exists a λ^* for which the expected excess risk of KRLS is smaller than the one of KOLS. As discussed in Table 1 of [Bach, 2013], if $d^* = n$ and the kernel is sufficiently

“rich”, namely universal [Micchelli et al., 2006], then d_{eff} can be less than a fractional power of d^* , so that $d_{\text{eff}} \ll d^*$ and

$$\mathbb{E}R(\bar{f}_{\lambda^*}) \ll \mathbb{E}R(f_{\text{ols}}).$$

Second, note that the choice of the regularization parameter depends on a form of signal to noise ratio, which is usually unknown. In practice, a regularization path⁹ is computed and then a model selected or found by aggregation [Hastie et al., 2001]. Assuming the selection/aggregation step to have negligible computational cost, the complexity of performing training *and* model selection is then $O(n^2)$ in memory and $O(n^3|\Lambda|)$ in time. These latter requirements can become prohibitive when n is large and the question is whether the same statistical accuracy of KRLS can be achieved while reducing time/memory requirements.

Early Stopping and Nyström Methods

In this section, we first recall how early stopping regularization allows to achieve the same statistical accuracy of KRLS with potential saving in time complexity. Then, we recall how subsampling ideas can be used in the framework of Tikhonov regularization to reduce the space complexity with no loss of statistical accuracy.

Iterative Regularization by Early Stopping The idea is to consider the gradient descent minimization of Problem (4.15) for a fixed number of steps t , as seen in Section 3.4. We now introduce the notation used in this section for early stopping. The algorithm is

$$\check{f}_t(x) = \sum_{i=1}^n \check{\alpha}_{t,i} K(x_i, x), \quad (4.20)$$

$$\check{\alpha}_t = \check{\alpha}_{t-1} - \frac{\gamma}{n} (K_n \check{\alpha}_{t-1} - Y), \quad (4.21)$$

where $\gamma < 1/\|K_n\|$ and $\check{\alpha}_0 = 0$. The only tuning parameter is the number of steps, which, as shown next, controls at the same time the computational complexity and statistical accuracy of the algorithm. The following theorem compares the expected excess risk of early stopping with the one of KRLS.

Theorem 4. *When $\gamma < 1/\|K_n\|$ and $t \geq 2$ the following holds*

$$\mathbb{E}R(\check{f}_{\gamma,t}) \leq c_t \mathbb{E}R(\bar{f}_{\frac{1}{\gamma t}}).$$

with $c_t = 4 \left(1 + \frac{1}{t-1}\right)^2 \leq 16$.

⁹The set of solutions corresponding to regularization parameters in a discrete set $\Lambda \subset \mathbb{R}$.

The above theorem follows as a corollary of our main result given in Theorem 6 and recovers results essentially given in [Raskutti et al., 2014]. Combining the above result with Theorem 3, and setting $t^* = \frac{1}{\gamma\lambda^*} = \frac{\text{SNR}}{\gamma}$, we have that

$$\mathbb{E}R(\check{f}_{\gamma,t^*}) \approx \mathbb{E}R(\bar{f}_{\lambda^*}) \leq \mathbb{E}R(f_{\text{ols}}).$$

The statistical accuracy of early stopping is essentially the same as KRLS and can be vastly better than a naïve ERM approach. Note that the cost of computing the best possible solution with early stopping is $O(n^2t^*) = O(n^2\text{SNR})$. Thus, the computational time of early stopping is proportional to the signal to noise ratio. Hence, it could be much better than KRLS for noisy problems, that is when SNR is small. The main bottle neck of early stopping regularization is that it has the same space requirements of KRLS. Subsampling approaches have been proposed to tackle this issue.

Subsampling and Regularization Recall that the solution of the standard KRLS problem belongs to \mathcal{H}_n , as in (4.5). We know from Subsection 4.2.2 that the basic idea of Nyström KRLS (NKRLS) is to restrict Problem (4.18) to a subspace $\mathcal{H}_m \subseteq \mathcal{H}_n$ defined as

$$\mathcal{H}_m = \left\{ \sum_{i=1}^m c_i K(\cdot, \tilde{x}_i) \mid c_1, \dots, c_m \in \mathbb{R} \right\}, \quad (4.22)$$

where $M = \{\tilde{x}_1, \dots, \tilde{x}_m\}$ is a subset of the training set and $m \leq n$. It is easy to see that the corresponding solution is given by

$$\tilde{f}_{m,\lambda}(x) = \sum_{i=1}^m (\tilde{\alpha}_{m,\lambda})_i K(x, \tilde{x}_i), \quad (4.23)$$

$$\tilde{\alpha}_{m,\lambda} = (K_{nm}^\top K_{nm} + \lambda n K_{mm})^\dagger K_{nm}^\top Y, \quad (4.24)$$

for all $x \in \mathcal{X}$, where $(\cdot)^\dagger$ is the pseudoinverse, $\lambda > 0$, $K_{nm} \in \mathbb{R}^{n \times m}$ with $(K_{nm})_{ij} = K(x_i, \tilde{x}_j)$ and $K_{mm} \in \mathbb{R}^{m \times m}$ with $(K_{mm})_{i,j} = K(\tilde{x}_i, \tilde{x}_j)$. A more efficient formulation can also be derived. Indeed, we rewrite Problem (4.18), restricted to \mathcal{H}_m , as

$$\tilde{\alpha}_{m,\lambda} = \arg \min_{\alpha \in \mathbb{R}^m} \|K_{nm}\alpha - Y\|^2 + \lambda \alpha^\top K_{mm} \alpha \quad (4.25)$$

$$= R \arg \min_{\beta \in \mathbb{R}^k} \|K_{nm}R\beta - Y\|^2 + \lambda \|\beta\|^2, \quad (4.26)$$

where in the last step we performed the change of variable $\alpha = R\beta$ where $R \in \mathbb{R}^{m \times k}$ is a matrix such that $RR^\top = K_{mm}^\dagger$ and k is the rank of K_{mm} . Then, we can obtain the following closed form expression,

$$\tilde{\alpha}_{m,\lambda} = R(A^\top A + \lambda n I_n)^{-1} A^\top Y. \quad (4.27)$$

(see Proposition 2 in Section A of the appendix of [Camoriano et al., 2016a] for a complete proof). This last formulation is convenient because it is possible to compute R by $R = ST^{-1}$ where $K_{mm} = SD$ is the economic QR decomposition of K_{mm} , with $S \in \mathbb{R}^{m \times k}$ such that $S^\top S = I_k$, $D \in \mathbb{R}^{k \times m}$ an upper triangular matrix and $T \in \mathbb{R}^{k \times k}$ an invertible triangular matrix that is the Cholesky decomposition of $S^\top K_{mm} S$. Assuming $k \approx m$, the complexity of NKRLS is then $O(nm)$ in space and $O(nm^2 + m^3|\Lambda|)$ in time. The following known result establishes the statistical accuracy of the solution obtained by suitably choosing the points in M .

Theorem 5 (Theorem 1 of [Bach, 2013]). *Let $m \leq n$ and $M = \{\tilde{x}_1, \dots, \tilde{x}_m\}$ be a subset of the training set uniformly chosen at random. Let $\tilde{f}_{m,\lambda}$ be as in (4.23) and \bar{f}_λ as in (4.19) for any $\lambda > 0$. Let $\delta \in (0, 1)$, when*

$$m \geq \left(\frac{32\tilde{d}(\lambda)}{\delta} + 2 \right) \log \frac{\|K_n\| n}{\delta\lambda}$$

with $\tilde{d}(\lambda) = n \sup_{1 \leq i \leq n} (K_n(K_n + \lambda n I_n)^{-1})_{ii}$, then the following holds

$$\mathbb{E}_M \mathbb{E} R(\tilde{f}_{m,\lambda}) \leq (1 + 4\delta) \mathbb{E} R(\bar{f}_\lambda).$$

The above result shows that the space/time complexity of NKRLS can be adaptive to the statistical properties of the data while preserving the same statistical accuracy of KRLS. Indeed, using Theorem 3, we have that

$$\mathbb{E}_M \mathbb{E} R(\tilde{f}_{m,\lambda^*}) \approx \mathbb{E} R(\bar{f}_{\lambda^*}) \leq \mathbb{E} R(f_{\text{ols}}),$$

requiring $O(n\tilde{d}(\lambda^*) \log \frac{n}{\lambda^*})$ memory and $O(n\tilde{d}(\lambda^*)^2 (\log \frac{n}{\lambda^*})^2)$ time. Hence, NKRLS is more efficient with respect to KRLS when $\tilde{d}(\lambda^*)$ is smaller than $\frac{n}{\log \frac{n}{\lambda^*}}$, that is when the problem is mildly complex.

Given the above discussion, it is natural to ask whether subsampling and early stopping ideas can be fruitfully combined. Providing a positive answer to this question is the main contribution of this section, and we discuss it next.

4.3.3 Proposed Algorithm and Main Results

We begin by describing the proposed algorithm incorporating the Nyström approach described above in iterative regularization by early stopping. The intuition is that the algorithm thus obtained could have memory and time complexity adapted to the statistical accuracy allowed by the data, while automatically computing the whole regularization path. Indeed, this intuition is then confirmed through a statistical analysis of the corresponding excess risk. Our result indicates in which regimes KRLS, NKRLS, Early Stopping and NYTRO are preferable.

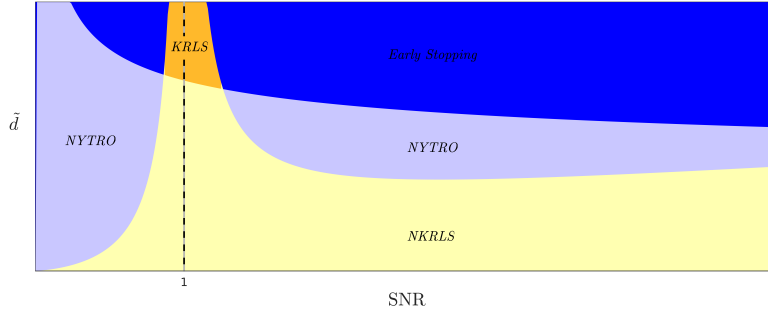


Figure 4.3: The graph represents the family of learning problems parametrized by the dimensionality \tilde{d} and the signal-to-noise ratio SNR (see (4.16), (4.17)). The four different regions represent the regimes where some algorithm is faster than the others. Purple: NYTRO is faster, Blue: Early Stopping is faster, Orange: KRLS is faster, Yellow: NKRLS is faster – see Section 4.3.3.

The Algorithm

NYTRO is obtained considering a finite number of iterations of the gradient descent minimization of the empirical risk in Problem (4.14) over the space in (4.22). The algorithm thus obtained is given by,

$$\hat{f}_{m,\gamma,t}(x) = \sum_{i=1}^m (\hat{\alpha}_{m,\gamma,t})_i K(\tilde{x}_i, x), \quad (4.28)$$

$$\hat{\beta}_{m,\gamma,t} = \hat{\beta}_{m,\gamma,t-1} - \frac{\gamma}{n} R^\top (K_{nm}^\top (K_{nm} \hat{\beta}_{m,\gamma,t-1} - Y)), \quad (4.29)$$

$$\hat{\alpha}_{m,\gamma,t} = R \hat{\beta}_{m,\gamma,t}, \quad (4.30)$$

for all $x \in \mathcal{X}$, where $\gamma = 1/(\sup_{1 \leq i \leq n} K(x_i, x_i))$ and $\hat{\beta}_{m,0} = 0$. Considering that the cost of computing R is $O(m^3)$, the total cost for the above algorithm is $O(nm)$ in memory and $O(nmt + m^3)$ in time.

In the previous section, we have seen that NKRLS has an accuracy comparable to the one of the standard KRLS under a suitable choice of m . We next show that, under the same conditions, the accuracy of NYTRO is comparable with the ones of KRLS and NKRLS, for suitable choices of t and m .

Error Analysis

We next establish excess risk bounds for NYTRO by providing a direct comparison with NKRLS and KRLS.

Theorem 6 (NYTRO and NKRLS). *Let $m \leq n$ and M be a subset of the training set. Let $\hat{f}_{m,\gamma,t}$ be the NYTRO solution as in (4.28), $\tilde{f}_{m,\frac{1}{\gamma t}}$ the NKRLS solution as in (4.23). When $t \geq 2$ and $\gamma < \|K_{nm}R\|^2$ (for example $\gamma = 1/\max_i K(x_i, x_i)$) the following holds*

$$\mathbb{E}R\left(\hat{f}_{m,\gamma,t}\right) \leq c_t \mathbb{E}R\left(\tilde{f}_{m,\frac{1}{\gamma t}}\right).$$

with $c_t = 4\left(1 + \frac{1}{t-1}\right)^2 \leq 16$.

Note that the above result holds for any $m \leq n$ and any selection strategy of the Nyström subset M . The proof of Theorem 6 is different from the one of Theorem 5 and is based only on geometric properties of the estimator and tools from spectral theory and inverse problems see [Engl et al., 1996]. In the next corollary we compare NYTRO and KRLS, by combining Theorems 5 and 6, hence considering M to be chosen uniformly at random from the training set.

Corollary 1. *Let $t \geq 2$, $\gamma = 1/\|K_n\|$, $\delta \in (0, 1)$ and m be chosen as*

$$m \geq \left(32 \frac{\tilde{d}(1/(\gamma t))}{\delta} + 2\right) \log \frac{n \|K_n\| \gamma t}{\delta}.$$

Let $\bar{f}_{\frac{1}{\gamma t}}$ be the KRLS solution as in (4.19) and $\hat{f}_{m,\gamma,t}$ be the NYTRO solution. When the subset M is chosen uniformly at random from the training set, the following holds

$$\mathbb{E}_M \mathbb{E}R\left(\hat{f}_{m,\gamma,t}\right) \leq c_{t,\delta} \mathbb{E}R\left(\bar{f}_{\frac{1}{\gamma t}}\right)$$

where $c_{t,\delta} = 4\left(1 + \frac{1}{t-1}\right)^2 (1 + 4\delta) \leq 80$.

The above result shows that NYTRO can achieve essentially the same results as KRLS. In the following we compare NYTRO to the other regularization algorithms introduced so far, by discussing how their computational complexity adapts to the statical accuracy in the data. In particular, by parametrizing the learning problems with respect to their dimension and their signal-to-noise ratio, we characterize the regions of the problem space where one algorithm is more efficient than the others.

Discussion

In Subsection 4.3.2 we have compared the expected excess risk of different regularization algorithms. More precisely, we have seen that there exists a suitable choice of λ that is $\lambda^* = \frac{1}{\text{SNR}}$, where SNR is the signal-to-noise ratio associated to the learning problem, such that the expected risk of KRLS is smaller than the one of KOLS, and indeed potentially much smaller. For

this reason, in the other result, statistical accuracy of the other methods was directly compared to that of KRLS with $\lambda = \lambda^*$.

We exploit these results to analyze the complexity of the algorithms with respect to the statistical accuracy allowed by the data. If we choose $m \approx \tilde{d}(\lambda^*) \log(n/\lambda^*)$ and $t = \frac{1}{\gamma\lambda^*}$, then combining Theorem 3 with Corollary 1 and with Theorem 5, respectively, we see that the expected excess risk of both NYTRO and NKRLS is in the same order of the one of KRLS. Both algorithms have a memory requirement of $O(nm)$ (compared to $O(n^2)$ for KRLS), but they differ in their time requirement. For NYTRO we have $O(n \frac{\tilde{d}(\lambda^*)}{\lambda^*} \log \frac{n}{\lambda^*})$, while for NKRLS it is $O(n\tilde{d}(\lambda^*)^2 (\log \frac{n}{\lambda^*})^2)$. Now note that $\tilde{d}(\lambda^*)$ by definition is bounded by

$$d_{\text{eff}}(\lambda) \leq \tilde{d}(\lambda) \leq \frac{1}{\lambda}, \quad \forall \lambda > 0,$$

thus, by comparing the two computational times, two regimes can be identified,

$$\begin{cases} d_{\text{eff}}(\lambda^*) \leq \tilde{d}(\lambda^*) \leq \frac{1}{\lambda^* \log \frac{n}{\lambda^*}} & \implies \text{NKRLS faster} \\ \frac{1}{\lambda^* \log \frac{n}{\lambda^*}} \leq \tilde{d}(\lambda^*) \leq \frac{1}{\lambda^*} & \implies \text{NYTRO faster} \end{cases}$$

To illustrate the regimes in which different algorithms can be preferable from a computational point of view while achieving the same error as KRLS with λ^* (see Figure 4.3), it is useful to parametrize the family of learning problems with respect to the signal-to-noise ratio defined in (4.17) and to the dimensionality of the problem $\tilde{d} := \tilde{d}(\lambda^*)$ defined in (4.16). We choose \tilde{d} as a measure of dimensionality with respect to d_{eff} , because \tilde{d} directly affects the computational properties of the analyzed algorithms. In Figure 4.3, the parameter space describing the learning problems is partitioned in regions given by the curve

$$c_1(\text{SNR}) = \frac{n}{|\log(n\text{SNR})|},$$

that separates the subsampling methods from the standard methods and

$$c_2(\text{SNR}) = \frac{\text{SNR}}{|\log(\text{SNR})|},$$

that separates the iterative from Tikhonov methods.

As illustrated in Figure 4.3, NYTRO is preferable when $\text{SNR} \leq 1$, that is when the problem is quite noisy. When $\text{SNR} > 1$, then NYTRO is faster when the dimension of the problem is sufficiently large. Note that, in particular, the area of the NYTRO region on $\text{SNR} > 1$ increases with n , and the curve c_1 is quite flat when n is very large. On the opposite extremes

Table 4.2: Specifications of the datasets used in time-accuracy comparison experiments. σ is the bandwidth of the Gaussian kernel.

Dataset	n	n_{test}	d	σ
InsuranceCompany	5822	4000	85	3
Adult	32562	16282	123	6.6
Ijcnn	49990	91701	22	1
YearPrediction	463715	51630	90	1
CoverttypeBinary	522910	58102	54	1

Table 4.3: Time-accuracy comparison on benchmark datasets.

Dataset		KOLS	KRLS	Early Stopping	NKRLS	NYTRO
InsuranceCompany $n = 5822$ $m = 2000$	Time (s)	1.04	97.48 \pm 0.77	2.92 \pm 0.04	20.32 \pm 0.50	5.49 \pm 0.12
	RMSE	5.179	0.4651 \pm 0.0001	0.4650 \pm 0.0002	0.4651 \pm 0.0003	0.4651 \pm 0.0003
	Par.	NA	3.27e-04	494 \pm 1.7	5.14e-04 \pm 1.42e-04	491 \pm 3
Adult $n = 32562$ $m = 1000$	Time (s)	112	4360 \pm 9.29	5.52 \pm 0.23	5.95 \pm 0.31	0.85 \pm 0.05
	RMSE	1765	0.645 \pm 0.001	0.685 \pm 0.002	0.6462 \pm 0.003	0.6873 \pm 0.003
	Par.	NA	4.04e-05 \pm 1.04e-05	39.2 \pm 1.1	4.04e-05 \pm 1.83e-05	44.9 \pm 0.3
Ijcnn $n = 49990$ $m = 5000$	Time (s)	271	825.01 \pm 6.81	154.82 \pm 1.24	160.28 \pm 1.54	80.9 \pm 0.4
	RMSE	730.62	0.615 \pm 0.002	0.457 \pm 0.001	0.469 \pm 0.003	0.457 \pm 0.001
	Par.	NA	1.07e-08 \pm 1.47e-08	489 \pm 7.2	1.07e-07 \pm 1.15e-07	328.7 \pm 2.6
YearPrediction $n = 463715$ $m = 10000$	Time (s)				1188.47 \pm 36.7	887 \pm 6
	RMSE	NA	NA	NA	0.1015 \pm 0.0002	0.1149 \pm 0.0002
	Par.				3.05e-07 \pm 1.05e-07	481 \pm 6.1
CoverttypeBinary $n = 522910$ $m = 10000$	Time (s)				1235.21 \pm 42.1	92.69 \pm 2.35
	RMSE	NA	NA	NA	1.204 \pm 0.008	0.918 \pm 0.006
	Par.				9.33e-09 \pm 1.12e-09	39.2 \pm 2.3

we have early stopping and NKRLS. Indeed, one is effective when the dimensionality is very large, while the second when it is very small. There is a peak around $\text{SNR} \approx 1$ for which it seems that the only useful algorithm is NKRLS when the dimensionality is sufficiently large. The only region where KRLS is more effective is when $\text{SNR} \approx 1$ and the dimensionality is close to n .

In the next subsection, the theoretical results are validated by an experimental analysis on benchmark datasets. We add one remark first.

Remark 3 (Empirical parameter choices and regularization path). *Note that an important aspect that is not covered by Figure 4.3 is that iterative algorithms have the further desirable property of computing the regularization path. In fact, for KRLS and NKRLS computations are slowed by a factor of $|\Lambda|$, where Λ is the discrete set of cross-validated λ s. This last aspect is very relevant in practice, because the optimal regularization parameter values are not known and need to be found via model selection/aggregation.*

4.3.4 Experiments

In this subsection we present an empirical evaluation of the NYTRO algorithm, showing regimes in which it provides a significant model selection speedup with respect to NKRLS and the other exact kernelized learning algorithms mentioned above (KOLS, KRLS and Early Stopping). We consider the Gaussian kernel and the subsampling of the training set points for kernel matrix approximation is performed uniformly at random. All experiments have been carried out on a server with $12 \times 2.10\text{GHz}$ Intel[®] Xeon[®] E5-2620 v2 CPUs and 132 GB of RAM.

We compare the algorithms on the benchmark datasets reported in Table 4.2¹⁰. In the table we also report the bandwidth parameter σ adopted for the Gaussian kernel computation. Following [Si et al., 2014], we measure performance by the root mean squared error (RMSE).

For the YearPredictionMSD dataset, outputs are scaled in $[0, 1]$.

For all the algorithms, model selection is performed via hold-out cross validation, where the validation set is composed of 20% of the training points chosen uniformly at random at each trial. We select the regularization parameter λ for NKRLS between 100 guesses logarithmically spaced in $[10^{-15}, 1]$, by computing the validation error for each model and choosing the λ^* associated with the lowest error. m is fixed for each learning task. NYTRO’s regularization parameter is the number of iterations t . We select the optimal t^* by considering the evolution of the validation error. As an early stopping rule, we choose an iteration such that the validation error ceases to be decreasing up to a given threshold chosen to be the 5% of the relative RMSE. After model selection, we evaluate the performance on the test set. We report the results in Table 4.3 and discuss them further below.

Time Complexity Comparison We start by showing how the time complexity changes with the subsampling level m , making NYTRO more convenient than NKRLS if m is large enough. For example, consider Figure 4.4. We performed training on the `cpuSmall`¹¹ dataset ($n = 6554$, $d = 12$), with m spanning between 100 and 4000 at 100-points linear intervals. The experiment is repeated 5 times, and we report the mean and standard deviation of the NYTRO and NKRLS model selection times. We consider 100 guesses for λ , while the NYTRO iterations are fixed to a maximum of 500. As revealed by the plot, the time complexity grows linearly with m for NYTRO and quadratically for NKRLS. This is consistent with the time complexities outlined in Sections 4.3.2 and 4.3.3 ($O(nm^2 + m^3)$ for NKRLS and $O(nmt + m^3)$ for NYTRO).

¹⁰All the datasets are available at <http://archive.ics.uci.edu/ml> or <https://www.csie.ntu.edu.tw/~cjlin/libsvmtools/datasets/>

¹¹<http://www.cs.toronto.edu/~delve/data/datasets.html>

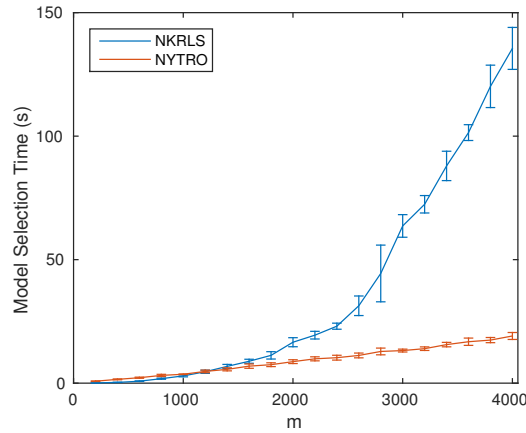


Figure 4.4: Training time of NKRLS and NYTRO on the `cpuSmall` dataset as the subsampling level m varies linearly between 100 and 4000. Experiment with 5 repetitions. mean and standard deviation reported.

Time-accuracy Benchmarking We also compared the training time and accuracy performances for KRLS, KOLS, Early Stopping (ES), NKRLS and NYTRO, reporting the selected hyperparameter (λ^* for KRLS and NKRLS, t^* for ES and NYTRO), the model selection time and the test error in Table 4.3. All the experiments are repeated 5 times. The standard deviation of the results is negligible. Notably, NYTRO achieves comparable or superior predictive performances with respect to its counterparts in a fraction of the model selection time. In particular, the absolute time gains are most evident on large-scale datasets such as `Covertypes` and `YearPredictionMSD`, for which a reduction of an order of magnitude in cross-validation time corresponds to saving tens of minutes. Note that exact methods such as KOLS, KRLS and ES cannot be applied to such large scale datasets due to their prohibitive memory requirements. Remarkably, NYTRO’s predictive performance is not significantly penalized in these regimes and can even be improved with respect to other methods, as in the `Covertypes` case, where it requires 90% less time for model selection.

Chapter 5

Speeding up by Data-independent Subsampling

5.1 Setting

As we have seen in Chapter 1, a basic problem in machine learning is estimating a function from random noisy data [Vapnik, 1998; Cucker and Smale, 2002]. The function to be learned is typically fixed, but unknown, and flexible nonlinear/nonparametric models are needed for good results. A general class of models is based on functions of the form,

$$\hat{f}(x) = \sum_{i=1}^m \alpha_i q(x, \omega_i), \quad (5.1)$$

where q is a nonlinear function, $\omega_1, \dots, \omega_m \in \mathbb{R}^d$ are the *centers*, $\alpha_1, \dots, \alpha_m \in \mathbb{R}$ are the coefficients, and $m = m_n$ could/should *grow* with the number of data points n . In this context, the problem of learning reduces to the problem of computing from data the parameters $\omega_1, \dots, \omega_m, \alpha_1, \dots, \alpha_m$ and m . Among others, one-hidden layer networks [Bishop, 2006], or RBF networks [Poggio and Girosi, 1990], are examples of classical approaches considering these models. Here, parameters are computed by considering a non-convex optimization problem, typically hard to solve and study [Pinkus, 1999]. Kernel methods, introduced in Chapter 2, are another notable example [Schölkopf and Smola, 2002]. In this case, q is assumed to be a positive definite function [Aronszajn, 1950] (the kernel function) and it is shown that choosing the centers to be the input points, hence $m = n$, suffices for optimal statistical results [Kimeldorf and Wahba, 1970; Schölkopf et al., 2001; Caponnetto and De Vito, 2007]. In kernel methods, computations reduce to finding the coefficients α_i , which can be typically done by convex

optimization. While theoretically sound and remarkably effective in small and medium size problems, memory requirements make kernel methods rapidly become unfeasible as datasets grow large. A current challenge is then to design scalable non-parametric procedures, while not giving up the nice theoretical properties of kernel methods.

A simple, yet effective, idea is that of sampling the centers at random, either in a data-dependent or in a data-independent way. Notable examples of this idea include Nyström [Smola and Schölkopf, 2000; Williams and Seeger, 2000] and random features approaches [Rahimi and Recht, 2007]. Given random centers, computations still reduce to convex optimization with potential big memory gains, if centers are fewer than data-points. In practice, the choice of the number of centers is based on heuristics or memory constraints and the question arises of characterizing theoretically which choices provide optimal learning bounds. For data-dependent subsampling, a.k.a. Nyström methods, some results in the fixed design setting were given in [Cortes et al., 2010; Bach, 2013; Alaoui and Mahoney, 2014], while in the context of statistical learning a fairly exhaustive analysis was recently provided in [Rudi et al., 2015], as we will see in Chapter 4. These latter results show, in the statistical learning theory framework, that a number of centers smaller than the number of data points suffices for optimal generalization properties.

The results on data-independent subsampling, a.k.a. random features, are fewer and require a number of centers in the order of n to attain basic generalization bounds [Rahimi and Recht, 2009; Cortes et al., 2010; Bach, 2015]. The study presented in this Chapter, based on [Rudi et al., 2016], improves on these results by

1. Deriving optimal learning bounds for regularized learning with random features.
2. Proving that the optimal bounds are achievable with a number of random features substantially smaller than the number of examples.

Following [Rudi et al., 2015], we further show that the number of random features/centers can be seen as a form of “computational” regularization, controlling at the same time statistical and computational aspects. Theoretical findings are complemented by numerical experiments, validating the bounds and showing the regularization properties of random features. The rest of the paper is organized as follows. In Section 5.2, we review relevant results on learning with kernels and least squares. In Section 5.3, we introduce regularized learning with random features. In Section 5.3.1, we present and discuss our main results, while proofs are deferred to the appendix. Finally, numerical experiments are presented in Section 5.4.

Notation. For the sake of readability, we denote by $f(n) \lesssim g(n)$ the condition $f(n) \leq cg(n)(\log n)^s$ for any $n \in \mathbb{N}$ and $c > 0$, $s \geq 0$, for two

functions $f, g : \mathbb{N} \rightarrow \mathbb{R}$. We denote by $f(n) \approx g(n)$ the condition $f(n) \lesssim g(n)$ and $g(n) \lesssim f(n)$. The symbol \gtrsim is defined accordingly.

5.2 Background: Generalization Properties of KRLS

A main motivation of this chapter is showing how random features improve the computations of kernel methods, while retaining their good statistical properties. Recalling these latter results provide the background of the chapter. The computational aspects of Kernel Regularized Least Squares (KRLS) were already introduced in Section 2.4. Thus, to derive learning bounds we only need to first recall KRLS's generalization properties in this Section.

Let \mathcal{X} be a probability space and ρ a probability distribution on $\mathcal{X} \times \mathbb{R}$. For all $x \in \mathcal{X}$, denote by $\rho(y|x)$ the conditional probability of ρ , given x . We make basic assumptions on the probability distribution and the kernel [De Vito et al., 2005a; Caponnetto and De Vito, 2007].

Assumption 5. *There exists $f_\rho(x) = \int y d\rho(y|x)$ such that $\int |f_\rho(x)|^2 d\rho < \infty$. For $M, \sigma > 0$,*

$$\int |y - f_\rho(x)|^p d\rho(y|x) \leq \frac{1}{2} p! M^{p-2} \sigma^2, \quad \forall p \geq 2, \quad (5.2)$$

holds almost surely. The data $(x_1, y_1), \dots, (x_n, y_n)$ are independently and identically distributed according to ρ .

Note that (5.2) is satisfied when the random variable $|y - f_\rho(x)|$, with y distributed according to $\rho(y|x)$, is uniformly bounded, subgaussian or subexponential for any $x \in \mathcal{X}$.

Assumption 6. *K is measurable, bounded by κ^2 , $\kappa \geq 1$ and the associated RKHS \mathcal{H} is separable.*

We need one further assumption to control the approximation (bias) and the estimation (variance) properties of KRLS. Let $L^2(\mathcal{X}, \rho) = \{f : \mathcal{X} \rightarrow \mathbb{R} : \|f\|_\rho^2 = \int |f(x)|^2 d\rho < \infty\}$ be the space of square integrable functions on \mathcal{X} , and define the integral operator $L : L^2(\mathcal{X}, \rho) \rightarrow L^2(\mathcal{X}, \rho)$,

$$Lf(x) = \int K(x, x') f(x') d\rho, \quad \forall f \in L^2(\mathcal{X}, \rho),$$

almost everywhere. The operator L is known to be symmetric, positive definite and trace class under Assumption 6 [De Vito et al., 2005b]. We make the following common assumption [Caponnetto and De Vito, 2007; Steinwart et al., 2009].

Assumption 7 (Source & Capacity Conditions). *There exist $r \geq 1/2$ and $R \in [1, \infty)$ such that*

$$\|L^{-r} f_\rho\|_\rho \leq R. \quad (5.3)$$

Moreover, for $\lambda > 0$ let $\mathcal{N}(\lambda) = \text{Tr}((L + \lambda I)^{-1} L)$, then there exist $\gamma \in (0, 1]$ and $Q > 0$ such that

$$\mathcal{N}(\lambda) \leq Q^2 \lambda^{-\gamma}. \quad (5.4)$$

We add some comments. The *Mercer* source condition (5.3) is better illustrated recalling that, according to Mercer theorem [Cucker and Smale, 2002], functions in \mathcal{H} are functions $f \in L^2(\mathcal{X}, \rho)$ such that $f = L^{1/2}g$ for some $g \in L^2(\mathcal{X}, \rho)$. Note that, under Assumption 5, we only have $f_\rho \in L^2(\mathcal{X}, \rho)$. Then, by 5.3, for $r = 1/2$ we are assuming f_ρ to belong to \mathcal{H} , while for larger r we are strengthening this condition assuming f_ρ to belong to smaller subspaces of \mathcal{H} . This condition is known to control the bias of KRLS [Caponnetto and De Vito, 2007; Steinwart et al., 2009].

The assumption in (5.4) is a natural capacity condition on the space \mathcal{H} . If \mathcal{H} is finite dimensional, then $\mathcal{N}(\lambda) \leq \dim(\mathcal{H})$, for all $\lambda \geq 0$. More generally, it can be seen as an assumption on the “effective” dimension at scale λ [Caponnetto and De Vito, 2007]. It is always true in the limit case $Q = \kappa$, $\gamma = 1$, sometimes referred to as the capacity independent setting [Cucker and Zhou, 2007]. However, when $\gamma < 1$ faster learning bounds can be achieved. Assumption 7 corresponds to a “polynomial” rates regime that can be specialized common smoothness classes in non-parametric statistics, such as Sobolev spaces [Steinwart and Christmann, 2008]. Other regimes, e.g. exponential decays or finite dimensional cases [Zhang et al., 2013], can also be derived with minor modifications. This discussion is omitted.

Before giving the generalization bounds for KRLS, we introduce the *generalization error* of an estimator $f \in L^2(\mathcal{X}, \rho_{\mathcal{X}})$, that will be useful in the rest of the paper and is measured by the excess risk [Cucker and Smale, 2002; Steinwart and Christmann, 2008]

$$\mathcal{E}(f) - \mathcal{E}(f_\rho), \quad \text{with} \quad \mathcal{E}(f) = \int (y - f(x))^2 d\rho(x, y). \quad (5.5)$$

The following theorem is the generalization bound for KRLS and is taken from [Caponnetto and De Vito, 2007], see also [Smale and Zhou, 2007; Steinwart et al., 2009].

Theorem 7. *Let $\tau \geq 0$. Under Assumptions 5, 6, 7, if $\lambda_n \approx n^{-\frac{1}{2r+\gamma}}$ and $\widehat{f}_n = \widehat{f}_{\lambda_n}$ of (2.6), then the following holds with probability at least $1 - e^{-\tau}$*

$$\mathcal{E}(\widehat{f}_n) - \mathcal{E}(f_\rho) \lesssim \tau^2 n^{-\frac{2v}{2v+\gamma}}, \quad v = \min\{r, 1\}.$$

The above result can be shown to be optimal, i.e. matching a corresponding lower bound [Caponnetto and De Vito, 2007; Steinwart et al., 2009].

Theorem 8. For any measurable estimator \hat{f}_n depending on n training examples, there exists a probability measure ρ , satisfying Assumptions 5, 6, 7, such that

$$\mathbb{E} \mathcal{E}(\hat{f}_n) - \mathcal{E}(f_\rho) \gtrsim n^{-\frac{2r}{2r+\gamma}}.$$

Beyond KRLS. Summarizing, the generalization properties of KRLS are optimal, since the upper bound of Thm. 7 matches the lower bound in Thm. 8. However, for KRLS, optimal statistical properties come at the cost of high computational complexity. As seen from (2.6), KRLS requires $O(n^2)$ in space, to store the matrix $K_{n,n}$, and roughly $O(n^3)$ in time, to solve a corresponding linear system. While the time complexity can be reduced without hindering generalization, by considering *iterative & online techniques* [Engl et al., 1996; Bauer et al., 2007; Caponnetto and Yao, 2010; Blanchard and Krämer, 2010], in general lowering the space requirements is a challenge. The question is, then, if it is possible to design a form of computational regularization controlling at once generalization, time *and space* requirements. Indeed, this can be done considering random features, as we show next.

5.3 Regularized Learning with Random Features

Following the discussion in the introduction, the idea is to consider a general non-linear function in (5.1), but now taking the centers at random according to a known probability distribution [Rahimi and Recht, 2007]. More precisely, let (Ω, θ) be a known probability space and $\psi : \Omega \times \mathcal{X} \rightarrow \mathbb{R}$. Given $\omega_1, \dots, \omega_m$ independently and identically distributed according to θ , the idea is to consider functions in the linear span of the set of *random features*

$$\left\{ \frac{1}{\sqrt{m}} \psi(\omega_1, \cdot), \dots, \frac{1}{\sqrt{m}} \psi(\omega_m, \cdot) \right\}.$$

In particular, given a dataset, we consider the estimator defined by,

$$\tilde{f}_{m,\lambda}(x) = \sum_{j=1}^m \frac{1}{\sqrt{m}} \psi(\omega_j, x) \tilde{\alpha}_j, \quad \tilde{\alpha}_{m,\lambda} = \left(\tilde{S}_n^\top \tilde{S}_n + \lambda I \right)^{-1} \tilde{S}_n^\top \hat{y}, \quad \forall x \in \mathcal{X}, \quad (5.6)$$

where $(\tilde{\alpha}_1, \dots, \tilde{\alpha}_m) = \tilde{\alpha}_{m,\lambda}$, $\hat{y} = \bar{y}/\sqrt{n}$, and $\tilde{S}_n \in \mathbb{R}^{n \times m}$ with entries $(\tilde{S}_n)_{i,j} = \psi(\omega_j, x_i)/\sqrt{nm}$. Some observations are in order. First, note that the above estimator is exactly of the form discussed in the introduction (see (5.1)), where the non-linear function is now denoted by ψ and the centers can belong to an abstract probability space (see e.g. Example 1 or Appendix F of [Rudi et al., 2016]). Second, it is easy to see that the above estimator follows from the minimization problem,

$$\min_{\alpha \in \mathbb{R}^m} \frac{1}{n} \sum_{i=1}^n \left(\sum_{j=1}^m \frac{1}{\sqrt{m}} \psi(\omega_j, x_i) \alpha_j - y_i \right)^2 + \lambda \|\alpha\|_m^2, \quad (5.7)$$

where $\|\cdot\|_m$ is the Euclidean norm in \mathbb{R}^m (so we will refer to it as the RF-KRLS estimator). Finally, by comparing (2.6) and (5.6), it is clear that if m is smaller than n , then the time/space requirements of the above approach can be much smaller than those of KRLS. Indeed, computing (5.6) requires $O(mn)$ in space and roughly $O(nm^2 + m^3)$ in time. The question is then if the potential computational gain comes at the expense of generalization properties. While the above approach is general, to answer this latter question random features will be related to kernels.

Assumptions on random features. We first need a basic assumption on the random features.

Assumption 8. ψ is measurable and there exists $\tilde{\kappa} \geq 1$ such that $|\psi(\omega, x)| \leq \tilde{\kappa}$ almost surely.

Under Assumption 8 the integral below exists and defines the kernel induced by ψ ,

$$K(x, x') = \int_{\Omega} \psi(\omega, x)\psi(\omega, x')d\theta(\omega), \quad \forall x, x' \in \mathcal{X}. \quad (5.8)$$

Indeed it is easy to see that K is a positive definite function, measurable and bounded almost surely. We still need a minor assumption.

Assumption 9. The RKHS \mathcal{H} associated to the kernel in (5.8) is separable.

Note that, Assumptions 8, 9 are mild and satisfied by essentially all examples of random features (see Appendix F of [Rudi et al., 2016]).

Example 1 (Gaussian random features [Rahimi and Recht, 2007]). When $\mathcal{X} = \mathbb{R}^d$, $d \in \mathbb{N}$, by setting $\Omega = \mathbb{R}^d \times \mathbb{R}$ and $\psi(\omega, x) = \cos(\beta^\top x + b)$, with $\omega = (\beta, b) \in \Omega$, then there exists a probability distribution on Ω , such that (5.8) holds for the Gaussian kernel $K(x, x') = e^{-\gamma\|x-x'\|^2}$, $x, x' \in \mathbb{R}^d$. Then, random features are continuous, hence measurable, and bounded. Moreover, the RKHS associated to the Gaussian kernel is separable [Steinwart and Christmann, 2008].

In general, the space Ω and its distribution θ need not to be related to the data space and distribution. However, we will see in the following that better results can be obtained if they are *compatible* in a sense made precise by the next assumption [Bach, 2015].

Assumption 10 (Random Features Compatibility). For $\lambda > 0$, let

$$\mathcal{F}_\infty(\lambda) = \operatorname{ess\,sup}_{\omega \in \Omega} \left\| (L + \lambda I)^{-1/2} \psi(\omega, \cdot) \right\|_\rho^2, \quad (5.9)$$

then there exists $\alpha \in (0, 1]$ and $F \geq \tilde{\kappa}$ such that,

$$\mathcal{F}_\infty(\lambda) \leq F^2 \lambda^{-\alpha}, \quad \forall \lambda > 0. \quad (5.10)$$

Note that the condition above is always satisfied when $\alpha = 1$ and $F = \tilde{\kappa}$. However, when $\alpha < 1$, the assumption leads to better results in terms of the number of random features required for optimal generalization (see Theorem 11). Moreover, Assumption 10 allows to extend our analysis to more refined ways of selecting the random features, as discussed in the next remark.

Remark 1 (Beyond uniform sampling for RF). *A natural question is if sampling the random features non-uniformly, allows to use less features. This approach can be cast in our setting, considering $\theta' = \theta q$ and $\psi' = \psi/\sqrt{q}$, where q is the sampling distribution. For example, when considering the data-dependent distribution proposed in [Bach, 2015], Assumption 10 is satisfied with $\alpha = \gamma$.*

5.3.1 Main Results

We next state results proving the optimal generalization properties of learning with random features. Our main results in Theorems 9, 10, 11 characterize the number of random features required by the RF-KRLS estimator in (5.6), to achieve the optimal learning bounds under different regularity conditions. In the theorem below, we analyze the generalization properties in a basic scenario, where the only requirement is that f_ρ is in \mathcal{H} .

Theorem 9. *Let $\tau > 0$. Under Assumptions 5, 8, 9, and that $f_\rho \in \mathcal{H}$, there exists $n_0 \in \mathbb{N}$ (see proof, for the explicit constant) such that, when $n \geq n_0$,*

$$\lambda_n \approx n^{-\frac{1}{2}}, \quad m_n \gtrsim \lambda_n^{-1}$$

and $\tilde{f}_n = \tilde{f}_{m_n, \lambda_n}$ as in (5.6), then the following holds with probability at least $1 - e^{-\tau}$

$$\mathcal{E}(\tilde{f}_n) - \mathcal{E}(f_\rho) \lesssim \tau^2 n^{-\frac{1}{2}}. \quad (5.11)$$

We add some comments. First, the RF-KRLS estimator in (5.6) achieves the optimal learning bound in this scenario. Indeed the condition $f_\rho \in \mathcal{H}$ is equivalent to Assumption 7 with $r = 1/2, \gamma = 1$ and so, the bound of Theorem 9 matches the ones in Theorem 7, 8. Moreover, RF-KRLS attains the optimal bound with a number of random features that is roughly

$$m_n \approx \sqrt{n}.$$

Thus, RF-KRLS generalizes optimally by requiring $O(n^{1.5})$ in space and $O(n^2)$ in time, compared to $O(n^2)$ in space and $O(n^3)$ in time for KRLS.

We next show that when the learning task satisfies additional regularity assumptions, it is possible to achieve faster learning rates than $n^{-1/2}$ (compare with Theorem 7). In particular, the next theorem shows that under Assumption 7, the RF-KRLS estimator achieves fast learning rates, again for a number of random features smaller than n .

Theorem 10. *Let $\tau > 0$ and $v = \min(r, 1)$. Under Assumptions 5, 7, 8, 9, there exists $n_0 \in \mathbb{N}$ (see proof in the Appendix E of [Rudi et al., 2016], for the explicit constant) such that when $n \geq n_0$,*

$$\lambda_n \approx n^{-\frac{1}{2v+\gamma}}, \quad m_n \gtrsim \lambda_n^{-c}, \quad \text{with } c = 1 + \gamma(2v - 1),$$

and $\tilde{f}_n = \tilde{f}_{m_n, \lambda_n}$ as in (5.6), then the following holds with probability at least $1 - e^{-\tau}$,

$$\mathcal{E}(\tilde{f}_n) - \mathcal{E}(f_\rho) \lesssim \tau^2 n^{-\frac{2v}{2v+\gamma}}.$$

Comparing Theorem 10 with Theorem 7, we see that the RF-KRLS algorithm achieves optimal learning bounds that are possibly faster than $n^{-1/2}$. In particular, when f_ρ is regular (that is r is close to 1) and the effective dimension is small (that is γ close to 0), RF-KRLS achieves a fast learning bound of n^{-1} , with a number of random features that is only $m_n \approx n^{1/2}$. However, with other combinations of r, γ , RF-KRLS may require more random features to attain the faster rates. The relation between the number of features for optimal rates and the parameters r, γ is illustrated in Figure 5.1 (top-left).

Note that in Theorem 10, the possible interaction between the feature map ψ , the feature distribution θ and the data distribution ρ is not taken into account. In the next theorem we consider this interaction, by means of the *compatibility condition* in (5.10). In particular we prove that the number or random features needed to achieve the optimal bounds may be even smaller than $n^{1/2}$ when the compatibility index α is smaller than 1.

Theorem 11. *Let $\tau > 0$ and $v = \min(r, 1)$. Under Assumptions 5, 7, 8, 9, 10, there exists $n_0 \in \mathbb{N}$ (see proof, for the explicit constant) such that when $n \geq n_0$,*

$$\lambda_n \approx n^{-\frac{1}{2v+\gamma}}, \quad m_n \gtrsim \lambda_n^{-c}, \quad \text{with } c = \alpha + (1 + \gamma - \alpha)(2v - 1),$$

and $\tilde{f}_n = \tilde{f}_{m_n, \lambda_n}$ as in (5.6), then the following holds with probability at least $1 - e^{-\tau}$

$$\mathcal{E}(\tilde{f}_n) - \mathcal{E}(f_\rho) \lesssim \tau^2 n^{-\frac{2v}{2v+\gamma}}.$$

Again, the RF-KRLS estimator achieves the optimal learning bounds, depending on the regularity conditions of the learning task. Note that the assumption in (5.10) affects only the number of random features needed to achieve the optimal bound. In particular, in the less favorable case, that is, when $\alpha = 1$, we recover exactly the results of Theorem 10, while in the favorable case when α is close to γ , a number of random features that is typically smaller than $n^{1/2}$ is required to achieve the optimal bounds. For example, even with $r = 1/2$, it is possible to achieve the fast bound of

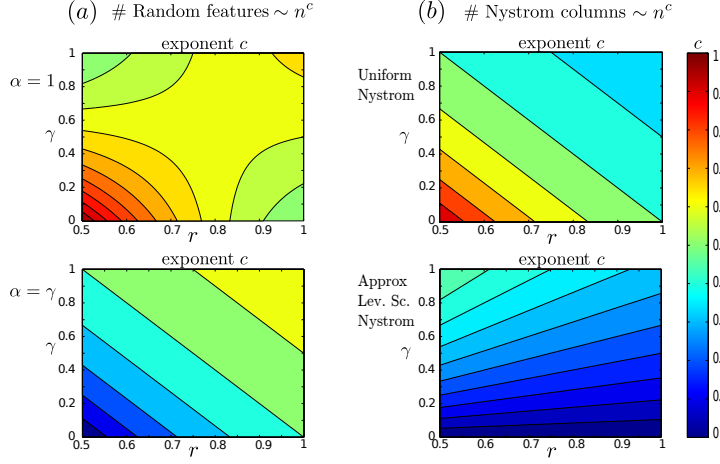


Figure 5.1: Predicted behaviour of the number of features/centers required to achieve optimal learning rates for (a) random features (see Theorem 11) and (b) Nyström (see [Rudi et al., 2015]) as a function of r, γ, α .

$n^{-1/(1+\gamma)}$, with $m_n \approx n^{-\gamma/(1+\gamma)}$. This means, a fast learning rate of $n^{-3/4}$ with $m_n \approx n^{1/4}$, when $\gamma = 1/3$, and, more surprisingly, a fast learning rate of n^{-1} with $m_n \approx 1$ when the effective dimension of the learning task is very small, that is γ close to 0. Figure 5.1 (bottom-left) is an illustration of the number of random features needed for optimal learning rates when $\alpha = \gamma$. Note that, in general this latter condition depends on the unknown data-distribution. In other words, recalling Remark 1, we see that while non-uniform sampling can in principle have a dramatic effect on the number of features required for optimal rates, how to design practical sampling schemes is an open question (see also discussion in [Bach, 2015]). Before giving a sketch of the proof, we first comment on the regularization role of m_n .

The number of random features as a regularizer. While in Theorems 9, 10, 11, the number of features m_n is typically viewed as the computational budget and generalization properties are governed by λ_n , following [Rudi et al., 2015], an interesting observation can be derived exchanging the roles of m and λ . For example, in the worst-case scenario we can set

$$m_n \approx \sqrt{n} \quad \text{and} \quad \lambda_n \approx m_n^{-1}.$$

Clearly the obtained estimator achieves the optimal error bound in (5.11), but the number of features can now be seen a regularization parameter controlling at once generalization properties and also time/space requirements. As noted in [Rudi et al., 2015], an advantage of this parameterization is that the solutions corresponding to different numbers of features

can be efficiently computed with an incremental strategy (see Appendix C). Note that, in practice, parameters are tuned by cross validation and an incremental approach allows for a fast computation of the whole regularization path, resulting in efficient model selection¹.

Sketch of the proof. Theorem 11 is the main technical contribution of the paper from which Theorems 9, 10 are derived. The extended version of Theorem 11 with explicit constants is given in Theorem 8 in the appendix of [Rudi et al., 2016]. Its proof relies on a novel error decomposition separates functional analytic results from probabilistic estimates. For the sake of conciseness, we omit to report the proofs, which can be found in the appendix of [Rudi et al., 2016]. Here we illustrate some basic ideas. From Theorem 6 of [Rudi et al., 2016] we have

$$\mathcal{E}(\tilde{f}_{m,\lambda}) - \mathcal{E}(f_\rho) \lesssim (\mathcal{S}(\lambda, n) + \mathcal{C}(\lambda, m) + R\lambda^v)^2. \quad (5.12)$$

The estimation error $\mathcal{S}(\lambda, n)$ is bounded in Lemma 7 of [Rudi et al., 2016] and depends on the noise, the regularization level and an empirical version of the effective dimension $\mathcal{N}(\lambda)$ which takes into account the random sampling of the data and of the random features. The empirical version of the effective dimension $\mathcal{N}(\lambda)$ is decomposed analytically in Proposition 8 of [Rudi et al., 2016] and bounded in terms of its continuous version in Lemma 3 of [Rudi et al., 2016]. The approximation error $R\lambda^v$ is independent of the data or the random features. It depends only on the regularization level and is controlled by the Mercer source condition (5.3). Finally, the term $\mathcal{C}(\lambda, m)$ is obtained by means of an interpolation inequality for linear operators in Lemma 2 of [Rudi et al., 2016], depending on the source condition (5.3). It is bounded in Lemma 6 of [Rudi et al., 2016] in terms of the effective dimension $\mathcal{N}(\lambda)$, but also the random features compatibility term $\mathcal{F}_\infty(\lambda)$. Learning rates (Theorems 9-11, and Theorem 8 of [Rudi et al., 2016]) are obtained by optimizing the bound (5.12).

5.3.2 Comparison with Previous Works

Most theoretical works on random features have focused on the approximation of the kernel function K in (5.8) by $\tilde{K}(x, x') = \frac{1}{m} \sum_{j=1}^m \psi(\omega_j, x)\psi(\omega_j, x')$, $x, x' \in \mathcal{X}$, see for example [Rahimi and Recht, 2007; Raginsky and Lazebnik, 2009; Rahimi and Recht, 2009], and [Sriperumbudur and Szabó, 2015] for more refined results. While the question of kernel approximation is interesting in its own right, it does not directly yield information on generalization properties of learning with random features.

¹In this view it is also useful to consider that, using results in [Caponnetto and Yao, 2010], it is possible to prove that optimal rates can be achieved adaptively if hold-out is used for parameter tuning.

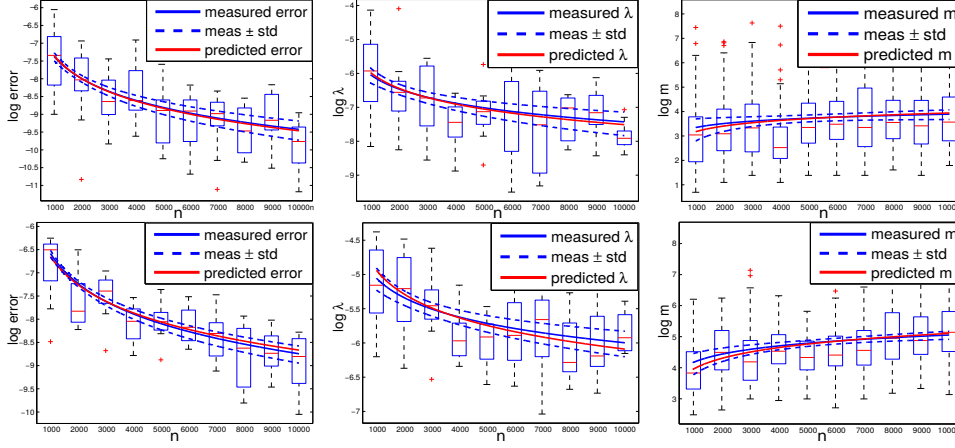


Figure 5.2: Comparison of theoretical and simulated rates for: excess risk $\mathcal{E}(f_{\lambda,m}) - \mathcal{E}(f_\rho)$, λ , m , with respect to n (100 repetitions). Model parameters $r = 11/16, \gamma = 1/8$ (top), and $r = 7/8, \gamma = 1/4$ (bottom).

Much fewer works have analyzed this latter question [Cortes et al., 2010; Rahimi and Recht, 2009; Bach, 2015]. In particular, [Rahimi and Recht, 2009] is the first work to study the generalization properties of random features, considering the empirical risk minimization on the space

$$\mathcal{H}_{R,\infty} = \left\{ f(\cdot) = \int \beta(\omega)\psi(\omega, \cdot)d\theta(\omega) \mid \|\beta\|_\infty \leq R, \beta : \Omega \rightarrow \mathbb{R} \right\},$$

for a fixed $R > 0$. The work in [Rahimi and Recht, 2009] proves the following bound

$$\mathcal{E}(\tilde{f}_n) - \inf_{f \in \mathcal{H}_{R,\infty}} \mathcal{E}(f) \lesssim Rn^{-1/2} \quad (5.13)$$

for a number of random features $m_n \approx n$. A corresponding bound on the excess risk can be derived considering

$$\mathcal{E}(\tilde{f}_n) - \mathcal{E}(f_\rho) = (\mathcal{E}(\tilde{f}_n) - \inf_{f \in \mathcal{H}_{R,\infty}} \mathcal{E}(f)) + (\inf_{f \in \mathcal{H}_{R,\infty}} \mathcal{E}(f) - \mathcal{E}(f_\rho))$$

however in this case the approximation error needs be taken into account and the bound in (5.13) leads to slow, possibly suboptimal rates. Most importantly it does not allow to derive results for a number of feature smaller than the number of points. Analogous results are given in [Bach, 2015] but replacing $\mathcal{H}_{R,\infty}$ with a larger space corresponding to a ball in the RKHS induced by a random features kernel. This latter paper further explores the potential benefit of non uniform sampling. Theorem 11 sharpen these latter results providing faster rates.

In this sense, our results are close to those for Nyström regularization given in [Rudi et al., 2015]. A graphical comparison of these results is given in Figure 5.1 and suggests that while in the worst-case Nyström

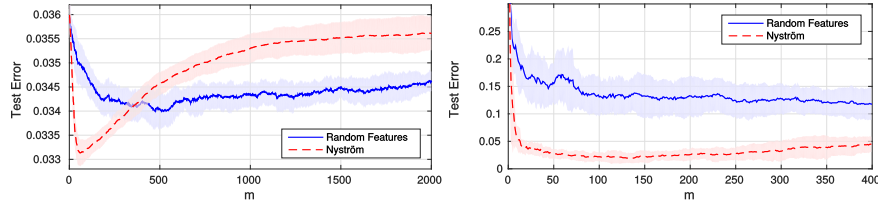


Figure 5.3: Test error with respect to m on *pumadyn32nh* with $\lambda = 10^{-9}$ and *breastCancer* with $\lambda = 10^{-2}$.

and random features behave similarly, in general Nyström methods could naturally adapt to the data distribution. However a definitive comparison would ultimately rely on deriving computational lower bounds giving the minimal possible number of features to achieve optimal rates.

5.4 Numerical results

In this section we provide several numerical experiments complementing the theoretical results. First of all we perform some numerical simulations to validate the rates derived theoretically and verify the number of features needed for optimal rates since theoretical lower bounds are missing. We consider a model where the excess risk can be computed analytically. In particular, we select $\mathcal{X} = \Omega = [0, 1]$, with both θ and $\rho_{\mathcal{X}}$ uniform densities, with $\rho_{\mathcal{X}}$ the marginal of ρ on \mathcal{X} . Given $\gamma \in (0, 1/2)$, $r \in [1/2, 1]$ and denoting with K_q the spline kernel of order $q > 1$ ([Wahba, 1990], Equation 2.1.7), we define $\psi(\omega, x) = K_{1/(2\gamma)}(\omega, x)$, $f_{\rho}(x) = K_{r/\gamma+1/2+\epsilon}(x, x_0)$, for $\epsilon > 0$, $x_0 \in \mathcal{X}$ and $\rho(y|x)$ a Gaussian density centered in $f_{\rho}(x)$. This setting can be shown to satisfy Assumptions 5-9 and 10, with $\alpha = \gamma$. We first compute the KRLS estimator with $n \in \{10^3, \dots, 10^4\}$ and select the λ minimizing the excess risk (computed analytically). Thus, we compute the RF-KRLS estimator and select the number of features m needed to obtain an excess risk within 5% of the one by KRLS. In Figure 5.2, the theoretical and estimated behavior of the excess risk, λ and m with respect to n are reported together with their standard deviation over 100 repetitions. The experiment shows that the predictions by Theorem 11 are quite accurate, since the probabilistic estimations are within one standard deviation from the values measured in the simulation.

Secondly, we test the regularization behavior of the number random features. In Figure 5.3 we plot the test error with respect to the number of random features m on two datasets, by using the random features in [Rahimi and Recht, 2007] approximating the Gaussian kernel. The experiment shows, for m , the typical curve of the bias-variance trade-off asso-

<i>Dataset</i>	n_{tr}	d	σ	Incremental RF RBF	Incremental Nyström RBF	KRLS RBF	Batch Nyström RBF	RF RBF	Fastfood RBF	Fastfood FFT
<i>Insurance</i>	5822	85	6	0.232	0.232	0.231	0.232	0.266	0.264	0.266
<i>CPU</i>	6554	21	0.904	8.593	2.847	7.271	6.758	7.103	7.366	4.544
<i>CT slices</i>	42800	384	5.261	22.627	7.111	NA	60.683	49.491	43.858	58.425
<i>YearPredMSD</i>	463715	90	1.889	0.132	0.105	NA	0.113	0.123	0.115	0.106
<i>Forest</i>	522910	54	1.122	0.977	0.964	NA	0.837	0.840	0.840	0.838

Table 5.1: Accuracy of RF-KRLS when cross-validating m vs. state of the art. d : Input dimensionality, σ : Kernel bandwidth.

ciated to a regularization parameter. The plots in Figure 5.3 also contrast random features and Nyström method, and seem to suggest that Nyström needs considerably fewer centers to achieve the same error.

In Table 5.1 we test, quantitatively, if considering m a regularization parameter and then cross-validating on it gives a better accuracy. We compared RF-KRLS cross-validated on λ and m with some state of the art methods [Williams and Seeger, 2000; Rahimi and Recht, 2007; Le et al., 2013; Rudi et al., 2015] on several small to medium size benchmark datasets, with the Gaussian kernel. The table shows that cross-validating on the number of random features gives a gain in the accuracy of the algorithm.

Part III

Incremental Approaches and Lifelong Learning

Chapter 6

Generalization Properties of Stochastic Gradient Methods

6.1 Setting

The stochastic gradient method (SGM), often called stochastic gradient descent, has become an algorithm of choice in machine learning, because of its simplicity and small computational cost especially when dealing with big data sets [Bousquet and Bottou, 2008].

Despite its widespread use, the generalization properties of the variants of SGM used in practice are relatively little understood. Most previous works consider generalization properties of SGM with only one pass over the data, see e.g. [Nemirovski et al., 2009] or [Orabona, 2014] and references therein, while in practice multiple passes are usually considered. The effect of multiple passes has been studied extensively for the optimization of an empirical objective [Boyd and Mutapcic, 2007], but the role for generalization is less clear. In practice, early-stopping of the number of iterations, for example monitoring a hold-out set error, is a strategy often used to regularize. Moreover, the step-size is typically tuned to obtain the best results. The study in this chapter is a step towards grounding theoretically these commonly used heuristics.

Our starting point are a few recent works considering the generalization properties of different variants of SGM. One first series of results focus on least squares, either with one [Ying and Pontil, 2008; Tarres and Yao, 2014; Dieuleveut and Bach, 2014], or multiple (deterministic) passes over the data [Rosasco and Villa, 2015]. In the former case, it is shown that, in general if only one pass over the data is considered, then the step-size needs to be tuned to ensure optimal results. In [Rosasco and Villa, 2015] it is shown that a universal step-size choice can be taken, if multiple passes are considered. In this case, it is the stopping time that needs to be tuned.

In our work, we are interested in general, possibly non smooth, convex loss

functions. The analysis for least squares heavily exploits properties of the loss and does not generalize to this more general setting. Here, our starting point are the results in [Lin et al., 2015; Hardt et al., 2016; Orabona, 2014] considering convex loss functions. In [Lin et al., 2015], early stopping of a (kernelized) batch subgradient method is analyzed, whereas in [Hardt et al., 2016] the stability properties of SGM for smooth loss functions are considered in a general stochastic optimization setting and certain convergence results derived. In [Orabona, 2014], a more complex variant of SGM is analyzed and shown to achieve optimal rates.

Since we are interested in analyzing regularization and generalization properties of SGM, we consider a general non-parametric setting. In this latter setting, the effects of regularization are typically more evident since it can directly affect the convergence rates. In this context, the difficulty of a problem is characterized by an assumption on the approximation error. Under this condition, the need for regularization becomes clear. Indeed, in the absence of other constraints, the good performance of the algorithm relies on a bias-variance trade-off that can be controlled by suitably choosing the step-size and/or the number of epochs. These latter parameters can be seen to act as regularization parameters. Here, we refer to the regularization as “implicit”, in the sense that it is achieved neither by penalization nor by adding explicit constraints. The two main variants of the algorithm are the same as in least squares: One pass over the data with tuned step-size, or, fixed step-size choice and number of passes appropriately tuned. While in principle optimal parameter tuning requires explicitly solving a bias-variance trade-off, in practice adaptive choices can be implemented by cross validation. In this case, both algorithm variants achieve optimal results, but different computations are entailed. In the first case, multiple single pass SGM need to be considered with different step-sizes, whereas in the second case, early stopping is used. Experimental results, complementing the theoretical analysis are given and provide further insights on the properties of the algorithms.

The rest of the chapter is organized as follows. In Section 6.2, we describe the supervised learning setting and the algorithm, and in Section 6.3 we state and discuss our main results. The detailed proofs can be found in the supplementary material of [Lin et al., 2016]. In Section 6.4 we present some numerical simulations on real datasets.

Notation. For notational simplicity, $[n]$ denotes $\{1, 2, \dots, n\}$ for any $n \in \mathbb{N}$. The notation $a_k \lesssim b_k$ means that there exists a universal constant $C > 0$ such that $a_k \leq Cb_k$ for all $k \in \mathbb{N}$. We denote by $\lceil a \rceil$ the smallest integer greater than a for any given $a \in \mathbb{R}$.

6.2 Learning with SGM

In this section, we introduce the SGM algorithm in the learning setting of interest.

Learning Setting. In the following, we use the definitions of data space, probabilistic data model and loss function introduced in Chapter 1. The goal is to find a function minimizing the expected risk given a sample (training set) $S_n = S = \{z_i = (x_i, y_i)\}_{i=1}^n$ of size $n \in \mathbb{N}$ independently drawn according to ρ . It is important to note that in this Chapter we deal with spaces of functions which are linearly parameterized. Consider a possibly non-linear feature map $\Phi : \mathcal{X} \rightarrow \mathcal{F}$, mapping the data space in \mathbb{R}^p , $p \leq \infty$, or more generally in a (real separable) Hilbert space space with inner product $\langle \cdot, \cdot \rangle$ and norm $\|\cdot\|$. Then, for $w \in \mathcal{F}$ we consider functions of the form

$$f_w(x) = \langle w, \Phi(x) \rangle, \quad \forall x \in \mathcal{X}. \quad (6.1)$$

Examples of the above setting include the case of infinite dictionaries, $\phi_j : \mathcal{X} \rightarrow \mathbb{R}$, $j = 1, \dots$, so that $\Phi(x) = (\phi_j(x))_{j=1}^\infty$, for all $x \in \mathcal{X}$, $\mathcal{F} = \ell_2$ and (6.1) corresponds to $f_w = \sum_{j=1}^p w^j \phi_j$. Also, this setting includes, and indeed is equivalent to considering, functions defined by a positive definite kernel $K : \mathcal{X} \times \mathcal{X} \rightarrow \mathbb{R}$, in which case $\Phi(x) = K(x, \cdot)$, for all $x \in \mathcal{X}$, $\mathcal{F} = \mathcal{H}$ and (6.1) corresponds to the reproducing property

$$f_w(x) = \langle w, K(x, \cdot) \rangle, \quad \forall x \in \mathcal{X}. \quad (6.2)$$

In the following, we assume the feature map to be measurable and define expected and empirical risks over functions of the form (6.1). For notational simplicity, we write $\mathcal{E}(f_w)$ as $\mathcal{E}(w)$, and $\widehat{\mathcal{E}}(f_w)$ as $\widehat{\mathcal{E}}(w)$.

Stochastic Gradient Method. For any fixed $y \in \mathcal{Y}$, assume the univariate loss function $\ell(y, \cdot)$ on \mathbb{R} to be convex, hence its left-hand derivative $\ell'_-(y, a)$ exists at every $a \in \mathbb{R}$ and is non-decreasing.

Algorithm 1. Given a sample S , the stochastic gradient method (SGM) is defined by $w_1 = 0$ and

$$w_{t+1} = w_t - \eta_t \ell'_-(y_{j_t}, \langle w_t, \Phi(x_{j_t}) \rangle) \Phi(x_{j_t}), \quad t = 1, \dots, \bar{t}, \quad (6.3)$$

for a non-increasing sequence of step-sizes $\{\eta_t > 0\}_{t \in \mathbb{N}}$ and a stopping rule $\bar{t} \in \mathbb{N}$. Here, $j_1, j_2, \dots, j_{\bar{t}}$ are independent and identically distributed (i.i.d.) random variables from the uniform distribution on $[n]$. The (weighted) averaged iterates are defined by

$$\bar{w}_t = \sum_{k=1}^t \eta_k w_k / a_t, \quad a_t = \sum_{k=1}^t \eta_k, \quad t = 1, \dots, \bar{t}. \quad (6.4)$$

Note that \bar{t} may be greater than n , indicating that we can use the sample more than once. We shall write $J(t)$ to mean $\{j_1, j_2, \dots, j_t\}$, which will be also abbreviated as J when there is no confusion.

The main purpose of the chapter is to estimate the expected excess risk of the last iterate

$$\mathbb{E}_{S,J}[\mathcal{E}(w_{\bar{t}}) - \inf_{w \in \mathcal{F}} \mathcal{E}(w)],$$

or similarly the expected excess risk of the averaged iterate $\bar{w}_{\bar{t}}$, and study how different parameter settings in Algorithm 1 affect the estimates.

6.3 Implicit Regularization for SGM

In this section, we present and discuss our main results. We begin in Subsection 6.3.1 by giving a universal convergence result and then provide finite sample bounds for smooth loss functions in Subsection 6.3.2, and for non-smooth functions in Subsection 6.3.3. As corollaries of these results we derive different implicit regularization strategies for SGM.

6.3.1 Convergence

We begin presenting a convergence result, involving conditions on both the step-sizes and the number of iterations. We need some basic assumptions.

Assumption 1. *There holds*

$$\kappa = \sup_{x \in X} \sqrt{\langle \Phi(x), \Phi(x) \rangle} < \infty. \quad (6.5)$$

Furthermore, the loss function is convex with respect to its second entry, and $|\ell|_0 := \sup_{y \in \mathcal{Y}} \ell(y, 0) < \infty$. Moreover, its left-hand derivative $\ell'_-(y, \cdot)$ is bounded:

$$|\ell'_-(y, a)| \leq a_0, \quad \forall a \in \mathbb{R}, y \in \mathcal{Y}. \quad (6.6)$$

The above conditions on K and ℓ are common in statistical learning theory [Steinwart and Christmann, 2008; Cucker and Zhou, 2007]. They are satisfied for example by the Gaussian kernel and the hinge loss $\ell(y, a) = |1 - ya|_+ = \max\{0, 1 - ya\}$ or the logistic loss $\ell(y, a) = \log(1 + e^{-ya})$ for all $a \in \mathbb{R}$, with a bounded domain \mathcal{Y} .

The bounded derivative condition (6.6) is implied by the requirement on the loss function to be Lipschitz in its second entry, when \mathcal{Y} is a bounded domain. Given these assumptions, the following result holds.

Theorem 1. *If Assumption 1 holds, then*

$$\lim_{n \rightarrow \infty} \mathbb{E}[\mathcal{E}(\bar{w}_{t^*(n)})] - \inf_{w \in \mathcal{F}} \mathcal{E}(w) = 0, \quad (6.7)$$

provided the sequence $\{\eta_k\}_k$ and the stopping rule $t^*(\cdot) : \mathbb{N} \rightarrow \mathbb{N}$ satisfy

$$(A) \lim_{n \rightarrow \infty} \frac{\sum_{k=1}^{t^*(n)} \eta_k}{n} = 0,$$

$$(B) \text{ and } \lim_{n \rightarrow \infty} \frac{1 + \sum_{k=1}^{t^*(n)} \eta_k^2}{\sum_{k=1}^{t^*(n)} \eta_k} = 0.$$

Conditions (A) and (B) arise from the analysis of suitable sample, computational, and approximation errors (see the appendix of [Lin et al., 2016]). Condition (B) is similar to the one required by stochastic gradient methods [Bertsekas, 1999; Boyd et al., 2003; Boyd and Mutapcic, 2007]. The difference is that here the limit is taken with respect to the number of points, but the number of passes on the data can be larger than one.

Theorem 1 shows that in order to achieve consistency, the step-sizes and the running iterations need to be appropriately chosen. For instance, given n sample points for SGM with one pass¹, i.e., $t^*(n) = n$, possible choices for the step-sizes are $\{\eta_k = n^{-\alpha} : k \in [n]\}$ and $\{\eta_k = k^{-\alpha} : k \in [n]\}$ for some $\alpha \in (0, 1)$. One can also fix the step-sizes a priori, and then run the algorithm with a suitable stopping rule $t^*(n)$.

These different parameters choices lead to different implicit regularization strategies, as we discuss next.

6.3.2 Finite Sample Bounds for Smooth Loss Functions

In this subsection, we give explicit finite sample bounds for smooth loss functions, considering a suitable assumption on the approximation error.

Assumption 2. *The approximation error associated to the triplet (ρ, ℓ, Φ) is defined by*

$$\mathcal{D}(\lambda) = \inf_{w \in \mathcal{F}} \left\{ \mathcal{E}(w) + \frac{\lambda}{2} \|w\|^2 \right\} - \inf_{w \in \mathcal{F}} \mathcal{E}(w), \quad \forall \lambda \geq 0. \quad (6.8)$$

We assume that for some $\beta \in (0, 1]$ and $c_\beta > 0$, the approximation error satisfies

$$\mathcal{D}(\lambda) \leq c_\beta \lambda^\beta, \quad \forall \lambda > 0. \quad (6.9)$$

Intuitively, condition (6.9) quantifies how hard it is to achieve the infimum of the expected risk. In particular, it is satisfied with $\beta = 1$ when $\exists w^* \in \mathcal{F}$ such that $\inf_{w \in \mathcal{F}} \mathcal{E}(w) = \mathcal{E}(w^*)$. More formally, the condition is related to classical quantities in approximation theory, such as K-functionals and interpolation spaces [Steinwart and Christmann, 2008; Cucker and Zhou, 2007]. The following remark is important for later discussions.

¹We slightly abuse the term ‘‘one pass’’ here. In practice, at each pass/epoch, that is n iterations, a sample point is selected randomly from the whole dataset, either with or without repetition.

Remark 4 (SGM and Implicit Regularization). *Assumption 2 is standard in statistical learning theory when analyzing Tikhonov regularization [Cucker and Zhou, 2007; Steinwart and Christmann, 2008]. In this view, our results show that SGM can implicitly implement a form of Tikhonov regularization by controlling the step-size and the number of epochs.*

A further assumption relates to the smoothness of the loss, and is satisfied for example by the logistic loss.

Assumption 3. *For all $y \in \mathcal{Y}$, $\ell(y, \cdot)$ is differentiable and $\ell'(y, \cdot)$ is Lipschitz continuous with a constant $L > 0$, i.e.*

$$|\ell'(y, b) - \ell'(y, a)| \leq L|b - a|, \quad \forall a, b \in \mathbb{R}.$$

The following result characterizes the excess risk of both the last and the average iterate for any fixed step-size and stopping time.

Theorem 2. *If Assumptions 1, 2 and 3 hold and $\eta_t \leq 2/(\kappa^2 L)$ for all $t \in \mathbb{N}$, then for all $t \in \mathbb{N}$,*

$$\begin{aligned} & \mathbb{E}[\mathcal{E}(\bar{w}_t) - \inf_{w \in \mathcal{F}} \mathcal{E}(w)] \\ & \lesssim \frac{\sum_{k=1}^t \eta_k}{n} + \frac{\sum_{k=1}^t \eta_k^2}{\sum_{k=1}^t \eta_k} + \left(\frac{1}{\sum_{k=1}^t \eta_k} \right)^\beta \end{aligned} \quad (6.10)$$

and

$$\begin{aligned} \mathbb{E}[\mathcal{E}(w_t) - \inf_{w \in \mathcal{F}} \mathcal{E}(w)] & \lesssim \frac{\sum_{k=1}^t \eta_k}{n} \sum_{k=1}^{t-1} \frac{\eta_k}{\eta_t(t-k)} \\ & + \left(\sum_{k=1}^{t-1} \frac{\eta_k^2}{\eta_t(t-k)} + \eta_t \right) + \frac{(\sum_{k=1}^t \eta_k)^{1-\beta}}{\eta_t t}. \end{aligned} \quad (6.11)$$

The proof of the above result follows more or less directly combining ideas and results in [Lin et al., 2015; Hardt et al., 2016] (as reported in the appendix of [Lin et al., 2016]). The constants in the bounds are omitted, but given explicitly in the proof. While the error bound for the weighted average looks more concise than the one for the last iterate, interestingly, both error bounds lead to similar generalization properties.

The error bounds are composed of three terms related to sample error, computational error, and approximation error. Balancing these three error terms to achieve the minimum total error bound leads to optimal choices for the step-sizes $\{\eta_k\}$ and total number of iterations t^* . In other words, both the step-sizes $\{\eta_k\}$ and the number of iterations t^* can play the role of a regularization parameter. Using the above theorem, general results for step-size $\eta_k = \eta t^{-\theta}$ with some $\theta \in [0, 1)$, $\eta = \eta(n) > 0$ can be found (see

Proposition 3 in the appendix of [Lin et al., 2016]). Here, as corollaries we provide four different parameter choices to obtain the best bounds, corresponding to four different regularization strategies.

The first two corollaries correspond to fixing the step-sizes a priori and using the number of iterations as a regularization parameter. In the first result, the step-size is constant and depends on the number of sample points.

Corollary 2. *If Assumptions 1, 2 and 3 hold and $\eta_t = \eta_1/\sqrt{n}$ for all $t \in \mathbb{N}$ for some positive constant $\eta_1 \leq 2/(\kappa^2 L)$, then for all $t \in \mathbb{N}$, and $g_t = \bar{w}_t$ (or w_t),*

$$\mathbb{E}[\mathcal{E}(g_t) - \inf_{w \in \mathcal{F}} \mathcal{E}(w)] \lesssim \frac{t \log t}{\sqrt{n^3}} + \frac{\log t}{\sqrt{n}} + \left(\frac{\sqrt{n}}{t}\right)^\beta. \quad (6.12)$$

In particular, if we choose $t^* = \lceil n^{\frac{\beta+3}{2(\beta+1)}} \rceil$,

$$\mathbb{E}[\mathcal{E}(g_{t^*}) - \inf_{w \in \mathcal{F}} \mathcal{E}(w)] \lesssim n^{-\frac{\beta}{\beta+1}} \log n. \quad (6.13)$$

In the second result the step-sizes decay with the iterations.

Corollary 3. *If Assumptions 1, 2 and 3 hold and $\eta_t = \eta_1/\sqrt{t}$ for all $t \in \mathbb{N}$ with some positive constant $\eta_1 \leq 2/(\kappa^2 L)$, then for all $t \in \mathbb{N}$, and $g_t = \bar{w}_t$ (or w_t),*

$$\mathbb{E}[\mathcal{E}(g_t) - \inf_{w \in \mathcal{F}} \mathcal{E}(w)] \lesssim \frac{\sqrt{t} \log t}{n} + \frac{\log t}{\sqrt{t}} + \frac{1}{t^{\beta/2}}. \quad (6.14)$$

Particularly, when $t^* = \lceil n^{\frac{2}{\beta+1}} \rceil$, we have (6.13).

In both the above corollaries the step-sizes are fixed a priori, and the number of iterations becomes the regularization parameter controlling the total error. Ignoring the logarithmic factor, the dominating terms in the bounds (6.12), (6.14) are the sample and approximation errors, corresponding to the first and third terms of the right hand side. Stopping too late may lead to a large sample error, while stopping too early may lead to a large approximation error. The ideal stopping time arises from a form of bias variance trade-off and requires in general more than one pass over the data. Indeed, if we reformulate the results in terms of number of epochs, we have that $\lceil n^{\frac{1-\beta}{2(1+\beta)}} \rceil$ epochs are needed for the constant step-size $\{\eta_t = \eta_1/\sqrt{n}\}_t$, while $\lceil n^{\frac{1-\beta}{1+\beta}} \rceil$ epochs are needed for the decaying step-size $\{\eta_t = \eta_1/\sqrt{t}\}_t$. These observations suggest in particular that while both step-size choices achieve the same bounds, the constant step-size can have a computational advantage since it requires less iterations.

Note that one pass over the data suffices only in the limit case when $\beta = 1$, while in general it will be suboptimal, at least if the step-size is fixed. In fact, Theorem 2 suggests that optimal results could be recovered if the step-size is suitably tuned. The next corollaries show that this is indeed the case. The first result corresponds to a suitably tuned constant step-size.

Corollary 4. *If Assumptions 1, 2 and 3 hold and $\eta_t = \eta_1 n^{-\frac{\beta}{\beta+1}}$ for all $t \in \mathbb{N}$ for some positive constant $\eta_1 \leq 2/(\kappa^2 L)$, then for all $t \in \mathbb{N}$, and $g_t = \bar{w}_t$ (or w_t),*

$$\begin{aligned} & \mathbb{E}[\mathcal{E}(g_t) - \inf_{w \in \mathcal{F}} \mathcal{E}(w)] \\ & \lesssim n^{-\frac{\beta+2}{\beta+1}} t \log t + n^{-\frac{\beta}{\beta+1}} \log t + n^{\frac{\beta^2}{\beta+1}} t^{-\beta}. \end{aligned} \quad (6.15)$$

In particular, we have (6.13) for $t^* = n$.

The second result corresponds to tuning the decay rate for a decaying step-size.

Corollary 5. *If Assumptions 1, 2 and 3 hold and $\eta_t = \eta_1 t^{-\frac{\beta}{\beta+1}}$ for all $t \in \mathbb{N}$ for some positive constant $\eta_1 \leq 2/(\kappa^2 L)$, then for all $t \in \mathbb{N}$, and $g_t = \bar{w}_t$ (or w_t),*

$$\begin{aligned} & \mathbb{E}[\mathcal{E}(g_t) - \inf_{w \in \mathcal{F}} \mathcal{E}(w)] \\ & \lesssim n^{-1} t^{\frac{1}{\beta+1}} \log t + t^{-\frac{\beta}{\beta+1}} \log t + t^{-\frac{\beta}{\beta+1}}. \end{aligned} \quad (6.16)$$

In particular, we have (6.13) for $t^* = n$.

The above two results confirm that good performances can be attained with only one pass over the data, provided the step-sizes are suitably chosen, that is using the step-size as a regularization parameter.

Finally, the following remark relates the above results to data-driven parameter tuning used in practice.

Remark 5 (Bias-Variance and Cross Validation). *The above results show how the number of iterations/passes controls a bias-variance trade-off, and in this sense act as a regularization parameter. In practice, the approximation properties of the algorithm are unknown and the question arises of how the parameter can be chosen. As it turns out, cross validation can be used to achieve adaptively the best rates, in the sense that the rate in (6.13) is achieved by cross validation or more precisely by hold-out cross validation. These results follow by an argument similar to that in Chapter 6 from [Steinwart and Christmann, 2008] and are omitted.*

6.3.3 Finite Sample Bounds for Non-smooth Loss Functions

Theorem 2 holds for smooth loss functions, and it is natural to ask if a similar result holds for non-smooth losses such as the hinge loss. Indeed, analogous results hold albeit current bounds are not as sharp.

Theorem 3. *Instate Assumptions 1 and 2. Then for all $t \in \mathbb{N}$,*

$$\begin{aligned} & \mathbb{E}[\mathcal{E}(\bar{w}_t) - \inf_{w \in \mathcal{F}} \mathcal{E}(w)] \\ & \lesssim \sqrt{\frac{\sum_{k=1}^t \eta_k}{n} + \frac{\sum_{k=1}^t \eta_k^2}{\sum_{k=1}^t \eta_k}} + \left(\frac{1}{\sum_{k=1}^t \eta_k} \right)^\beta, \end{aligned} \quad (6.17)$$

and

$$\begin{aligned} \mathbb{E}[\mathcal{E}(w_t) - \inf_{w \in \mathcal{F}} \mathcal{E}(w)] &\lesssim \sqrt{\frac{\sum_{k=1}^t \eta_k}{n} \sum_{k=1}^{t-1} \frac{\eta_k}{\eta_t(t-k)}} \\ &+ \sum_{k=1}^{t-1} \frac{\eta_k^2}{\eta_t(t-k)} + \eta_t + \frac{(\sum_{k=1}^t \eta_k)^{1-\beta}}{\eta_t t}. \end{aligned} \quad (6.18)$$

The proof of the above theorem is based on ideas from [Lin et al., 2015], where tools from Rademacher complexity [Bartlett and Mendelson, 2003; Meir and Zhang, 2003] are employed (the proof is reported in the appendix of [Lin et al., 2016]).

Using the above result with concrete step-sizes as those for smooth loss functions, we have the following explicit error bounds and corresponding stopping rules.

Corollary 6. *Instate Assumptions 1 and 2. Let $\eta_t = 1/\sqrt{n}$ for all $t \in \mathbb{N}$. Then for all $t \in \mathbb{N}$, and $g_t = \bar{w}_t$ (or w_t),*

$$\mathbb{E}[\mathcal{E}(g_t) - \inf_{w \in \mathcal{F}} \mathcal{E}(w)] \lesssim \frac{\sqrt{t} \log t}{n^{3/4}} + \frac{\log t}{\sqrt{n}} + \left(\frac{\sqrt{n}}{t}\right)^\beta. \quad (6.19)$$

In particular, if we choose $t^* = \lceil n^{\frac{2\beta+3}{4\beta+2}} \rceil$,

$$\mathbb{E}[\mathcal{E}(g_{t^*}) - \inf_{w \in \mathcal{F}} \mathcal{E}(w)] \lesssim n^{-\frac{\beta}{2\beta+1}} \log n. \quad (6.20)$$

Corollary 7. *Instate Assumptions 1 and 2. Let $\eta_t = 1/\sqrt{t}$ for all $t \in \mathbb{N}$. Then for all $t \in \mathbb{N}$, and $g_t = \bar{w}_t$ (or w_t),*

$$\mathbb{E}[\mathcal{E}(g_t) - \inf_{w \in \mathcal{F}} \mathcal{E}(w)] \lesssim \frac{t^{1/4} \log t}{\sqrt{n}} + \frac{\log t}{\sqrt{t}} + \frac{1}{t^{\beta/2}}. \quad (6.21)$$

In particular, if we choose $t^* = \lceil n^{\frac{2}{2\beta+1}} \rceil$, there holds (6.20).

From the above two corollaries, we see that the algorithm with constant step-size $1/\sqrt{n}$ can stop earlier than the one with decaying step-size $1/\sqrt{t}$ when $\beta \leq 1/2$, while they have the same convergence rate, since $n^{\frac{2\beta+3}{4\beta+2}}/n^{\frac{2}{2\beta+1}} = n^{\frac{2\beta-1}{4\beta+1}}$. Note that the bound in (6.20) is slightly worse than that in (6.13), see discussion in Subsection 6.3.4.

Similar to the smooth case, we also have the following results for SGM with one pass where regularization is realized by step-size.

Corollary 8. *Instate Assumptions 1 and 2. Let $\eta_t = n^{-\frac{2\beta}{2\beta+1}}$ for all $t \in \mathbb{N}$. Then for all $t \in \mathbb{N}$, and $g_t = \bar{w}_t$ (or w_t),*

$$\begin{aligned} &\mathbb{E}[\mathcal{E}(g_t) - \inf_{w \in \mathcal{F}} \mathcal{E}(w)] \\ &\lesssim n^{-\frac{4\beta+1}{4\beta+2}} \sqrt{t} \log t + n^{-\frac{2\beta}{2\beta+1}} \log t + n^{\frac{2\beta^2}{2\beta+1}} t^{-\beta}. \end{aligned} \quad (6.22)$$

In particular, (6.20) holds for $t^* = n$.

Corollary 9. *Instate Assumptions 1 and 2. Let $\eta_t = t^{-\frac{2\beta}{2\beta+1}}$ for all $t \in \mathbb{N}$. Then for all $t \in \mathbb{N}$, and $g_t = \bar{w}_t$ (or w_t),*

$$\begin{aligned} & \mathbb{E}[\mathcal{E}(g_t) - \inf_{w \in \mathcal{F}} \mathcal{E}(w)] \\ & \lesssim n^{-\frac{1}{2}} t^{\frac{1}{4\beta+2}} \log t + t^{-\frac{\min(2\beta,1)}{2\beta+1}} \log t + t^{-\frac{\beta}{2\beta+1}}. \end{aligned} \quad (6.23)$$

In particular, (6.20) holds for $t^* = n$.

6.3.4 Discussion and Proof Sketch

As mentioned in the introduction, the literature on theoretical properties of the iteration in Algorithm 1 is vast, both in learning theory and in optimization. A first line of works focuses on a single pass and convergence of the expected risk. Approaches in this sense include classical results in optimization (see [Nemirovski et al., 2009] and references therein), but also approaches based on so called “online to batch” conversion (see [Orabona, 2014] and references therein). The latter are based on analyzing a sequential prediction setting and then on considering the averaged iterate to turn regret bounds in expected risk bounds. A second line of works focuses on multiple passes, but measures the quality of the corresponding iteration in terms of the minimization of the empirical risk. In this view, the iteration in Algorithm 1 is seen as an instance of incremental methods for the minimization of objective functions that are sums of a finite, but possibly large, number of terms [Bertsekas, 2011]. These latter works, while interesting in their own right, do not yield any direct information on the generalization properties of considering multiple passes.

Here, we follow the approach in [Bousquet and Bottou, 2008] advocating the combination of statistical and computational errors. The general proof strategy is to consider several intermediate steps to relate the expected risk of the empirical iteration to the minimal expected risk. The argument we sketch below is a simplified and less sharp version with respect to the one used in the actual proof, but it is easier to illustrate and still carry some important aspects useful to compare with related results.

Consider an intermediate element $\tilde{w} \in \mathcal{F}$ and decompose the excess risk as

$$\begin{aligned} & \mathbb{E}\mathcal{E}(w_t) - \inf_{w \in \mathcal{F}} \mathcal{E} = \\ & \mathbb{E}(\mathcal{E}(w_t) - \widehat{\mathcal{E}}(w_t)) + \mathbb{E}(\widehat{\mathcal{E}}(w_t) - \widehat{\mathcal{E}}(\tilde{w})) \\ & + \mathbb{E}\widehat{\mathcal{E}}(\tilde{w}) - \inf_{w \in \mathcal{F}} \mathcal{E}. \end{aligned}$$

The first term in the right hand side is the generalization error of the iterate. The second term can be seen as a computational error. To discuss the last

term, it is useful to consider a few different choices for \tilde{w} . Assuming the empirical and expected risks to have minimizers \hat{w}^* and w^* , a possibility is to set $\tilde{w} = \hat{w}^*$, this can be seen to be the choice made in [Hardt et al., 2016]. In this case, it is immediate to see that the last term is negligible since,

$$\mathbb{E}\hat{\mathcal{E}}(\tilde{w}) = \mathbb{E}\min_{w \in \mathcal{F}} \hat{\mathcal{E}}(w) \leq \min_{w \in \mathcal{F}} \mathbb{E}\hat{\mathcal{E}}(w) \leq \min_{w \in \mathcal{F}} \mathbb{E}\mathcal{E}(w),$$

and hence,

$$\mathbb{E}\hat{\mathcal{E}}(\tilde{w}) - \min_{w \in \mathcal{F}} \mathcal{E} \leq 0.$$

On the other hand, in this case the computational error depends on the norm $\|\hat{w}^*\|$ which is in general hard to estimate. A more convenient choice is to set $\tilde{w} = w^*$. A reasoning similar to the one above shows that the last term is still negligible and the computational error can still be controlled depending on $\|w^*\|$. In a non-parametric setting, the existence of a minimizer is not ensured and corresponds to a limit case where there is small approximation error. Our approach is then to consider an *almost* minimizer of the expected risk with a prescribed accuracy. Following [Lin et al., 2015], we do this introducing Assumption 2 and choosing $\tilde{w} = w_\lambda$ the unique minimizer of $\mathcal{E} + \lambda \|\cdot\|^2$, $\lambda > 0$. Then the last term in the error decomposition corresponds to the approximation error.

For the generalization error, the stability results from [Hardt et al., 2016] provide sharp estimates for smooth loss functions and in the “capacity independent” limit, that is under no assumptions on the covering numbers of the considered function space. For this setting, the obtained bound is optimal in the sense that it matches the best available bound for Tikhonov regularization [Steinwart and Christmann, 2008; Cucker and Zhou, 2007]. For the non-smooth case a standard Rademacher complexity argument can be used and easily extended to be capacity dependent. However, the corresponding bound is not sharp and improvements are likely to hinge on deriving better norm estimates for the iterates. The question does not seem to be straightforward and is deferred to a future work.

The computational error for the averaged iterates can be controlled using classic arguments [Boyd and Mutapcic, 2007], whereas for the last iterate the arguments in [Lin et al., 2015; Shamir and Zhang, 2013] are needed. Finally, Theorems 2, 3 result from estimating and balancing the various error terms with respect to the choice of the step-size and number of passes.

We conclude this section with some perspective on the results in the chapter. We note that since the primary goal of this study was to analyze the implicit regularization effect of step-size and number of passes, we have considered a very simple iteration. However, it would be very interesting to consider more sophisticated, “accelerated” iterations [Schmidt et al., 2013], and assess the potential advantages in terms of computational and generalization aspects. Similarly, we chose to keep our analysis rela-

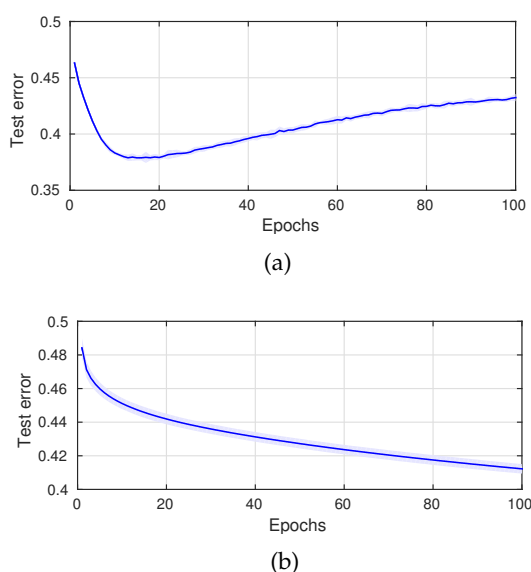


Figure 6.1: Test error for SIGM with fixed (a) and decaying (b) step-size with respect to the number of epochs on *adult* ($n = 1000$).

tively simple, but several improvements can be considered for example deriving high probability bounds and sharper errors under further assumptions. Some of these improvements are relatively straightforward, see e.g. [Lin et al., 2015], but others will require non-trivial extensions of results developed for Tikhonov regularization in the last few years. Finally, here we only referred to a simple cross validation approach to parameter tuning, but it would clearly be very interesting to find ways to tune parameters online. A remarkable result in this direction is derived in [Orabona, 2014], where it is shown that, in the capacity independent setting, adaptive online parameter tuning is indeed possible.

6.4 Numerical Simulations

We carry out some numerical simulations to illustrate our results. The experiments are executed 10 times each, on the benchmark datasets² reported in Table 6.1, in which the Gaussian kernel bandwidth σ used by SGM and SIGM³ for each learning problem is also shown. Here, the chosen loss function is the hinge loss. The experimental platform is a server with $12 \times$

²The datasets can be downloaded from archive.ics.uci.edu/ml and www.csie.ntu.edu.tw/~cjlin/libsvmtools/datasets/

³In what follows, we name one pass SGM and multiple passes SGM as SGM and SIGM (Stochastic Incremental Gradient Method), respectively.

Table 6.1: Benchmark datasets and Gaussian kernel width σ used in our experiments.

<i>Dataset</i>	<i>n</i>	<i>n_{test}</i>	<i>d</i>	<i>σ</i>
<i>breastCancer</i>	400	169	30	0.4
<i>adult</i>	32562	16282	123	4
<i>ijcnn1</i>	49990	91701	22	0.6

Intel[®] Xeon[®] E5-2620 v2 (2.10GHz) CPUs and 132 GB of RAM. Some of the experimental results, as specified in the following, have been obtained by running the experiments on subsets of the data samples chosen uniformly at random. In order to apply hold-out cross validation, the training set is split in two parts: One for empirical risk minimization and the other for validation error evaluation (80% - 20%, respectively). All the data points are randomly shuffled at each repetition.

6.4.1 Regularization in SGM and SIGM

In this subsection, we illustrate four concrete examples showing different regularization effects of the step-size in SGM and the number of passes in SIGM. In all these four examples, we consider the *adult* dataset with sample size $n = 1000$.

In the first experiment, the SIGM step-size is fixed as $\eta = 1/\sqrt{n}$. The test error computed with respect to the hinge loss at each epoch is reported in Figure 6.1(a). Note that the minimum test error is reached for a number of epochs smaller than 20, after which it significantly increases, a so-called overfitting regime. This result clearly illustrates the regularization effect of the number of epochs. In the second experiment, we consider SIGM with decaying step-size ($\eta = 1/4$ and $\theta = 1/2$). As shown in Figure 6.1(b), overfitting is not observed in the first 100 epochs. In this case, the convergence to the optimal solution appears slower than the one in the fixed step-size case. In the last two experiments, we consider SGM and show that the step-size plays the role of a regularization parameter. For the fixed step-size case, i.e., $\theta = 0$, we perform SGM with different $\eta \in (0, 1]$ (logarithmically scaled). We plot the errors in Figure 6.2(a), showing that a large step-size ($\eta = 1$) leads to overfitting, while a smaller one (e. g., $\eta = 10^{-3}$) is associated to oversmoothing. For the decaying step-size case, we fix $\eta_1 = 1/4$, and run SGM with different $\theta \in [0, 1]$. The errors are plotted in Figure 6.2(b), from which we see that the exponent θ has a regularization effect. In fact, a more “aggressive” choice (e. g., $\theta = 0$, corresponding to a fixed step-size) leads to overfitting, while for a larger θ (e. g., $\theta = 1$) we observe

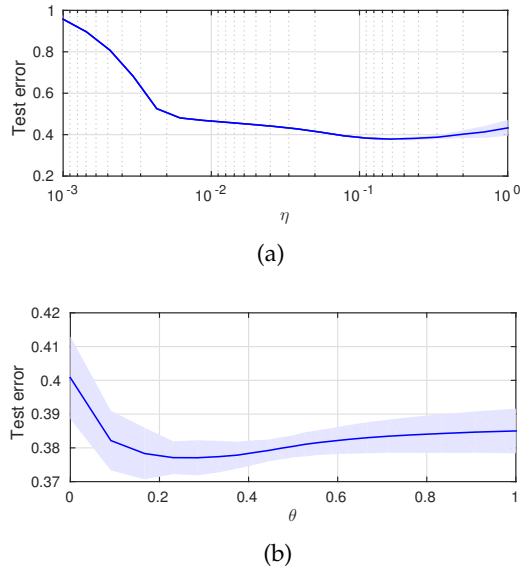


Figure 6.2: Test error for SGM with fixed (a) and decaying (b) step-size cross validation on *adult* ($n = 1000$).

oversmoothing.

6.4.2 Accuracy and Computational Time Comparison

In this subsection, we compare SGM with cross validation and SIGM with benchmark algorithm LIBSVM [Chang and Lin, 2011], both in terms of accuracy and computational time. For SGM, with 30 parameter guesses, we use cross-validation to tune the step-size (either setting $\theta = 0$ while tuning η , or setting $\eta = 1/4$ while tuning θ). For SIGM, we use two kinds of step-size suggested by Section 6.3: $\eta = 1/\sqrt{n}$ and $\theta = 0$, or $\eta = 1/4$ and $\theta = 1/2$, using early stopping via cross-validation. The testing errors with respect to the hinge loss, the testing relative misclassification errors and the computational times are collected in Table 6.2.

We first start comparing accuracies. The results in Table 6.2 indicate that SGM with constant and decaying step-sizes and SIGM with fixed step-size reach comparable test errors, which are in line with the LIBSVM baseline. Observe that SIGM with decaying step-size attains consistently higher test errors, a phenomenon already illustrated in Subsection 6.4.1 in theory.

We now compare the computational times for cross-validation. We see from Table 6.2 that the training times of SIGM and SGM, either with constant or decaying step-sizes, are roughly the same. We also observe that SGM and SIGM are significantly faster than LIBSVM on large datasets (*adult*

Table 6.2: Comparison of SGM and SIGM with cross-validation with decaying (D) and constant (C) step-sizes, in terms of computational time and accuracy. SGM performs cross validation on 30 step-sizes, while SIGM achieves implicit regularization via early stopping.

<i>Dataset</i>	<i>Algorithm</i>	<i>Step Size</i>	<i>Test Error (hinge loss)</i>	<i>Test Error (class. error)</i>	<i>Training Time (s)</i>
<i>breastCancer</i> $n = 400$	<i>SGM</i>	C	0.127 ± 0.022	$3.1 \pm 1.1\%$	1.7 ± 0.2
	<i>SGM</i>	D	0.135 ± 0.024	$3.0 \pm 1.1\%$	1.4 ± 0.3
	<i>SIGM</i>	C	0.131 ± 0.023	$3.2 \pm 1.1\%$	1.4 ± 0.8
	<i>SIGM</i>	D	0.204 ± 0.017	$3.9 \pm 1.0\%$	1.8 ± 0.5
	<i>LIBSVM</i>			$2.8 \pm 1.3\%$	0.2 ± 0.0
<i>adult</i> $n = 1000$	<i>SGM</i>	C	0.380 ± 0.003	$16.6 \pm 0.3\%$	5.7 ± 0.6
	<i>SGM</i>	D	0.378 ± 0.002	$16.2 \pm 0.2\%$	5.4 ± 0.3
	<i>SIGM</i>	C	0.383 ± 0.002	$16.1 \pm 0.0\%$	3.2 ± 0.4
	<i>SIGM</i>	D	0.450 ± 0.002	$23.6 \pm 0.0\%$	1.6 ± 0.2
	<i>LIBSVM</i>			$18.7 \pm 0.0\%$	5.8 ± 0.5
<i>adult</i> $n = 32562$	<i>SGM</i>	C	0.342 ± 0.001	$15.2 \pm 0.8\%$	320.0 ± 3.3
	<i>SGM</i>	D	0.340 ± 0.001	$15.1 \pm 0.7\%$	332.1 ± 3.3
	<i>SIGM</i>	C	0.343 ± 0.001	$15.7 \pm 0.9\%$	366.2 ± 3.9
	<i>SIGM</i>	D	0.364 ± 0.001	$17.1 \pm 0.8\%$	442.4 ± 4.2
	<i>LIBSVM</i>			$15.3 \pm 0.7\%$	6938.7 ± 171.7
<i>ijcnn1</i> $n = 1000$	<i>SGM</i>	C	0.199 ± 0.016	$8.4 \pm 0.8\%$	3.9 ± 0.3
	<i>SGM</i>	D	0.199 ± 0.009	$9.1 \pm 0.1\%$	3.8 ± 0.3
	<i>SIGM</i>	C	0.205 ± 0.010	$9.3 \pm 0.5\%$	1.7 ± 0.4
	<i>SIGM</i>	D	0.267 ± 0.006	$9.4 \pm 0.6\%$	2.2 ± 0.4
	<i>LIBSVM</i>			$7.1 \pm 0.7\%$	0.6 ± 0.1
<i>ijcnn1</i> $n = 49990$	<i>SGM</i>	C	0.041 ± 0.002	$1.5 \pm 0.0\%$	564.9 ± 6.3
	<i>SGM</i>	D	0.059 ± 0.000	$1.7 \pm 0.0\%$	578.9 ± 1.8
	<i>SIGM</i>	C	0.098 ± 0.001	$4.7 \pm 0.1\%$	522.2 ± 20.7
	<i>SIGM</i>	D	0.183 ± 0.000	$9.5 \pm 0.0\%$	519.3 ± 25.8
	<i>LIBSVM</i>			$0.9 \pm 0.0\%$	770.4 ± 38.5

with $n = 32562$, and *ijcnn1* with $n = 49990$). Moreover, for small datasets (*breastCancer* with $n = 400$, *adult* with $n = 1000$, and *ijcnn1* with $n = 1000$), SGM and SIGM are comparable with or slightly slower than LIBSVM.

Chapter 7

Incremental Classification: Adding New Classes in Constant Time

7.1 Setting

In order for autonomous robots to operate in unstructured environments, several perceptual capabilities are required. Most of these skills cannot be hard-coded in the system beforehand, but need to be developed and learned over time as the agent explores and acquires novel experience. As a prototypical example of this setting, in this chapter we consider the task of visual object recognition in robotics: Images depicting different objects are received one frame at a time and the system needs to incrementally update the internal model of known objects as new examples are gathered.

In the last few years, machine learning has achieved remarkable results in a variety of applications for robotics and computer vision [Krizhevsky et al., 2012; Simonyan and Zisserman, 2014; Schwarz et al., 2015; Eitel et al., 2015]. However, most of these methods have been developed for off-line (or “batch”) settings, where the entire training set is available beforehand. The problem of updating a learned model on-line has been addressed in the literature [French, 1999; Sayed, 2008; Duchi et al., 2011; Goodfellow et al., 2013], but most algorithms proposed in this context do not take into account challenges that are characteristic of realistic lifelong learning applications. Specifically, in on-line classification settings, a major challenge is to cope with the situation in which a novel class is added to the model. Indeed:

1. Most learning algorithms require the number of classes to be known beforehand and not grow indefinitely.
2. The imbalance between the few examples (potentially even a single

one) of the new class and the many examples of previously learned classes can lead to unexpected and undesired behaviors [Elkan, 2001].

More precisely, in this chapter we observe both theoretically and empirically that the new and under-represented class is likely to be ignored by the learning model in favor of classes for which more training examples have already been observed, until a sufficient number of examples are provided also for such class.

Several methods have been proposed in the literature to deal with class imbalance in the batch setting by “rebalancing” the misclassification errors accordingly [Elkan, 2001; Steinwart and Christmann, 2008; He and Garcia, 2009]. However, as we will point out in the following, exact rebalancing cannot be applied to the on-line setting without re-training the entire model from scratch every time a novel example is acquired. This would incur in computational learning times that increase at least linearly in the number of examples, which is clearly not feasible in scenarios where training data grow indefinitely. We propose a novel method that learns incrementally with respect to both the number of examples and classes, and accounts for potential class unbalance. Our algorithm builds on a recursive version of RLS for classification (RLSC) [Rifkin, 2002; Rifkin et al., 2003] to achieve constant incremental learning times both when adding new examples to the model and when dealing with imbalance between classes. We evaluate our approach on a standard machine learning benchmark for classification and two challenging visual object recognition datasets for robotics. Our results highlight the clear advantages of our approach when classes are learned incrementally.

The chapter is organized as follows: Section 7.2 reviews related work. Section 7.3 introduces the learning setting, discusses the impact of class imbalance and considers two approaches to deal with this problem. Section 7.4 reviews the incremental RLS algorithm, from which the approach proposed in this work is derived in Section 7.5. Section 7.6 reports the empirical evaluation of our method.

7.2 Related Work

Incremental Learning. The problem of learning from a continuous stream of data has been addressed in the literature from multiple perspectives. The simplest strategy is to re-train the system on the updated training set, whenever a new example is received [Xiao et al., 2014; Jain et al., 2014]. The model from the previous iteration can be used as an initialization to learn the new predictor, reducing training times. These approaches require to store all the training data, and to retrain over all the points at each iteration. Their computational complexity increases at least linearly with the number of examples.

Incremental approaches that do not require to keep previous data in memory can be divided in *stochastic* and *recursive* methods. Stochastic techniques assume training data to be randomly sampled from an unknown distribution and offer asymptotic convergence guarantees to the ideal predictor [Duchi et al., 2011]. However, it has been empirically observed that these methods do not perform well when seeing each training point only once, hence requiring to perform “multiple passes” [Hardt et al., 2016; Lin et al., 2016] over the data, as discussed in Chapter 6 for SGD. This effect has been referred to as the “catastrophic effect of forgetting” [French, 1999] and has recently attracted the attention of the Neural Networks literature [Srivastava et al., 2013; Goodfellow et al., 2013].

Recursive techniques are based, as the name suggests, on a recursive formulation of batch learning algorithms. This formulation typically allows to compute the current model in closed form (or with few operations independent from the number of examples) as a combination of the previous model and the new observed example [Sayed, 2008; Laskov et al., 2006]. As we discuss in more detail in Subsection 7.4.1, the algorithm proposed in this work is based on a recursive method.

Learning with an Increasing Number of Classes. Most classification algorithms have been developed for the batch settings and therefore require the number of classes to be known a priori. This assumption is often broken in incremental settings, since new examples could belong to previously unknown classes. The problem of dealing with an increasing number of classes has been addressed in the contexts of transfer learning or *learning to learn* [Thrun, 1996]. These settings consider a scenario where T linear predictors have been learned to model T classes. Then, when a new class is observed, the associated predictor is learned with the requirement of being “close” to a linear combination of the previous ones [Tommasi et al., 2010; Kuzborskij et al., 2013]. Other approaches have been recently proposed where a class hierarchy is built incrementally as new classes are observed, allowing to create a taxonomy (useful for instance for visual tasks) and exploit possible similarities among different classes [Xiao et al., 2014; Sun and Fox, 2016]. However, all these methods are not incremental in the number of examples and require to retrain the system every time a new point is received.

Class Imbalance. The problems related to class imbalance were previously studied in the literature [Elkan, 2001; He and Garcia, 2009; Steinwart and Christmann, 2008] and are addressed in Section 7.3. Methods to tackle this issue have been proposed, typically re-weighting the misclassification loss [Tommasi et al., 2010] to account for class imbalance. However, as we discuss in Subsection 7.5.2 for the case of the square loss, these methods cannot be implemented incrementally. This is problematic, since imbalance among multiple classes often arises in on-line settings, even if temporarily, for instance when examples of a new class are observed for the first time.

7.3 The Classification Setting and the Effect of Class Imbalance

We introduce the learning framework adopted in this work and then proceed to describe the disrupting effects of imbalance among class labels. We refer the reader to Chapter 1 and [Steinwart and Christmann, 2008] for more details about Statistical Learning Theory for classification problems. For the sake of simplicity, in the following we consider a binary classification setting, postponing the extension to multiclass classification to the end of this section.

7.3.1 Optimal Bayes Classifier and its Least Squares Surrogate

Let us consider a binary classification problem where input-output examples are sampled randomly according to a distribution ρ over $\mathcal{X} \times \{-1, 1\}$. The goal is to learn a function $b_* : \mathcal{X} \rightarrow \{-1, 1\}$ minimizing the overall *expected* classification error

$$b_* = \arg \min_{b: \mathcal{X} \rightarrow \{-1, 1\}} \int_{\mathcal{X} \times \{-1, 1\}} \mathbf{1}(b(x) - y) d\rho(x, y), \quad (7.1)$$

given a finite set of observations $\{x_i, y_i\}_{i=1}^n$, $x_i \in \mathcal{X}$, $y_i \in \{-1, 1\}$ randomly sampled from ρ . Here $\mathbf{1}(x)$ denotes the binary function taking value 0 if $x = 0$ and 1 otherwise. The solution to (7.1) is called the *optimal Bayes classifier* and it can be shown to satisfy the equation

$$b_*(x) = \begin{cases} 1 & \text{if } \rho(1|x) > \rho(-1|x) \\ -1 & \text{otherwise} \end{cases}, \quad (7.2)$$

for all $x \in \mathcal{X}$. Here we have denoted with $\rho(y|x)$ the *conditional* distribution of y given x . In this work we will denote $\rho(x)$ the *marginal* distribution of x , such that by Bayes' rule $\rho(x, y) = \rho(y|x)\rho(x)$.

Computing good estimates of $\rho(y|x)$ typically requires large training datasets and is often unfeasible in practice. Therefore, a so-called *surrogate* problem (see [Steinwart and Christmann, 2008; Bartlett et al., 2006]) is usually adopted to simplify the optimization problem at (7.1) and asymptotically recover the optimal Bayes classifier. In this sense, one well-known surrogate approach is to consider the least squares expected risk minimization

$$f_* = \arg \min_{f: \mathcal{X} \rightarrow \mathbb{R}} \int_{\mathcal{X} \times \{-1, 1\}} (y - f(x))^2 d\rho(x, y). \quad (7.3)$$

The solution to (7.3) allows to recover the optimal Bayes classifier. Indeed,

for any $f : \mathcal{X} \rightarrow \mathbb{R}$ we have

$$\begin{aligned} \int (y - f(x))^2 d\rho(x, y) &= \int \int (y - f(x))^2 d\rho(y|x) d\rho(x) \\ &= \int (1 - f(x))^2 \rho(1|x) - (f(x) + 1)^2 \rho(-1|x) d\rho(x), \end{aligned}$$

which implies that the minimizer of (7.3) satisfies

$$f_*(x) = 2\rho(1|x) - 1 = \rho(1|x) - \rho(-1|x) \quad (7.4)$$

for all $x \in \mathcal{X}$. The optimal Bayes classifier can be recovered from f_* by taking its sign: $b_*(x) = \text{sign}(f_*(x))$. Indeed, $f_*(x) > 0$ if and only if $\rho(1|x) > \rho(-1|x)$.

Empirical Setting. When solving the problem in practice, we are provided with a finite set $\{x_i, y_i\}_{i=1}^n$ of training examples. In these settings the typical approach is to find an estimator \hat{f} of f_* by minimizing the *regularized empirical risk*

$$\hat{f} = \arg \min_{f: \mathcal{X} \rightarrow \mathbb{R}} \frac{1}{n} \sum_{i=1}^n (y_i - f(x_i))^2 + R(f), \quad (7.5)$$

where R is a so-called *regularizer* preventing the solution \hat{f} to overfit. Indeed, it can be shown [Steinwart and Christmann, 2008; Shawe-Taylor and Cristianini, 2004] that, under mild assumptions on the distribution ρ , it is possible for \hat{f} to converge in probability to the ideal f_* as the number of training points grows indefinitely. In Section 7.4 we review a method to compute \hat{f} in practice, both in the batch and in the on-line settings.

7.3.2 The Effect of Unbalanced Data

The classification rule at (7.2) associates every $x \in \mathcal{X}$ to the class y with highest likelihood $\rho(y|x)$. However, in settings where the two classes are not balanced this approach could lead to unexpected and undesired behaviors. To see this, let us denote $\gamma = \rho(y = 1) = \int_{\mathcal{X}} d\rho(y = 1, x)$ and notice that, by (7.2) and the Bayes' rule, an example x is labeled $y = 1$ whenever

$$\rho(x|1) > \rho(x|-1) \frac{(1 - \gamma)}{\gamma}. \quad (7.6)$$

Hence, when γ is close to one of its extremal values 0 or 1 (i.e. $\rho(y = 1) \gg \rho(y = -1)$ or vice-versa), one class becomes clearly preferred with respect to the other and is almost always selected.

In Figure 7.1 we report an example of the effect of unbalanced data by showing how the decision boundary (white dashed curve) of the optimal

Bayes classifier from (7.2) varies as γ takes values from 0.5 (balanced case) to 0.9 (very unbalanced case). As it can be noticed, while the classes maintain the same shape, the decision boundary is remarkably affected by the value of γ .

Clearly, in an on-line robotics setting this effect could be critically sub-optimal for two reasons: 1) We would like the robot to recognize with high accuracy even objects that are less common to be seen. 2) In incremental settings, whenever a novel object is observed for the first time, only few training examples are available (in the extreme case even just one) and we need a loss weighting fairly also underrepresented classes.

7.3.3 Rebalancing the Loss

We consider a general approach to “rebalancing” the classification loss of the standard learning problem of (7.1), similar to the ones in [Elkan, 2001; Steinwart and Christmann, 2008]. We begin by noticing that in the balanced setting, namely for $\gamma = 0.5$, the classification rule at (7.6) is equivalent to assigning class 1 whenever $\rho(x|1) > \rho(x|-1)$ and vice-versa. Here we want to slightly modify the misclassification loss in (7.1) to recover this same rule also in unbalanced settings. To do so, we propose to apply a weight $w(y) \in \mathbb{R}$ to the loss $\mathbf{1}(b(x) - y)$, obtaining the problem

$$b_*^w = \arg \min_{b: \mathcal{X} \rightarrow \{-1,1\}} \int_{\mathcal{X} \times \{-1,1\}} w(y) \mathbf{1}(b(x) - y) d\rho(x, y).$$

Analogously to the non-weighted case, the solution to this problem is

$$b_*^w(x) = \begin{cases} 1 & \text{if } \rho(1|x)w(1) > \rho(-1|x)w(-1) \\ -1 & \text{otherwise} \end{cases}. \quad (7.7)$$

In this work we take the weights w to be $w(1) = 1/\gamma$ and $w(-1) = \gamma - w(1)$. Indeed, from the fact that $\rho(y|x) = \rho(x|y)(\rho(y)/\rho(x))$ we have that the rule at (7.7) is equivalent to

$$b_*^w(x) = \begin{cases} 1 & \text{if } \rho(x|1) > \rho(x|-1) \\ -1 & \text{otherwise} \end{cases}, \quad (7.8)$$

which corresponds to the (unbalanced) optimal Bayes classifier in the case $\gamma = 0.5$, as desired.

Figure 7.1 compares the unbalanced and rebalanced optimal Bayes classifiers for different values of γ . Notice that rebalancing leads to solutions that are invariant to the value of γ (compare the black decision boundary with the white one).

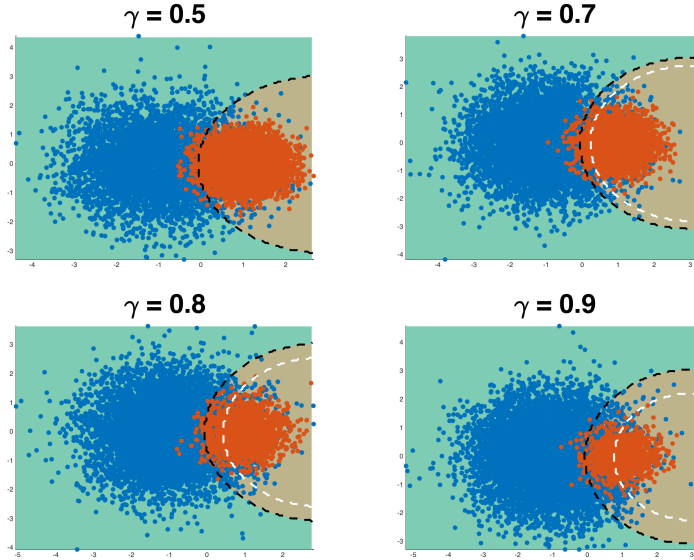


Figure 7.1: Bayes decision boundaries for standard (dashed white line) and rebalanced (dashed black line) binary classification loss for multiple values of $\gamma = \rho(y = 1)$ from 0.5 to 0.9. Data are sampled according to a Gaussian $\rho(x|y) \sim \mathcal{N}(\mu_y, \sigma_y)$ with $\mu_1 = (-1, 0)^\top$, $\mu_{-1} = (1, 0)^\top$, $\sigma_1 = 1$ and $\sigma_{-1} = 0.3$. The boundaries coincide when $\gamma = 0.5$ (balanced data), while they separate as γ increases.

7.3.4 Rebalancing and Recoding the Square Loss

Interestingly, the strategy of changing the weight of the classification error loss can be naturally extended to the least squares surrogate. Indeed, if we consider the weighted least squares problem,

$$f_*^w = \arg \min_{f: \mathcal{X} \rightarrow \mathbb{R}} \int_{\mathcal{X} \times \{-1, 1\}} w(y)(y - f(x))^2 d\rho(x, y), \quad (7.9)$$

we can again recover the (weighted) rule $b_*^w(x) = \text{sign}(f_*^w(x))$ as in the non-weighted setting. Indeed, by direct calculation it follows that (7.9) has solution

$$f_*^w(x) = \frac{\rho(1|x)w(1) - \rho(-1|x)w(-1)}{\rho(1|x)w(1) + \rho(-1|x)w(-1)}. \quad (7.10)$$

If we assume $w(1) > 0$ and $w(-1) > 0$ (as in this work), the denominator of (7.10) is always positive and therefore $\text{sign}(f_*^w(x)) > 0$ if and only if $\rho(1|x)w(1) > \rho(-1|x)w(-1)$, as desired.

Coding. An alternative approach to recover the rebalanced optimal Bayes classifier via least squares surrogate is to apply a suitable coding function

to the class labels $y = \{-1, 1\}$, namely

$$f_*^c = \arg \min_{f: \mathcal{X} \rightarrow \mathbb{R}} \int_{\mathcal{X} \times \{-1, 1\}} (c(y) - f(x))^2 d\rho(x, y), \quad (7.11)$$

where $c: \{-1, 1\} \rightarrow \mathbb{R}$ maps the labels y into scalar codes $c(y) \in \mathbb{R}$. Analogously to the unbalanced (and uncoded) case, the solution to (7.11) is

$$f_*^c(x) = c(1)\rho(1|x) - c(-1)\rho(-1|x), \quad (7.12)$$

which, for $c(y) = w(y)$, corresponds to the numerator of (7.10). Therefore, the optimal (rebalanced) Bayes classifier is recovered again by $b_*^w(x) = \text{sign}(f_*^c(x))$.

7.3.5 Multiclass Rebalancing and Recoding

In the multiclass setting, the optimal Bayes decision rule corresponds to the function $b_*: \mathcal{X} \rightarrow \{1, \dots, T\}$, assigning a label $t \in \{1, \dots, T\}$ to $x \in \mathcal{X}$ when $\rho(t|x) > \rho(s|x) \forall s \neq t$, with $t, s \in \{1, \dots, T\}$. Consequently, the rebalanced decision rule would assign class t , whenever $\rho(y = t|x)w(t) > \rho(y = s|x)w(s) \forall s \neq t$, where the function $w: \{1, \dots, T\} \rightarrow \mathbb{R}$ assigns a weight to each class. Generalizing the binary case, in this work we set $w(t) = 1/\rho(y = t)$, where we denote $\rho(y = t) = \int_{\mathcal{X}} d\rho(t, x)$, for each $t \in \{1, \dots, T\}$.

In multiclass settings, the surrogate least squares classification approach is recovered by adopting a *1-vs-all* strategy, formulated as the vector-valued problem

$$f_* = \arg \min_{f: \mathcal{X} \rightarrow \mathbb{R}^T} \int_{\mathcal{X} \times \{-1, 1\}} \|e_y - f(x)\|^2 d\rho(x, y), \quad (7.13)$$

where $e_t \in \mathbb{R}^T$ is a vector of the canonical basis $\{e_1, \dots, e_T\}$ of \mathbb{R}^T (with the t -th coordinate equal to 1 and the remaining 0). Analogously to the derivation of (7.4), it can be shown that the solution to this problem corresponds to $f_*(x) = (\rho(1|x), \dots, \rho(T|x))^\top \in \mathbb{R}^T$ for all $x \in \mathcal{X}$. Consequently, we recover the optimal Bayes classifier by

$$b_*(x) = \arg \max_{t=1, \dots, T} f(x)_t. \quad (7.14)$$

where $f(x)_t$ denotes the t -th entry of the vector $f(x) \in \mathbb{R}^T$.

The extensions of recoding and rebalancing approaches to this setting follow analogously to the binary setting discussed in Subsection 7.3.4. In particular, the coding function $c: \{e_1, \dots, e_T\} \rightarrow \mathbb{R}$ consists in mapping a vector of the basis e_t to $c(e_t) = e_t/\rho(y = t)$.

Note. In the previous sections we presented the analysis on the binary case by considering a $\{-1, 1\}$ coding for the class labels. This was done to offer a clear introduction to the classification problem, since we need to solve a single least squares problem to recover the optimal Bayes classifier. Alternatively, we could have followed the approach introduced in this section where classes have labels $y = 1, 2$ and adopt surrogate labels $e_1 = [1, 0]^\top$ and $e_2 = [0, 1]^\top$. This would have led to train two distinct classifiers and choose the predicted class as the *argmax* of their scores, according to (7.14). The two approaches are clearly equivalent since the Bayes classifier corresponds respectively to the inequalities $\rho(1|x) > \rho(-1|x)$ or $\rho(1|x) > \rho(2|x)$.

7.4 Incremental Multiclass Classification

In this section we review the standard algorithm for Regularized Least Squares Classification (RLSC) and its recursive formulation used for incremental updates.

7.4.1 Regularized Least Squares for Classification

Here we address the problem of solving the empirical risk minimization introduced at (7.5) in the multiclass setting. Let $\{x_i, y_i\}_{i=1}^n$ be a finite training set, with inputs $x_i \in \mathcal{X} = \mathbb{R}^d$ and labels $y_i \in \{1, \dots, T\}$. In this work, we will assume a linear model for the classifier \hat{f} , namely $f(x) = W^\top x$, with W a matrix in $\mathbb{R}^{d \times T}$. We can rewrite (7.5) in matrix notation as

$$\widehat{W} = \arg \min_{W \in \mathbb{R}^{d \times T}} \|Y - XW\|_F^2 + \lambda \|W\|_F^2 \quad (7.15)$$

with $\lambda > 0$ the *regularization parameter* and $X \in \mathbb{R}^{n \times d}$ and $Y \in \mathbb{R}^{n \times T}$ the matrices whose i -th row correspond respectively to $x_i \in \mathbb{R}^d$ and $e_{y_i} \in \mathbb{R}^T$. We denote by $\|\cdot\|_F^2$ the squared Frobenius norm of a matrix (i.e. the sum of its squared entries).

The solution to (7.15) is

$$\widehat{W} = (X^\top X + \lambda I_d)^{-1} X^\top Y \in \mathbb{R}^{d \times T}, \quad (7.16)$$

where I_d is the $d \times d$ identity matrix (see for instance [Boyd and Vandenberghe, 2004]).

Prediction. According to the rule introduced in Subsection 7.3.5, a given $x \in \mathbb{R}^d$ is classified according to

$$\hat{b}(x) = \arg \max_{i=1, \dots, T} \hat{f}(x)_i = (\widehat{W}^{(i)})^\top x \quad (7.17)$$

with $\widehat{W}^{(i)} \in \mathbb{R}^d$ denoting the i -th column of \widehat{W} .

7.4.2 Recursive Regularized Least Squares

The closed form for the solution at (7.16) allows to derive a recursive formulation to incrementally update \widehat{W} in constant time as new training examples are observed [Sayed, 2008]. Consider a learning process where training data are provided one at a time to the system. At iteration k we need to compute $W_k = (X_k^\top X_k + \lambda I_d)^{-1} X_k^\top Y_k$, where $X_k \in \mathbb{R}^{k \times d}$ and $Y_k \in \mathbb{R}^{k \times T}$ are the matrices whose rows correspond to the first k training examples. The computational cost for evaluating W_{k+1} according to (7.4) is $O(kd^2)$ (for the matrix products) and $O(d^3)$ (for the inversion). This is undesirable in the on-line setting, since k can grow indefinitely. Here we show that we can compute W_k incrementally from W_{k-1} in $O(Td^2)$.

To see this, first notice that by construction

$$X_k = [X_{k-1}^\top, x_k]^\top \quad Y_k = [Y_{k-1}^\top, e_{y_k}]^\top,$$

and therefore, if we denote $A_k = X_k^\top X_k + \lambda I_d$ and $b = X_k^\top Y_k$, we obtain the recursive formulations

$$\begin{aligned} A_k &= X_k^\top X_k + \lambda I_d \\ &= X_{k-1}^\top X_{k-1} + x_k^\top x_k + \lambda I_d \\ &= A_{k-1} + x_k^\top x_k + \lambda I_d \end{aligned} \quad (7.18)$$

and

$$b_k = X_k^\top Y_k = X_{k-1}^\top Y_{k-1} + x_k e_{y_k}^\top = b_{k-1} + x_k e_{y_k}^\top. \quad (7.19)$$

Now, computing b_k from b_{k-1} requires $O(d)$ operations (since e_{y_k} has all zero entries but one), computing A_k from A_{k-1} requires $O(d^2)$, while the inversion A_k^{-1} requires $O(d^3)$. To reduce the cost of the (incremental) inversion, we recall that for a positive definite matrix A_k for which its Cholesky decomposition $A_k = R_k^\top R_k$ is known (with $R_k \in \mathbb{R}^{d \times d}$ upper triangular), the inversion A_k^{-1} can be computed in $O(d^2)$ [Golub and Van Loan, 2012]. In principle, computing the Cholesky decomposition of A_k still requires $O(d^3)$, but we can apply a rank-one update to the Cholesky decomposition at the previous step, namely $A_k = R_k^\top R_k = R_{k-1}^\top R_{k-1} + x_k x_k^\top = A_{k-1} + x_k x_k^\top$, which is known to require $O(d^2)$ [Björck, 1996]. Several implementations are available for the Cholesky rank-one updates; in our experiments we used the MATLAB routine CHOLUPDATE.

Therefore, the update W_k from W_{k-1} can be computed in $O(Td^2)$, since the most expensive operation is the multiplication $A_k^{-1} b_k$. In particular, this computation is independent of the current number k of training examples seen so far, making this algorithm suited for the on-line setting.

7.5 Incremental Multiclass Classification with Class Extension and Recoding

In this section, we present our approach to incremental multiclass classification where we account for the possibility to extend the number of classes incrementally and apply the recoding approach introduced in Section 7.3. The algorithm is reported in Algorithm 7.1.

7.5.1 Class Extension

We introduce a modification of recursive RLSC, allowing to extend the number of classes in constant time with respect to the number of examples seen so far. Let T_k denote the number of classes seen up to iteration k . We have two possibilities:

1. The new sample (x_k, y_k) belongs to a known class, this meaning that $e_{y_k} \in \mathbb{R}^{T_{k-1}}$ and $T_k = T_{k-1}$.
2. (x_k, y_k) belongs to a previously unknown class, implying that $y_k = T_k = T_{k-1} + 1$.

In the first case, the update rules for A_k , b_k and W_k explained in Subsection 7.4.2 can be directly applied. In the second case, the update rule for A_k remains unchanged, while the update of b_k needs to account for the increase in size (since $b_k \in \mathbb{R}^{k \times (T_{k-1} + 1)}$). However, we can modify the update rule for b_k without increasing its computational cost by first adding a new column of zeros $\mathbf{0} \in \mathbb{R}^d$ to b_{k-1} , namely

$$b_k = [b_{k-1}, \mathbf{0}] + x_k^\top e_{y_k}, \quad (7.20)$$

which requires $O(d)$ operations. Therefore, with the strategy described above it is indeed possible to extend the classification capabilities of the incremental learner during on-line operation, without re-training it from scratch. In the following, we address the problem of dealing with class imbalance during incremental updates by performing incremental recoding.

7.5.2 Incremental Recoding

The main algorithmic difference between standard RLSC and the variant with recoding is in the matrix Y containing output training examples. Indeed, according to the recoding strategy, the vector e_{y_k} associated to an output label y_k is coded into $c(e_{y_k}) = e_{y_k} / \rho(y = y_k)$. In the batch setting, this can be formulated in matrix notation as

$$W = (X^\top X + \lambda I_d)^{-1} X^\top Y \Gamma$$

Algorithm 7.1: Incremental RLSC with Class Recoding

Input: Hyperparameters $\lambda > 0, \alpha \in [0, 1]$
Output: Learned weights W_k at each iteration
Initialize: $R_0 \leftarrow \sqrt{\lambda}I_d, b_0 \leftarrow \emptyset, \gamma_0 \leftarrow \emptyset, T \leftarrow 0$

Increment: Observed input $x_k \in \mathbb{R}^d$ and output label y_k :

```

if ( $y_k = T + 1$ ) then
   $T \leftarrow T + 1$ 
   $\gamma_{k-1} \leftarrow [\gamma_{k-1}^\top, 0]^\top$ 
   $b_{k-1} \leftarrow [b_{k-1}, \mathbf{0}]$ , with  $\mathbf{0} \in \mathbb{R}^d$ 
end if
 $\gamma_k \leftarrow \gamma_{k-1} + e_{y_k}$ 
 $\Gamma_k \leftarrow k \cdot \text{diag}(\gamma_k)^{-1}$ 
 $b_k \leftarrow b_{k-1} + x_k^\top e_{y_k}$ 
 $R_k \leftarrow \text{CHOLESKYUPDATE}(R_{k-1}, x_k)$ 
 $W_k \leftarrow R_k^{-1}(R_k^\top)^{-1}b_k\Gamma_k^\alpha$ 
return  $W_k$ 

```

where the original output matrix is substituted by its encoded version $Y^{(e)} = Y\Gamma \in \mathbb{R}^{n \times T}$, with Γ the $T \times T$ diagonal matrix whose t -th diagonal element is $\Gamma_{tt} = 1/\rho(y = t)$. Clearly, in practice the $\rho(y = t)$ are estimated empirically (e.g. by $\hat{\rho}(y = t) = n_t/n$, the ratio between the number n_t of training examples belonging to class t and the total number n of examples).

The above formulation is favorable for the on-line setting. Indeed, we have

$$X_k^\top Y_k \Gamma_k = b_k \Gamma_k = (b_{k-1} + x_k^\top y_k) \Gamma_k, \quad (7.21)$$

where Γ_k is the diagonal matrix of the (inverse) class distribution estimators $\hat{\rho}$ up to iteration k . Γ_k can be computed incrementally in $O(T)$ by keeping track of the number k_t of examples belonging to t and then computing $\hat{\rho}_k(y = t) = k_t/k$ (see Algorithm 7.1 for how this update was implemented in our experiments).

Note that the above step requires $O(dT)$, since updating the (uncoded) b_k from b_{k-1} requires $O(d)$ and multiplying b_k by a diagonal matrix requires $O(dT)$. All the above computations are dominated by the product $A_k^{-1}b_k$, which requires $O(Td^2)$. Therefore, our algorithm is computationally equivalent to the standard incremental RLSC approach.

Coding as a Regularization Parameter. Depending on the amount of training examples seen so far, the estimator k_t/k could happen to not approximate $\rho(y = t)$ well. In order to mitigate this issue, we propose to add a parameter $\alpha \in [0, 1]$ on Γ_k^α , regularizing the effect of coding. Clearly, for $\alpha = 0$ we recover the (uncoded) standard RLSC, since $\Gamma_k^0 = I_T$, while $\alpha = 1$

applies full recoding. In Subsection 7.6.3 we discuss an efficient heuristic to find α in practice.

Incremental Rebalancing. Note that the incremental loss-rebalancing algorithm (Subsection 7.3.4) cannot be implemented incrementally. Indeed, the solution of the rebalanced empirical RLS is

$$W_k = (X_k^\top \Sigma_k X_k + \lambda I_d)^{-1} X_k^\top \Sigma_k Y_k \quad (7.22)$$

with Σ_k a diagonal matrix whose i -th entry is equal to $(\Sigma_k)_{ii} = 1/\hat{\rho}(y = t_i)$ and t_i is the class to which the i -th training example y_i belongs. Since Σ_k changes at every iteration, it is not possible to derive a rank-one update rule for $(X_k^\top \Sigma_k X_k + \lambda I_d)^{-1}$ as for standard RLSC.

7.6 Experiments

We empirically assessed the performance of Algorithm 7.1 on a standard benchmark for machine learning and on two visual recognition tasks in robotics. We compared the classification accuracy of the proposed method with standard RLSC, to evaluate the improvement provided by incremental recoding, and with the rebalanced approach (7.22), which cannot be implemented incrementally, but is a competitor in terms of accuracy when classes are imbalanced.

7.6.1 Experimental Protocol

We adopted the following experimental protocol:

1. Given a dataset with T classes, we simulated a scenario where a new class is observed by selected $T - 1$ of them to be “balanced” and the remaining one to be under-represented.
2. We trained a classifier for the balanced classes, using a randomly sampled dataset containing n_{bal} examples per class. We sampled also a validation set with $n_{bal}/5$ examples per class. n_{bal} is specified below for each dataset.
3. We incrementally trained the classifier from the previous step by sampling on-line n_{imb} examples for the T -th class. Model selection was performed *using exclusively the validation set of the balanced classes*, following the strategy described in Subsection 7.6.3.
4. To measure performance, we sampled a separate test set containing n_{test} examples per class (both balanced and under-represented).

For each dataset, we performed 10 independent trials to account for statistical variability. We measured the performance of the algorithms on the test set while they were trained incrementally. In particular, in Table 7.1 we report the average test accuracy on the imbalanced class and on the entire test set to assess both the relative and overall performance.

7.6.2 Datasets

MNIST [LeCun et al., 1998] is a benchmark dataset composed of 60000 28×28 centered greyscale pictures of digits from 0 to 9. In our experiment, we considered a much smaller subset of MNIST, with $n_{bal} = 1000$ per balanced class. The test set was obtained by sampling $n_{test} = 200$ examples per class for all digits. The imbalanced class was chosen randomly at each trial. We used the raw pixels of the images as inputs for the linear classifiers (i.e. $x \in \mathbb{R}^{784}$).

iCubWorld28 [Pasquale et al., 2015] is a dataset for visual object recognition in robotics. It was collected during a series of sessions where a human teacher showed different objects to the iCub humanoid [Metta et al., 2010]. The task is to discriminate between 28 objects *instances* and contains ~ 1800 images per class. We used $n_{bal} = 700$ and $n_{test} = 700$ and chose the 28-th class to be under-represented. We performed feature extraction on *iCubWorld28* images by taking the output of the *fc7* activation layer of a CAFFENET [Jia et al., 2014] Convolutional Neural Network (CNN), pre-trained on the ImageNet dataset [Russakovsky et al., 2015] (see [Pasquale et al., 2015] for feature extraction details)

RGB-D [Lai et al., 2011] is a dataset for visual object *categorization* in robotics settings. The dataset has been collected while 300 objects from 51 categories were observed on a table from multiple points of view and scales. An average of ~ 900 images are available for each object category. While also depth information is available, in this work we focused only on *RGB* data. Feature extraction was performed analogously to *iCubWorld28*. We used $n_{bal} = 500$ and $n_{test} = 400$ and chose the *tomato* category to be under-represented.

7.6.3 Model Selection

In traditional batch learning settings for RLSC, model selection for the hyperparameter λ is typically performed via hold-out, k-fold or similar cross-validation techniques. In the incremental setting these strategies cannot be directly applied since examples are observed on-line, but a simple approach to create a validation set is to hold out every *i*-th example without using it for training (in our experiments we set $i = 6$). At each iteration, multiple candidate models are trained incrementally each for a different

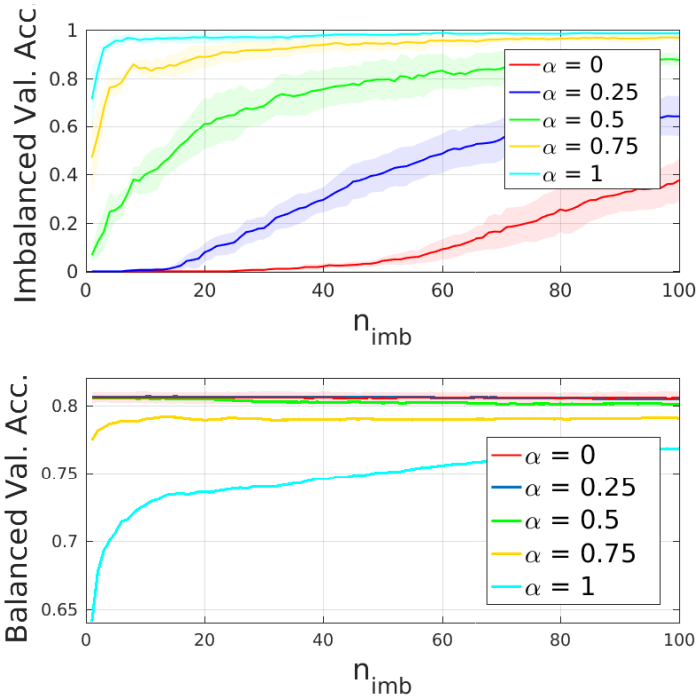


Figure 7.2: Classification accuracy on *iCubWorld28* imbalanced (top) and balanced (bottom) test classes for models trained according to Algorithm 7.1 with varying α and best λ within a pre-defined range (chosen at each iteration and for each α). Growing α from 0 to 1 allows to find a model that maintains same performance on known classes while improving on the under-represented one.

value of λ , and the one with highest validation accuracy is selected for prediction.

However, following the same argument of Section 7.3, in presence of class imbalance this strategy would often select classifiers that ignore the under-represented class. Rebalancing the validation loss (see Section 7.3) does not necessarily solve the issue, but could rather lead to overfit the under-represented class, degrading the accuracy on other classes since errors count less on them. Motivated by empirical evidence discussed below, in this work we have adopted a model selections heuristic for λ and α in Algorithm 7.1, which guarantees to not degrade accuracy on well-represented classes while at the same time achieving higher or equal accuracy on the under-represented one.

Our strategy evaluates the accuracy of the candidate models on the incremental validation set, but *only for classes that have a sufficient number of examples* (e.g. classes with less examples than a pre-defined threshold are

Table 7.1: Incremental classification accuracy on for the naïve (N) RLSC, Rebalanced (RB) and recoding Algorithm 7.1 (RC).

Dataset	n_{imb}	Total Acc. (%)			Imbalanced Acc. (%)			
		N	RB	RC	N	RB	RC	
<i>MNIST</i>	1	79.2 ± 0.3	79.7 ± 0.4	79.7 ± 0.6	0.0 ± 0.0	7.4 ± 7.7	9.5 ± 4.9	
	5	79.1 ± 0.3	82.5 ± 0.7	80.3 ± 0.6	0.0 ± 0.0	39.6 ± 6.2	17.5 ± 6.6	
	n_{bal} =	10	79.2 ± 0.3	83.6 ± 0.7	81.0 ± 0.6	0.0 ± 0.0	49.5 ± 5.7	25.1 ± 5.3
	1000	50	79.2 ± 0.3	85.5 ± 0.3	83.9 ± 0.5	0.0 ± 0.0	73.5 ± 3.3	49.1 ± 3.5
	100	79.2 ± 0.4	85.9 ± 0.4	85.1 ± 0.5	2.0 ± 0.9	75.5 ± 2.7	62.7 ± 2.9	
	500	85.5 ± 0.3	86.2 ± 0.3	86.1 ± 0.3	66.9 ± 1.1	78.5 ± 0.9	77.8 ± 1.1	
<i>iCub</i>	1	77.6 ± 0.3	76.8 ± 0.1	77.7 ± 0.3	0.0 ± 0.0	0.4 ± 0.6	8.0 ± 11.4	
	5	77.6 ± 0.3	77.9 ± 0.1	78.6 ± 0.3	0.0 ± 0.0	8.1 ± 3.9	38.5 ± 9.7	
	n_{bal} =	10	77.6 ± 0.3	78.3 ± 0.4	78.9 ± 0.2	0.0 ± 0.0	23.7 ± 10.8	49.6 ± 5.6
	700	50	77.7 ± 0.2	80.0 ± 0.2	80.0 ± 0.1	5.4 ± 4.1	73.9 ± 7.3	75.0 ± 5.5
	100	78.6 ± 0.1	80.2 ± 0.1	80.1 ± 0.2	39.1 ± 3.6	85.9 ± 4.0	86.5 ± 3.0	
	500	80.2 ± 0.2	80.1 ± 0.1	80.1 ± 0.2	89.3 ± 2.5	93.8 ± 2.0	94.8 ± 1.9	
<i>RGB-D</i>	1	80.4 ± 2.2	78.6 ± 3.2	83.3 ± 3.2	0.0 ± 0.0	62.0 ± 42.1	72.2 ± 26.3	
	5	80.4 ± 2.2	83.0 ± 2.1	83.9 ± 2.6	0.0 ± 0.0	91.7 ± 12.8	99.9 ± 0.3	
	n_{bal} =	10	80.4 ± 2.2	83.8 ± 1.8	83.6 ± 2.6	2.8 ± 2.4	94.7 ± 8.4	100.0 ± 0.0
	500	50	82.3 ± 2.2	84.3 ± 1.9	83.5 ± 2.9	96.6 ± 3.7	100.0 ± 0.0	100.0 ± 0.0
	100	82.4 ± 2.1	84.4 ± 2.0	83.5 ± 2.8	100.0 ± 0.0	100.0 ± 0.0	100.0 ± 0.0	
	500	82.3 ± 2.1	84.1 ± 2.0	84.1 ± 2.8	100.0 ± 0.0	100.0 ± 0.0	100.0 ± 0.0	

not used for validation). Then, we choose the model with largest $\alpha \in [0, 1]$ for which such accuracy is higher or equal to the one measured for $\alpha = 0$, namely without coding. Indeed, as can be seen in Figure 7.2 for validation experiments on *iCubWorld28*, as α grows from 0 to 1, the classification accuracy on the under-represented class increases, Figure 7.2 (Top), while it decreases on the remaining ones, Figure 7.2 (Bottom). Our heuristic chooses the best trade-off for α so that performance does not degrade on well-known classes, but at the same time it will often improve on the under-represented one.

7.6.4 Results

In Table 7.1 we report the classification accuracy of the three models evaluated in our experiments over *MNIST*, *iCubWorld28* and *RGB-D*. The RLSC baseline and Algorithm 7.1 were trained incrementally as new examples of the under-represented class were fed to the system, while the balanced approach was trained from scratch at each iteration. As can be noticed, Algorithm 7.1 consistently outperforms the RLSC baseline, which does not account for class imbalance and learns models which ignore the under-represented class. To offer a clear intuition of the improvement provided by our approach, in Figure 7.3 we report the test accuracy of both RLSC and Algorithm 7.1 on the balanced and under-represented classes as they

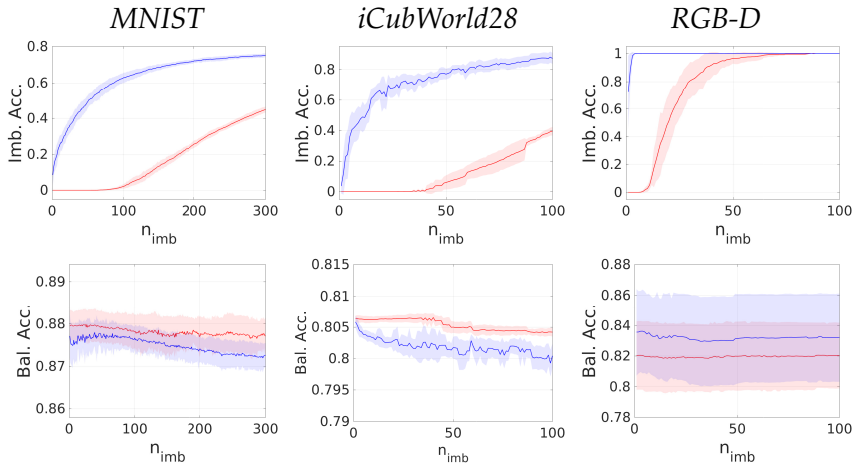


Figure 7.3: Average test classification accuracy of the standard incremental RLSC (red) and the variant proposed in this work (blue) over the imbalanced (top) and balanced (bottom) classes. The models are incrementally trained as n_{imb} grows, as described in Subsection 7.6.1.

are trained on new examples. Interestingly, on the two robotics tasks, our method significantly outperforms also the rebalanced approach. This is favorable, since the rebalanced approach cannot be implemented incrementally (Subsection 7.5.2).

We care to point out that for the *RGB-D* dataset, the overall classification accuracy of Algorithm 7.1 when trained with all available examples for all classes (last row in Table 7.1) is approximately 84%, which is comparable with the state of the art on this dataset [Schwarz et al., 2015]. Moreover, notice that the under-represented category (*tomato*) is in general easy to be distinguished, since all classifiers end up achieving 100% accuracy on this class when sufficient examples are observed. However, RLSC completely ignores this class when only few examples are available, showing that even for “easy” classes the imbalance can heavily affect accuracy and that our approach successfully addresses this issue.

On On-line Backpropagation and Fine-tuning. In principle, for the experiments performed on *iCubWorld28* and *RGB-D*, we could have directly trained the CaffeNet convolutional neural network on-line by stochastic gradient descent (backpropagation) rather than using it just as a feature extractor. Indeed, it has been empirically observed that in batch settings, *fine-tuning* a network previously trained on a large-scale dataset (such as ImageNet [Russakovsky et al., 2015] for the case of CaffeNet) typically leads to remarkable performance improvements [Chatfield et al., 2014]. However, our preliminary results in this direction showed that performing fine-

tuning on-line without using training data from previous classes led to overfit the new class and overall extremely poor results, which we did not include in this work. This is in line with the previous literature studying the “catastrophic effect of forgetting” [French, 1999; Srivastava et al., 2013; Goodfellow et al., 2013], which occurs when training a stochastic model only on new examples while ignoring previous ones.

Chapter 8

Incremental Inverse Dynamics Learning

8.1 Setting

In order to control a robot a model describing the relation between the actuator inputs, the interactions with the world and bodies accelerations is required. This model is called the *dynamics* model of the robot. A dynamics model can be obtained from first principles in mechanics, using the techniques of Rigid Body Dynamics (RBD) [Featherstone and Orin, 2008], resulting in a *parametric model* in which the values of physically meaningful parameters must be provided to complete the fixed structure of the model. Alternatively, the dynamical model can be obtained from experimental data using black-box machine learning techniques, resulting in a *nonparametric model*.

Traditional dynamics parametric methods are based on several assumptions, such as rigidity of links or that friction has a simple analytical form, which may not be accurate in real systems. On the other hand, nonparametric methods based on algorithms such as Kernel Ridge Regression (KRR) [Hoerl and Kennard, 1970; Saunders et al., 1998; Cristianini and Shawe-Taylor, 2000], Kernel Regularized Least Squares (KRLS — see Section 2.4) [Rifkin et al., 2003] or Gaussian Processes [Rasmussen and Williams, 2006] can model dynamics by extrapolating the input-output relationship directly from the available data¹. If a suitable kernel function is chosen, then the nonparametric model is a universal approximator which can account for the dynamics effects which are not considered by the parametric model. Still, nonparametric models have no prior knowledge about the target function to be approximated. Therefore, they need a sufficient amount of train-

¹Note that KRR and KRLS have a very similar formulation, and that these are also equivalent to the techniques derived from Gaussian Processes, as explained for instance in Chapter 6 of [Cristianini and Shawe-Taylor, 2000].

Table 8.1: Schematic comparison of this work with related ones on semi-parametric or incremental robot dynamics learning.

Author, Year	Parametric	Nonparametric
[Nguyen-Tuong and Peters, 2010]	Batch	Batch
[Gijsberts and Metta, 2011]	-	Incremental
[Wu and Movellan, 2012]	Batch	Batch
[Sun de la Cruz et al., 2012]	CAD*	Incremental
[Um et al., 2014]	CAD	Batch
[Camoriano et al., 2016c]	Incremental	Incremental

* In [Sun de la Cruz et al., 2012] the parametric part is used only for initializing the nonparametric model.

ing examples in order to produce accurate predictions on the entire input space. If the learning phase has been performed offline, both approaches are susceptible to the variation of the mechanical properties over long time spans, which are mainly caused by temperature shifts and wear. Even the inertial parameters can change over time. For example if the robot grasps a heavy object, the resulting change in dynamics can be described by a change of the inertial parameters of the hand. A solution to this problem is to address the variations of the identified system properties by learning *incrementally*, continuously updating the model as long as new data becomes available. In this Chapter, we propose a novel technique that joins parametric and nonparametric model learning in an incremental fashion.

Classical methods for physics-based dynamics modeling can be found in [Featherstone and Orin, 2008]. These methods require to identify the mechanical parameters of the rigid bodies composing the robot [Yamane, 2011; Traversaro et al., 2013; Ogawa et al., 2014; Hollerbach et al., 2008], which can then be employed in model-based control and state estimation schemes.

In [Nguyen-Tuong and Peters, 2010], the authors present a learning technique which combines prior knowledge about the physical structure of the mechanical system and learning from available data with Gaussian Process Regression (GPR) [Rasmussen and Williams, 2006]. Similar approaches are presented in [Wu and Movellan, 2012; Um et al., 2014]. Both techniques require an offline training phase and are not incremental, limiting them to scenarios in which the properties of the system do not change significantly over time.

In [Sun de la Cruz et al., 2012], an incremental semiparametric robot dynamics learning scheme based on Locally Weighted Projection Regression (LWPR) [Vijayakumar and Schaal, 2000] is presented, that is initialized using a linearized parametric model. However, this approach uses a fixed parametric model, that is not updated as new data becomes avail-

able. Moreover, LWPR has been shown to underperform with respect to other methods (e.g. [Gijsberts and Metta, 2011]).

In [Gijsberts and Metta, 2011], a fully nonparametric incremental approach for inverse dynamics learning with constant update complexity is presented, based on kernel methods [Schölkopf and Smola, 2002] (in particular KRR) and random features [Rahimi and Recht, 2007] (see Chapter 5). The incremental nature of this approach allows for adaptation to changing conditions in time. The authors also show that the proposed algorithm outperforms other methods such as LWPR, GPR and Local Gaussian Processes (LGP) [Nguyen-Tuong et al., 2009], both in terms of accuracy and prediction time. Nevertheless, the fully nonparametric nature of this approach undermines the interpretability of the inverse dynamics model.

In this chapter we propose a method that is incremental with fixed update complexity (as [Gijsberts and Metta, 2011]) and semiparametric (as [Nguyen-Tuong and Peters, 2010] and [Wu and Movellan, 2012]). The fixed update complexity and prediction time are key properties of our method, enabling real-time performances. Both the parametric and nonparametric parts can be updated, as opposed to [Sun de la Cruz et al., 2012] in which only the nonparametric part is. A comparison between the existing literature and our incremental method is reported in Table 8.1. We validate the proposed method with experiments performed on an arm of the iCub humanoid robot [Metta et al., 2010].

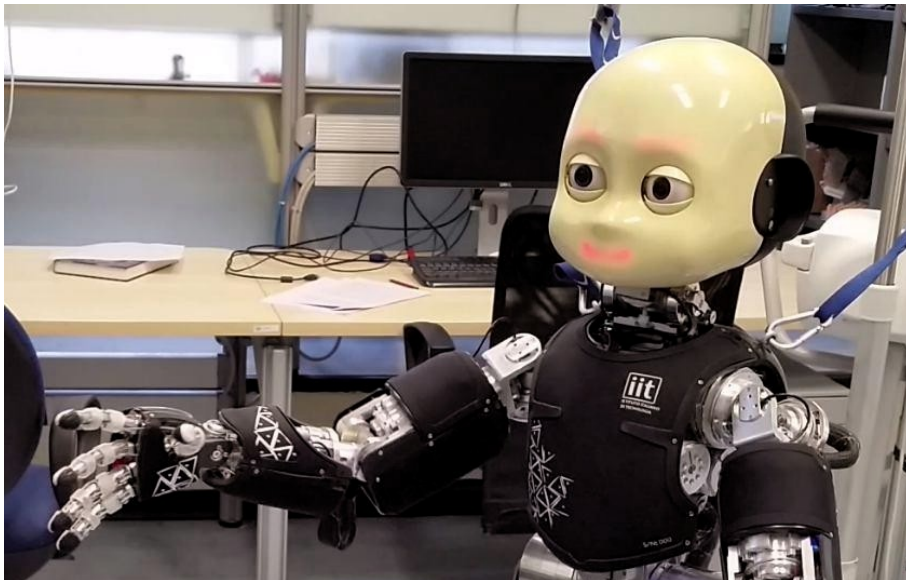


Figure 8.1: iCub learning its right arm's dynamics.

The chapter is organized as follows. Section 8.2 introduces the existing

techniques for parametric and nonparametric robot dynamics learning. In Section 8.3, a complete description of the proposed semiparametric incremental learning technique is introduced. Section 8.4 presents the validation of our approach on the iCub humanoid robotic platform.

8.2 Background

8.2.1 Parametric Models of Robot Dynamics

Robot dynamics parametric models are used to represent the relation connecting the geometric and inertial parameters with some dynamic quantities that depend uniquely on the robot model. A typical example is obtained by writing the robot's inverse dynamics equation in linear form with respect to the robot inertial parameters π :

$$\boldsymbol{\tau} = M(\mathbf{q})\ddot{\mathbf{q}} + C(\mathbf{q}, \dot{\mathbf{q}})\dot{\mathbf{q}} + g(\mathbf{q}) = \Phi(x)\boldsymbol{\pi}, \quad (8.1)$$

where: $\mathbf{q} \in \mathbb{R}^{n_{dof}}$ is the vector of joint positions, $\boldsymbol{\tau} \in \mathbb{R}^{n_{dof}}$ is the vector of joint torques, $\boldsymbol{\pi} \in \mathbb{R}^{n_p}$ is the vector of the identifiable (base) inertial parameters [Featherstone and Orin, 2008], $\Phi(x) \in \mathbb{R}^{n_{dof} \times n_p}$ is the “regressor”, i.e. a matrix that depends only on the robot kinematic parameters. In the rest of the chapter we will indicate with $x \in \mathbb{R}^{3n_{dof}}$ the input triple given by $(\mathbf{q}, \dot{\mathbf{q}}, \ddot{\mathbf{q}})$. Other parametric models write different measurable quantities as a product of a regressor and a vector of parameters, for example the total energy of the robot [Gautier and Khalil, 1988], the instantaneous power provided to the robot [Gautier, 1997], the sum of all external forces acting on the robot [Ayusawa et al., 2014] or the center of pressure of the ground reaction forces [Baelemans et al., 2013]. Regardless of the choice of the measured variable $y \in \mathbb{R}^T$ (row vector), the structure of the regressor is similar:

$$y^\top = \Phi(\mathbf{q}, \dot{\mathbf{q}}, \ddot{\mathbf{q}})\boldsymbol{\pi} = \Phi(x)\boldsymbol{\pi}. \quad (8.2)$$

The $\boldsymbol{\pi}$ vector is composed of certain linear combinations of the inertial parameters of the links, the *base inertial parameters* [Khalil and Dombre, 2004]. In particular, the inertial parameters of a single body are the mass m , the first moment of mass $m\mathbf{c} \in \mathbb{R}^3$ expressed in a body fixed frame and the inertia matrix $I \in \mathbb{R}^{3 \times 3}$ expressed in the orientation of the body fixed frame and with respect to its origin. In *parametric modeling* of robot dynamics, the regressor structure depends on the kinematic parameters of the robot, that are obtained from CAD models of the robot through kinematic calibration techniques. Similarly, the inertial parameters $\boldsymbol{\pi}$ can also be obtained from CAD models of the robot, however these models may be unavailable, for example because the manufacturer of the robot does not provide them. In this case the usual approach is to estimate $\boldsymbol{\pi}$ from experimental data [Hollerbach et al., 2008]. To do that, given n measures of the measured

quantity y_i (with $i = 1 \dots n$), stacking (8.2) for the n samples it is possible to write:

$$\begin{bmatrix} y_1^\top \\ y_2^\top \\ \vdots \\ y_n^\top \end{bmatrix} = \begin{bmatrix} \Phi(x_1) \\ \Phi(x_2) \\ \vdots \\ \Phi(x_n) \end{bmatrix} \boldsymbol{\pi}. \quad (8.3)$$

This equation can then be solved in least squares (LS) sense to find an estimate $\hat{\boldsymbol{\pi}}$ of the base inertial parameters. Given the training trajectories, it is possible that not all parameters in $\boldsymbol{\pi}$ can be estimated well as the problem in (8.3) can be ill-posed, hence this equation is usually solved as a Regularized Least Squares (RLS — see Section 1.10) problem. Defining

$$\bar{\mathbf{y}}_n = \begin{bmatrix} y_1^\top \\ y_2^\top \\ \vdots \\ y_n^\top \end{bmatrix}, \quad \bar{\boldsymbol{\Phi}}_n = \begin{bmatrix} \Phi(x_1) \\ \Phi(x_2) \\ \vdots \\ \Phi(x_n) \end{bmatrix},$$

the RLS problem that is solved for the parametric identification is:

$$\hat{\boldsymbol{\pi}} = \arg \min_{\boldsymbol{\pi} \in \mathbb{R}^{n_p}} (\|\bar{\boldsymbol{\Phi}}_n \boldsymbol{\pi} - \bar{\mathbf{y}}_n\|^2 + \lambda \|\boldsymbol{\pi}\|^2), \lambda > 0. \quad (8.4)$$

8.2.2 Nonparametric Modeling with Kernel Methods

Kernel methods in the Statistical Learning Theory framework are the form of nonparametric modeling of interest for this chapter, and have already been discussed in Chapters 1 and 2. In a nonparametric modeling setting, the goal is to find a function $f^* : \mathcal{X} \rightarrow \mathcal{Y}$ such that

$$f^* = \arg \min_{f \in \mathcal{H}} \underbrace{\int_{\mathcal{X} \times \mathcal{Y}} \ell(f(x), y) d\rho(x, y)}_{\mathcal{E}(f)}, \quad (8.5)$$

In the rest of this work, we will consider the squared loss $\ell(f(x), y) = \|f(x) - y\|^2$. The optimization problem outlined in (8.5) can be approached empirically by means of many different algorithms, among which one of the most widely used is Kernel Regularized Least Squares (KRLS) [Saunders et al., 1998; Rifkin et al., 2003]. In KRLS, as discussed in Section 2.4, a regularized solution $\hat{f}_\lambda : \mathcal{X} \rightarrow \mathcal{Y}$ is found solving

$$\hat{f}_\lambda = \arg \min_{f \in \mathcal{H}} \sum_{i=1}^n \|f(x_i) - y_i\|^2 + \lambda \|f\|_{\mathcal{H}}^2, \quad \lambda > 0, \quad (8.6)$$

where for simplicity we do not divide the sum of the point-wise errors by n , and it can be conveniently expressed as

$$\hat{f}_\lambda(x) = \sum_{i=1}^n \alpha_i K(x_i, x) \quad (8.7)$$

with $\alpha = (K_n + \lambda I_n)^{-1} Y \in \mathbb{R}^{n \times T}$, α_i i -th row of α and $Y = [y_1^\top, \dots, y_n^\top]^\top$. As we know, it is necessary to invert and store the kernel matrix $K_n \in \mathbb{R}^{n \times n}$, which implies $O(n^3)$ and $O(n^2)$ time and memory complexities, respectively. Such complexities render the above-mentioned KRLS approach prohibitive in settings where n is large, including the one treated in this work. This limitation can be dealt with by resorting to approximated methods such as random features (see Chapter 5), which will now be recalled in this setting.

Random Feature Maps for Kernel Approximation

The empirical kernel matrix K_n can become too cumbersome to invert and store as n grows. In this chapter, we introduce a random feature map $\tilde{\phi} : \mathbb{R}^d \rightarrow \mathbb{R}^D$ directly approximating the infinite-dimensional Gaussian kernel feature map ϕ , so that

$$K(x, x') = e^{-\frac{\|x-x'\|^2}{2\sigma^2}} = \langle \phi(x), \phi(x') \rangle_{\mathcal{H}} \approx \tilde{\phi}(x) \tilde{\phi}(x')^\top. \quad (8.8)$$

The number of random features D can be chosen according to the desired approximation accuracy, as guaranteed by the convergence bounds reported in [Rahimi and Recht, 2007, 2008]. The approximated feature map in this case is $\tilde{\phi}(x) = [e^{ix\omega_1}, \dots, e^{ix\omega_D}]$, where

$$\omega \sim p(\omega) = (2\pi)^{-\frac{D}{2}} e^{-\frac{\|\omega\|^2}{2\sigma^2}}, \quad (8.9)$$

with $\omega \in \mathbb{R}^D$ column vector. Therefore, it is possible to map the input data as $\tilde{x} = \tilde{\phi}(x) \in \mathbb{R}^D$, with \tilde{x} row vector, to obtain a nonlinear and nonparametric model of the form

$$\tilde{f}(x) = \tilde{x} \tilde{W} \approx \hat{f}_\lambda(x) = \sum_{i=1}^n \alpha_i K(x_i, x) \quad (8.10)$$

approximating the exact kernelized solution $\hat{f}_\lambda(x)$, with $\tilde{W} \in \mathbb{R}^{D \times T}$. Note that the approximated model is nonlinear in the input space, but linear in the random features space. We can therefore introduce the regularized linear regression problem in the random features space as follows:

$$\tilde{W}^\lambda = \arg \min_{\tilde{W} \in \mathbb{R}^{D \times T}} \left(\|\tilde{X} \tilde{W} - Y\|^2 + \lambda \|\tilde{W}\|^2 \right), \quad \lambda > 0, \quad (8.11)$$

where $\tilde{X} \in \mathbb{R}^{n \times D}$ is the matrix of the training inputs where each row has been mapped by $\tilde{\phi}$. The main advantage of performing a random feature mapping is that it allows us to obtain a nonlinear model by applying linear regression methods. For instance, Regularized Least Squares (RLS — see Section 1.10) can compute the solution \tilde{W}^λ of (8.11) with $O(nD^2)$ time and $O(D^2)$ memory complexities. Once \tilde{W}^λ is known, the prediction $\hat{y} \in \mathbb{R}^{1 \times T}$ for a mapped sample \tilde{x} can be computed as $\hat{y} = \tilde{x}\tilde{W}^\lambda$.

8.2.3 RLS for Parametric and Nonparametric Learning

We now see in detail how RLS can be applied to solve both the parametric RBD and nonparametric random features-based dynamics learning problems. Let $Z \in \mathbb{R}^{a \times b}$ and $U \in \mathbb{R}^{a \times c}$ be two matrices of real numbers, with $a, b, c \in \mathbb{N}^+$. RLS computes a solution $W^\lambda \in \mathbb{R}^{b \times c}$ of the potentially ill-posed problem $ZW = U$. Considering the Tikhonov regularization scheme, $W^\lambda \in \mathbb{R}^{b \times c}$ is the solution to the problem

$$W^\lambda = \arg \min_{W \in \mathbb{R}^{b \times c}} \underbrace{(\|ZW - U\|^2 + \lambda \|W\|^2)}_{J(W, \lambda)}, \quad \lambda > 0. \quad (8.12)$$

As we know, the minimizing solution is

$$W^\lambda = (Z^\top Z + \lambda I_b)^{-1} Z^\top U. \quad (8.13)$$

Both the parametric identification problem (8.4) and the nonparametric random features problem (8.11) are *specific instances* of the general problem (8.12). In particular, the parametric problem (8.4) is equivalent to (8.12) with

$$W^\lambda = \hat{\pi}, \quad Z = \bar{\Phi}_n, \quad U = \bar{y}_n,$$

while the random features learning problem (8.11) is equivalent to (8.12) with

$$W^\lambda = \tilde{W}^\lambda, \quad Z = \tilde{X}, \quad U = Y.$$

Hence, both problems for a given training set can be solved applying (8.13).

8.2.4 Recursive RLS with Cholesky Update

In scenarios in which supervised samples become available sequentially, a very useful extension of the RLS algorithm consists in the definition of an update rule for the model which allows it to be incrementally trained, increasing adaptivity to changes of the system properties through time. This algorithm is called Recursive Regularized Least Squares (RRLS), already discussed in Subsection 8.2.4 in its classification variant. We consider RRLS with the Cholesky update rule [Björck, 1996], which is numerically more stable than others (e.g. the Sherman-Morrison-Woodbury update rule). In

adaptive filtering, this update rule is known as the *QR algorithm* [Sayed, 2008].

Let us define $A = Z^\top Z + \lambda I_b$, with $\lambda > 0$, and $B = Z^\top U$. Our goal is to update the model (fully described by A and B) with a new supervised sample (z_{k+1}, u_{k+1}) , with $z_{k+1} \in \mathbb{R}^b$, $u_{k+1} \in \mathbb{R}^c$ row vectors. Consider the Cholesky decomposition $A = R^\top R$. It can always be obtained, since A is positive definite for $\lambda > 0$. Thus, we can express the update problem at step $k + 1$ as:

$$\begin{aligned} A_{k+1} &= R_{k+1}^\top R_{k+1} \\ &= A_k + z_{k+1}^\top z_{k+1} \\ &= \tilde{R}_k^\top R_k + z_{k+1}^\top z_{k+1}, \end{aligned} \quad (8.14)$$

where R is full rank and unique, and $R_0 = \sqrt{\lambda} I_b$.

By defining

$$\tilde{R}_k = \begin{bmatrix} R_k \\ z_{k+1} \end{bmatrix} \in \mathbb{R}^{b+1 \times b}, \quad (8.15)$$

we can write $A_{k+1} = \tilde{R}_k^\top \tilde{R}_k$. However, in order to compute R_{k+1} from the obtained A_{k+1} it would be necessary to recompute its Cholesky decomposition, requiring $O(b^3)$ computational time. There exists a procedure, based on Givens rotations, which can be used to compute R_{k+1} from \tilde{R}_k with $O(b^2)$ time complexity. A recursive expression can be obtained also for B_{k+1} as follows:

$$\begin{aligned} B_{k+1} &= Z_{k+1}^\top U_{k+1} \\ &= Z_k^\top U_k + z_{k+1}^\top u_{k+1}. \end{aligned} \quad (8.16)$$

Once R_{k+1} and B_{k+1} are known, the updated weights matrix W_k can be obtained via back and forward substitution as

$$W_{k+1} = R_{k+1} \setminus (R_{k+1}^\top \setminus B_{k+1}). \quad (8.17)$$

The time complexity for updating W is $O(b^2)$.

As for RLS, the RRLS incremental solution can be applied to both the parametric (8.4) and nonparametric with random features (8.11) problems, assuming $\lambda > 0$. In particular, RRLS can be applied to the parametric case by noting that the arrival of a new sample (Φ_r, y_r) adds T rows to $Z_k = \bar{\Phi}_{r-1}$ and $U_k = \bar{y}_{r-1}$. Consequently, the update of A must be decomposed in T update steps using (8.16). For each one of these T steps we consider only one row of Φ_r and y_r^\top , namely:

$$z_{k+i} = (\Phi_r)_i, \quad u_{k+i} = (y_r^\top)_i, \quad i = 1 \dots T$$

where $(V)_i$ is the i -th row of the matrix V or the i -th element of vector V .

On the other hand, in the nonparametric random features case, RRLS can be applied considering

$$z_{k+1} = \tilde{x}_r, \quad u_{k+1} = y_r,$$

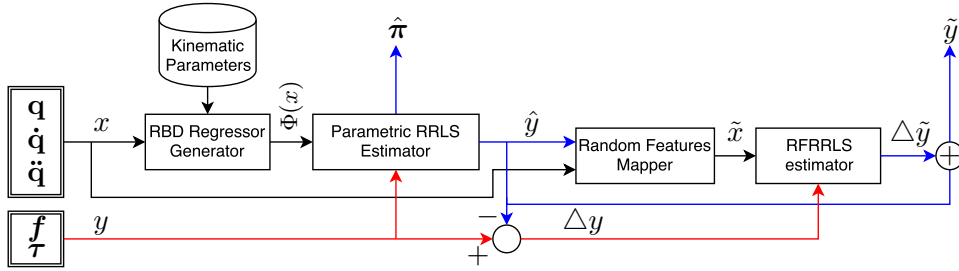


Figure 8.2: Block diagram displaying the functioning of the proposed prioritized semiparametric inverse dynamics estimator. \mathbf{f} and $\boldsymbol{\tau}$ indicate measured force and torque components, concatenated in the measured output vector y . The parametric part is composed of the RBD regressor generator and of the parametric estimator based on RRLS. Its outputs are the estimated parameters $\hat{\boldsymbol{\pi}}$ and the predicted output \hat{y} . The nonparametric part maps the input to the random features space with the Random Features Mapper block, and the RFRRLS estimator predicts the residual output $\Delta\tilde{y}$, which is then added to the parametric prediction \hat{y} to obtain the semiparametric prediction \tilde{y} .

where (\tilde{x}_r, y_r) is the supervised sample at step r .

8.3 Semiparametric Incremental Dynamics Learning

We propose a semiparametric incremental inverse dynamics estimator, designed to have better generalization properties with respect to fully parametric and nonparametric ones, both in terms of accuracy and convergence rates. The estimator, whose functioning is illustrated by the block diagram in Figure 8.2, is composed of two main parts. The first one is an incremental parametric estimator taking as input the rigid body dynamics regressors $\Phi(x)$ and computing two quantities at each step:

- An estimate \hat{y} of the output quantities of interest.
- An estimate $\hat{\boldsymbol{\pi}}$ of the base inertial parameters of the links composing the rigid body structure.

The employed learning algorithm is RRLS. Since it is supervised, during the model update step the real measured output y is used by the learning algorithm as ground truth. The parametric estimation is performed first, and is independent of the nonparametric part. This property is desirable in order to give priority to the identification of the inertial parameters $\boldsymbol{\pi}$. Moreover, since the estimator is incremental, the estimated inertial parameters $\hat{\boldsymbol{\pi}}$ adapt to changes in the inertial properties of the links, which can

occur if the end-effector is holding a heavy object. Still, this adaptation cannot address changes in nonlinear effects which do not respect the rigid body assumptions.

The second estimator is also RRLS-based, fully nonparametric and incremental. It leverages the approximation of the kernel function via random Fourier features, as outlined in Subsection 8.2.2, to obtain a nonlinear model that can be updated incrementally with constant update complexity $O(D^2)$ (see Subsection 8.2.4). This estimator receives as inputs the current vectorized x and the parametric estimation \hat{y} , normalized and mapped to the random features space approximating an infinite-dimensional feature space introduced by the Gaussian kernel. The supervised output, used for training the nonparametric part, is the residual $\Delta y = y - \hat{y}$. The nonparametric estimator provides as output the estimate $\Delta \tilde{y}$ of the residual, which is then added to \hat{y} to obtain the final semiparametric estimate \tilde{y} . Similarly to the parametric part, in the nonparametric one the estimator's internal nonlinear model can be updated during operation, which constitutes an advantage in the case in which the robot has to explore a previously unseen area of the state space, or when the mechanical conditions change (e.g. due to wear, tear or temperature shifts).

8.4 Experimental Results

8.4.1 Software

For implementing the proposed algorithm we used two existing open source libraries. For the RRLS learning part we used GURLS [Tacchetti et al., 2013], a regression and classification library based on the Regularized Least Squares (RLS) algorithm, available for Matlab and C++. For the computations of the regressors $\Phi(\mathbf{q}, \dot{\mathbf{q}}, \ddot{\mathbf{q}})$ we used iDynTree² (see [Nori et al., 2015]), a C++ dynamics library designed for free floating robots. Using SWIG [Beazley et al., 1996], iDynTree supports calling its algorithms in several programming languages, such as Python, Lua and Matlab. For producing the presented results, we used the Matlab interfaces of iDynTree and GURLS.

8.4.2 Robotic Platform

iCub is a full-body humanoid with 53 degrees of freedom [Metta et al., 2010]. For validating the presented approach, we learned the dynamics of the right arm of the iCub as measured from the proximal six-axis force/torque (F/T) sensor embedded in the arm (see Figure 8.3). The considered output y is the reading of the F/T sensor, and the inertial parameters π are the

²<https://github.com/robotology/idyntree>

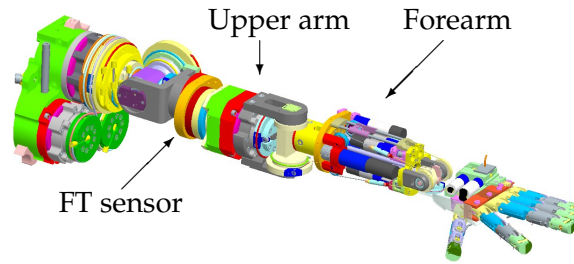


Figure 8.3: CAD drawing of the iCub arm used in the experiments. The six-axis F/T sensor used for validation is visible in the middle of the upper arm link.

base parameters of the arm [Traversaro et al., 2015]. As y is not a input variable for the system, the output of the dynamic model is not directly usable for control, but it is still a proper benchmark for the dynamics learning problem, as also shown in [Gijsberts and Metta, 2011]. Nevertheless, the joint torques could be computed seamlessly from the F/T sensor readings if needed for control purposes, by applying the method presented in [Ivaldi et al., 2011].

8.4.3 Validation

We now present the results of the experimental validation of the proposed semiparametric model. The model includes a parametric part, based on physical modeling. This part is expected to provide acceptable prediction accuracy for the force components in the whole workspace of the robot, since it is based on prior knowledge about the structure of the robot itself, which does not abruptly change as the trajectory changes. On the other hand, the nonparametric part can provide higher prediction accuracy in specific areas of the input space for a given trajectory, since it also models nonrigid body dynamics effects by learning directly from data. To provide empirical foundations to the above insights, a validation experiment has been set up using the right arm of the iCub humanoid robot, considering as input the positions, velocities and accelerations of the 3 shoulder joints and of the elbow joint, and as outputs the 3 force and 3 torque components measured by the six-axis F/T sensor in-built in the upper arm. We employ two datasets for this experiment, collected at $10Hz$ as the end-effector tracks (using the Cartesian controller presented in [Pattacini et al., 2010]) circumferences with $10cm$ radius on the transverse (XY) and sagittal (XZ) planes³ at approximately $0.6m/s$. The total number of points for each

³For more information on the iCub reference frames, see <http://eris.liralab.it/wiki/ICubForwardKinematics>

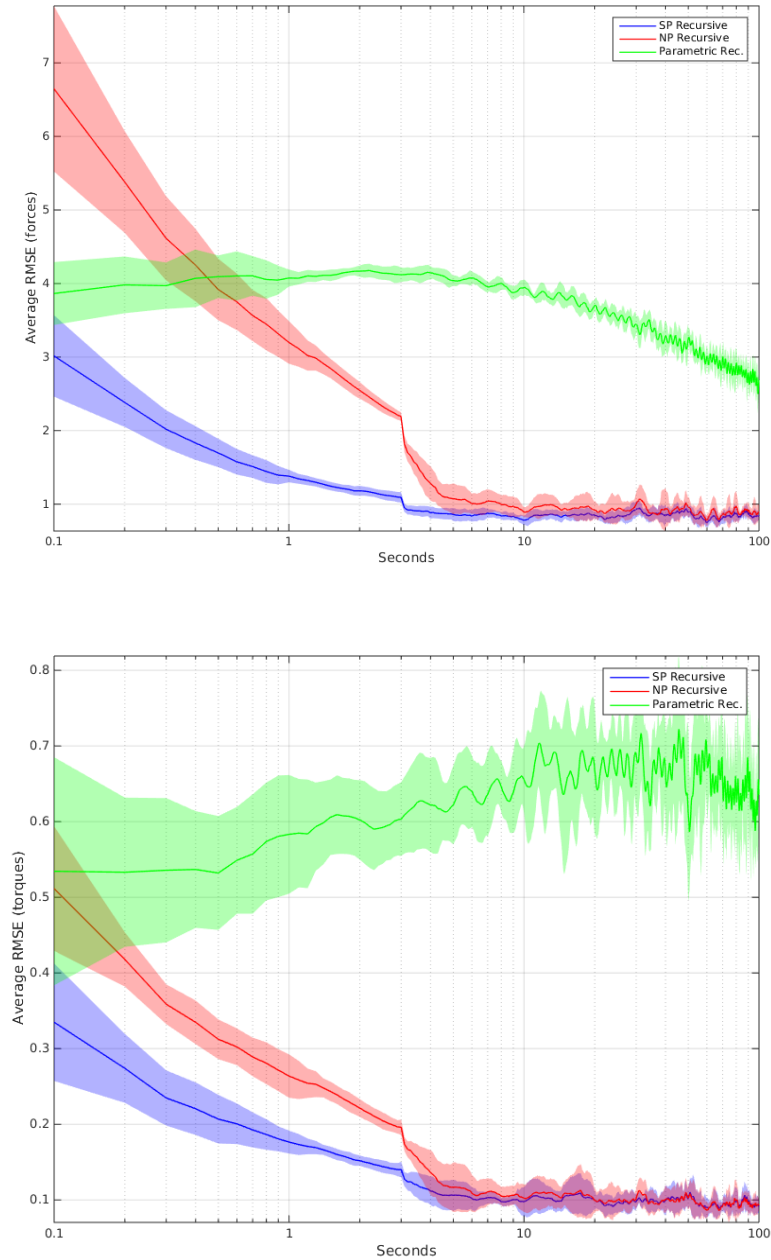


Figure 8.4: Predicted forces (top) and torques (bottom) components average RMSE (y axis) in time (x axis), averaged over a 30-samples window for the recursive SP (blue), NP (red) and P (green) estimators. The transparent areas correspond to the standard deviation over 10 repetitions.

dataset is 10000, corresponding to approximately 17 minutes of continuous operation. The steps of the validation experiment are the following:

1. Initialize the recursive parametric, nonparametric and semiparametric models to zero. The inertial parameters are also initialized to zero
2. Train the models on the whole XY dataset (10000 points)
3. Split the XZ dataset in 10 sequential parts of 1000 samples each. Each part corresponds to 100 seconds of continuous operation
4. Test and update the models independently on the 10 splitted datasets, one sample at a time.

In Figure 8.4 we present the means and standard deviations of the average root mean squared error (RMSE) of the predicted force and torque components on the 10 different test sets for the three models, averaged over a 3-seconds sliding window. At steady state, the nonparametric (NP) and the semiparametric (SP) models provide more accurate predictions than the parametric (P) model with statistical significance. In fact, their force prediction error is approximately $1N$, while the one of the P model is approximately 2 to 3 times larger. Similarly, the torque prediction error is around $0.1Nm$ for SP and NP, which is considerably better than the $0.5Nm$ to $0.7Nm$ average RMSE of the P model. The SP model outperforms the P model, both in the transient and at regime, since it makes use of both the prior physical information and of the available data. It is particularly interesting to note that the error of the SP model is considerably lower than the NP one *in the initial transient*, both for forces and torques. This indicates that the SP model takes advantage of the prior knowledge about the physical structure of the system in an area of the state space that is new for the fully data-driven NP model.

Given these experimental results, we can conclude that in terms of predictive accuracy the proposed incremental semiparametric method outperforms the incremental parametric one and matches the fully nonparametric one. The SP method also shows a smaller standard deviation of the error with respect to the competing methods. Considering the previous results and observations, the proposed method has been shown to be able to combine the main advantages of parametric modeling (i.e. interpretability) with the ones of nonparametric modeling (i.e. capacity of modeling nonrigid body dynamics phenomena). The incremental nature of the algorithm, in both its P and NP parts, allows for adaptation to changing conditions of the robot itself and of the surrounding environment. Note that the introduction of a forgetting factor to assign smaller weights to older or less relevant samples might be necessary to avoid saturation phenomena in long time spans and properly track the changing system dynamics (see

[Paleologu et al., 2008] and references therein). This interesting aspect will be addressed in future work.

Chapter 9

Conclusion

In this work, we address several open problems in large-scale machine learning and propose some applications of our methods to the solution of challenging lifelong robot learning tasks. In particular, we focus on randomized methods to scale up kernel machines to tackle learning problems with a large (and potentially growing) number of training examples. We analyze the generalization properties of randomized learning algorithms in the statistical learning theory framework, outlining the tight relationship between statistics and optimization giving rise to novel computational regularization schemes, provably allowing for optimal generalization with reduced computational burden.

First, in Part II we analyze the generalization properties of two of the most widely used randomized subsampling schemes for kernel methods, namely Nyström methods and random features. Theoretical results are accompanied by numerical simulations and experiments on large-scale benchmark datasets. In particular, Chapter 4 is focused on data-dependent subsampling schemes, namely Nyström methods. In this context, in Section 4.2 we prove novel optimal generalization bounds for Nyström-based kernel methods with Tikhonov regularization (NKRLS), provided that the subsampling level is appropriately chosen. Moreover, we show that the subsampling level controls regularization and computations at the same time. In Section 4.3 we investigate if iterative regularization/early stopping and Nyström methods can be fruitfully combined. We answer this question by introducing the NYTRO (NYström iTerative RegularizatiOn) algorithm, and by analyzing its statistical and computational properties in different regimes. On the other hand, in Chapter 5 we show that a number of random features smaller than the number of examples can be sufficient to achieve optimal learning rates. We also show that random features mapping can be interpreted as a form of regularization, in which the number of random features is not limited to be a computational efficiency parameter, but also controls a bias-variance trade-off.

Part III is devoted to the investigation of the generalization performance of online/incremental learning methods, and to their application in lifelong learning scenarios of interest for robotics, such as visual object recognition and dynamics learning. Chapter 6 is concerned with the generalization properties of the stochastic gradient method (SGM) for learning with convex loss functions and linearly parametrized functions. We show that the stability and approximation properties of the algorithm can be controlled by the number of passes over the training data or the step-size, without any additional penalization or constraints, thus implementing a form of implicit regularization. Interestingly, depending on the statistical properties of the data distribution, multiple passes might be required for optimal performance. Numerical results complement our theoretical findings.

In Chapter 7 we address the problem of learning on-line with an increasing number of classes. Motivated by the visual object recognition applications in a lifelong learning robotic setting, we focus on the problems related to class imbalance, which naturally arises when a new class/object is observed for the first time. To address these issues, we propose a variant of the incremental Regularized Least Squares for Classification (RLSC) algorithm that incorporates new classes and dynamically applies class recoding when new examples are observed. Updates are performed in constant time with respect to the number of training examples seen so far. We evaluate the proposed algorithm on a standard machine learning benchmark and on two datasets for visual object recognition in robotics, showing that our approach is indeed favorable in on-line settings when classes are imbalanced. In line with the literature on “learning to learn” and transfer learning [Thrun, 1996], future research will focus on strategies to exploit knowledge of previous, well-represented classes, to improve classification accuracy on novel and under-represented ones. Indeed, as empirically observed in recent work [Tommasi et al., 2010; Kuzborskij et al., 2013; Sun and Fox, 2016], sharing information and structures among classification tasks can dramatically improve performance.

Finally, in Chapter 8 we present a novel incremental semiparametric modeling approach for inverse dynamics learning, joining together the advantages of parametric modeling derived from rigid body dynamics equations and of nonparametric learning methods. A distinctive trait of the proposed approach lies in its incremental nature, encompassing both the parametric and nonparametric parts and allowing for the prioritized update of both the identified base inertial parameters and the nonparametric weights. This feature is key to enabling robotic systems to adapt to mutable conditions of the environment and their own mechanical properties throughout extended time periods. We validate our approach on the iCub humanoid robot by analyzing the performances of a semiparametric inverse dynamics model of its right arm and comparing them with the ones obtained by state of the art fully nonparametric and parametric approaches.

Bibliography

- Alaoui, A. and Mahoney, M. W. (2014). Fast Randomized Kernel Methods With Statistical Guarantees. *arXiv*.
- Aronszajn, N. (1950). Theory of reproducing kernels. *Transactions of the AMS*, 68(3):337–404.
- Ayusawa, K., Venture, G., and Nakamura, Y. (2014). Identifiability and identification of inertial parameters using the underactuated base-link dynamics for legged multibody systems. *The International Journal of Robotics Research*, 33(3):446–468.
- Bach, F. (2013). Sharp analysis of low-rank kernel matrix approximations. In *COLT*, volume 30 of *JMLR Proceedings*, pages 185–209. JMLR.org.
- Bach, F. (2015). On the Equivalence between Quadrature Rules and Random Features. *ArXiv e-prints*.
- Baelemans, J., van Zutven, P., and Nijmeijer, H. (2013). Model parameter estimation of humanoid robots using static contact force measurements. In *Safety, Security, and Rescue Robotics (SSRR), 2013 IEEE International Symposium on*, pages 1–6.
- Bartlett, P., Jordan, M., and McAuliffe, J. (2006). Convexity, classification, and risk bounds. *Journal of the American Statistical Association*.
- Bartlett, P. L. and Mendelson, S. (2003). Rademacher and Gaussian complexities: Risk bounds and structural results. *The Journal of Machine Learning Research*, 3:463–482.
- Bauer, F., Pereverzev, S., and Rosasco, L. (2007). On regularization algorithms in learning theory. *Journal of complexity*, 23(1):52–72.
- Beazley, D. M. et al. (1996). SWIG: An easy to use tool for integrating scripting languages with C and C++. In *Proceedings of the 4th USENIX Tcl/Tk workshop*, pages 129–139.
- Bertero, M. and Boccacci, P. (1998). *Introduction to inverse problems in imaging*. CRC press.

- Bertsekas, D. P. (1999). *Nonlinear programming*.
- Bertsekas, D. P. (2011). Incremental gradient, subgradient, and proximal methods for convex optimization: A survey. *Optimization for Machine Learning*, 2010:1–38.
- Bishop, C. (2006). *Pattern Recognition and Machine Learning*. Springer.
- Björck, A. (1996). *Numerical Methods for Least Squares Problems*.
- Blanchard, G. and Krämer, N. (2010). Optimal learning rates for kernel conjugate gradient regression. In *Advances in Neural Information Processing Systems*, pages 226–234.
- Bottou, L. (2007). *Large-scale kernel machines*. MIT Press.
- Bottou, L. and Bousquet, O. (2007). The Tradeoffs of Large Scale Learning. In *NIPS*.
- Bousquet, O. and Bottou, L. (2008). The tradeoffs of large scale learning. In *Advances in neural information processing systems*, pages 161–168.
- Boyd, S. and Mutapcic, A. (2007). *Stochastic Subgradient Methods*.
- Boyd, S. and Vandenberghe, L. (2004). *Convex optimization*. Cambridge university press.
- Boyd, S., Xiao, L., and Mutapcic, A. (2003). Subgradient methods. Lecture notes of EE392o, Stanford University.
- Camoriano, R., Angles, T., Rudi, A., and Rosasco, L. (2016a). NYTRO: When Subsampling Meets Early Stopping. In *Proceedings of the 19th International Conference on Artificial Intelligence and Statistics*, pages 1403–1411.
- Camoriano, R., Pasquale, G., Ciliberto, C., Natale, L., Rosasco, L., and Metta, G. (2016b). Incremental Robot Learning of New Objects with Fixed Update Time. *arXiv preprint arXiv:1605.05045*.
- Camoriano, R., Pasquale, G., Ciliberto, C., Natale, L., Rosasco, L., and Metta, G. (2017). Incremental Robot Learning of New Objects with Fixed Update Time. (to appear) *IEEE International Conference on Robotics and Automation (ICRA)*.
- Camoriano, R., Traversaro, S., Rosasco, L., Metta, G., and Nori, F. (2016c). Incremental semiparametric inverse dynamics learning. In *2016 IEEE International Conference on Robotics and Automation (ICRA)*, pages 544–550. IEEE.

- Caponnetto, A. and De Vito, E. (2007). Optimal rates for the regularized least-squares algorithm. *Foundations of Computational Mathematics*, 7(3):331–368.
- Caponnetto, A. and Yao, Y. (2010). Adaptive rates for regularization operators in learning theory. *Analysis and Applications*, 08.
- Chang, C.-C. and Lin, C.-J. (2011). LIBSVM: A library for support vector machines. *ACM Transactions on Intelligent Systems and Technology*, 2:27:1–27:27.
- Chatfield, K., Simonyan, K., Vedaldi, A., and Zisserman, A. (2014). Return of the Devil in the Details: Delving Deep into Convolutional Nets. In *British Machine Vision Conference*.
- Cohen, M. B., Lee, Y. T., Musco, C., Musco, C., Peng, R., and Sidford, A. (2015). Uniform Sampling for Matrix Approximation. In *ITCS*, pages 181–190. ACM.
- Cortes, C., Mohri, M., and Talwalkar, A. (2010). On the Impact of Kernel Approximation on Learning Accuracy. In *AISTATS*, volume 9 of *JMLR Proceedings*, pages 113–120. JMLR.org.
- Crevier, D. (1993). *AI: The tumultuous history of the search for artificial intelligence*. Basic Books, Inc.
- Cristianini, N. and Shawe-Taylor, J. (2000). *An Introduction to Support Vector Machines and Other Kernel-based Learning Methods*. Cambridge University Press.
- Cucker, F. and Smale, S. (2002). On the mathematical foundations of learning. *Bulletin of the AMS*, 39:1–49.
- Cucker, F. and Zhou, D.-X. (2007). *Learning Theory: an Approximation Theory Viewpoint*, volume 24. Cambridge University Press.
- Dai, B., 0002, B. X., He, N., Liang, Y., Raj, A., Balcan, M.-F., and Song, L. (2014). Scalable Kernel Methods via Doubly Stochastic Gradients. In *NIPS*, pages 3041–3049.
- De Vito, E., Caponnetto, A., and Rosasco, L. (2005a). Model selection for regularized least-squares algorithm in learning theory. *Foundations of Computational Mathematics*, 5(1):59–85.
- De Vito, E., Rosasco, L., Caponnetto, A., Giovannini, U. D., and Odone, F. (2005b). Learning from examples as an inverse problem. In *Journal of Machine Learning Research*, pages 883–904.

- De Vito, E., Rosasco, L., and Verri, A. (2006). Spectral methods for regularization in learning theory.
- Dieuleveut, A. and Bach, F. (2014). Non-parametric stochastic approximation with large step sizes. *arXiv preprint arXiv:1408.0361*.
- Drineas, P., Magdon-Ismael, M., Mahoney, M. W., and Woodruff, D. P. (2012). Fast approximation of matrix coherence and statistical leverage. *JMLR*, 13:3475–3506.
- Drineas, P. and Mahoney, M. W. (2005). On the Nyström Method for Approximating a Gram Matrix for Improved Kernel-Based Learning. *JMLR*, 6:2153–2175.
- Duchi, J., Hazan, E., and Singer, Y. (2011). Adaptive subgradient methods for online learning and stochastic optimization. *Journal of Machine Learning Research*.
- Eitel, A., Springenberg, J. T., Spinello, L., Riedmiller, M., and Burgard, W. (2015). Multimodal deep learning for robust rgb-d object recognition. In *Intelligent Robots and Systems (IROS), 2015 IEEE/RSJ International Conference on*. IEEE.
- Elkan, C. (2001). The foundations of cost-sensitive learning. In *International joint conference on artificial intelligence*.
- Engl, H. W., Hanke, M., and Neubauer, A. (1996). *Regularization of inverse problems*, volume 375. Springer Science & Business Media.
- Featherstone, R. and Orin, D. E. (2008). Dynamics. In Siciliano, B. and Khatib, O., editors, *Springer Handbook of Robotics*, pages 35–65. Springer.
- French, R. M. (1999). Catastrophic forgetting in connectionist networks. *Trends in cognitive sciences*.
- Gautier, M. (1997). Dynamic identification of robots with power model. In *ICRA*, volume 3, pages 1922–1927. IEEE.
- Gautier, M. and Khalil, W. (1988). On the identification of the inertial parameters of robots. In *Decision and Control, 1988., Proceedings of the 27th IEEE Conference on*, pages 2264–2269. IEEE.
- Gerfo, L. L., Rosasco, L., Odone, F., De Vito, E., and Verri, A. (2008a). Spectral algorithms for supervised learning. *Neural Computation*, 20(7):1873–1897.
- Gerfo, L. L., Rosasco, L., Odone, F., Vito, E. D., and Verri, A. (2008b). Spectral Algorithms for Supervised Learning. *Neural Computation*, 20(7):1873–1897.

- Gijsberts, A. and Metta, G. (2011). Incremental learning of robot dynamics using random features. In *ICRA*, pages 951–956. IEEE.
- Gittens, A. and Mahoney, M. W. (2013). Revisiting the Nystrom method for improved large-scale machine learning. *28*:567–575.
- Golub, G. H. and Van Loan, C. F. (2012). *Matrix computations*, volume 3. JHU Press.
- Goodfellow, I. J., Mirza, M., Xiao, D., Courville, A., and Bengio, Y. (2013). An empirical investigation of catastrophic forgetting in gradient-based neural networks. *arXiv preprint arXiv:1312.6211*.
- Hardt, M., Recht, B., and Singer, Y. (2016). Train faster, generalize better: Stability of stochastic gradient descent. *International Conference on Machine Learning*.
- Hastie, T., Tibshirani, R., Friedman, J., and Franklin, J. (2001). The elements of statistical learning: data mining, inference and prediction. *The Mathematical Intelligencer*, *27*(2):83–85.
- He, H. and Garcia, E. A. (2009). Learning from imbalanced data. *IEEE Transactions on knowledge and data engineering*.
- Hoerl, A. E. and Kennard, R. W. (1970). Ridge Regression: Biased Estimation for Nonorthogonal Problems. *Technometrics*, *12*:55–67.
- Hofmann, T., Schölkopf, B., and Smola, A. J. (2008). Kernel Methods in Machine Learning. *Annals of Statistics*, *36*(3).
- Hollerbach, J., Khalil, W., and Gautier, M. (2008). Model identification. In *Springer Handbook of Robotics*, pages 321–344. Springer.
- Huang, P.-S., Avron, H., Sainath, T. N., Sindhvani, V., and Ramabhadran, B. (2014). Kernel methods match deep neural networks on timit. In *Acoustics, Speech and Signal Processing (ICASSP), 2014 IEEE International Conference on*, pages 205–209. IEEE.
- Ivaldi, S., Fumagalli, M., Randazzo, M., Nori, F., Metta, G., and Sandini, G. (2011). Computing robot internal/external wrenches by means of inertial, tactile and F/T sensors: Theory and implementation on the iCub. In *Humanoids*, pages 521–528.
- Jain, L. C., Seera, M., Lim, C. P., and Balasubramaniam, P. (2014). A review of online learning in supervised neural networks. *Neural Computing and Applications*.

- Jia, Y., Shelhamer, E., Donahue, J., Karayev, S., Long, J., Girshick, R., Guadarrama, S., and Darrell, T. (2014). Caffe: Convolutional Architecture for Fast Feature Embedding. In *Proceedings of the ACM International Conference on Multimedia - MM '14*. ACM Press.
- Jin, R., Yang, T., Mahdavi, M., Li, Y.-F., and Zhou, Z.-H. (2013). Improved Bounds for the Nyström Method With Application to Kernel Classification. *Information Theory, IEEE Transactions on*, 59(10):6939–6949.
- Khalil, W. and Dombre, E. (2004). *Modeling, identification and control of robots*. Butterworth-Heinemann.
- Kimeldorf, G. S. and Wahba, G. (1970). A correspondence between Bayesian estimation on stochastic processes and smoothing by splines. *The Annals of Mathematical Statistics*, 41(2):495–502.
- Krizhevsky, A., Sutskever, I., and Hinton, G. (2012). ImageNet Classification with Deep Convolutional Neural Networks. In *Advances in Neural Information Processing Systems*.
- Kumar, S., Mohri, M., and Talwalkar, A. (2009). Ensemble Nyström Method. In *NIPS*, pages 1060–1068. Curran Associates, Inc.
- Kumar, S., Mohri, M., and Talwalkar, A. (2012). Sampling Methods for the Nyström Method. *JMLR*, 13(1):981–1006.
- Kuzborskij, I., Orabona, F., and Caputo, B. (2013). From n to $n+1$: Multi-class transfer incremental learning. In *Computer Vision and Pattern Recognition (CVPR)*.
- Lai, K., Bo, L., Ren, X., and Fox, D. (2011). A large-scale hierarchical multi-view rgb-d object dataset. In *Robotics and Automation (ICRA), 2011 IEEE International Conference on*. IEEE.
- Laskov, P., Gehl, C., Krüger, S., and Müller, K.-R. (2006). Incremental support vector learning: Analysis, implementation and applications. *Journal of machine learning research*.
- Le, Q. V., Sarló, T., and Smola, A. J. (2013). Fastfood - Computing Hilbert Space Expansions in loglinear time. In *ICML*, volume 28 of *JMLR Proceedings*, pages 244–252. JMLR.org.
- LeCun, Y., Bottou, L., Bengio, Y., and Haffner, P. (1998). Gradient-based learning applied to document recognition. *IEEE Proceedings*.
- Li, M., Kwok, J. T., and Lu, B.-L. (2010). Making Large-Scale Nyström Approximation Possible. In *ICML*, pages 631–638. Omnipress.

- Lin, J., Camoriano, R., and Rosasco, L. (2016). Generalization Properties and Implicit Regularization for Multiple Passes SGM. *International Conference on Machine Learning*.
- Lin, J., Rosasco, L., and Zhou, D.-X. (2015). Iterative Regularization for Learning with Convex Loss Functions. *The Journal of Machine Learning Research, To appear*.
- Lu, Z., May, A., Liu, K., Bagheri Garakani, A., Guo, D., Bellet, A., Fan, L., Collins, M., Kingsbury, B., Picheny, M., and Sha, F. (2014). How to Scale Up Kernel Methods to Be As Good As Deep Neural Nets. *ArXiv e-prints*.
- Meir, R. and Zhang, T. (2003). Generalization error bounds for Bayesian mixture algorithms. *The Journal of Machine Learning Research, 4*:839–860.
- Mendelson, S. and Neeman, J. (2010). Regularization in kernel learning. *The Annals of Statistics, 38*(1):526–565.
- Metta, G., Natale, L., Nori, F., Sandini, G., Vernon, D., Fadiga, L., von Hofsten, C., Rosander, K., Lopes, M., Santos-Victor, J., Bernardino, A., and Montesano, L. (2010). The iCub Humanoid Robot: An Open-systems Platform for Research in Cognitive Development. *Neural Netw., 23*(8-9):1125–1134.
- Micchelli, C. A., Xu, Y., and Zhang, H. (2006). Universal kernels. *The Journal of Machine Learning Research, 7*:2651–2667.
- Minsky, M. and Papert, S. (1969). Perceptrons.
- Nemirovski, A., Juditsky, A., Lan, G., and Shapiro, A. (2009). Robust stochastic approximation approach to stochastic programming. *SIAM Journal on Optimization, 19*(4):1574–1609.
- Nguyen-Tuong, D. and Peters, J. (2010). Using model knowledge for learning inverse dynamics. In *ICRA*, pages 2677–2682. IEEE.
- Nguyen-Tuong, D., Seeger, M., and Peters, J. (2009). Model Learning with Local Gaussian Process Regression. *Advanced Robotics, 23*(15):2015–2034.
- Nori, F., Traversaro, S., Eljaik, J., Romano, F., Del Prete, A., and Pucci, D. (2015). iCub Whole-body Control through Force Regulation on Rigid Noncoplanar Contacts. *Frontiers in Robotics and AI, 2*(6).
- Ogawa, Y., Venture, G., and Ott, C. (2014). Dynamic parameters identification of a humanoid robot using joint torque sensors and/or contact forces. In *Humanoids*, pages 457–462. IEEE.

- Orabona, F. (2014). Simultaneous Model Selection and Optimization through Parameter-free Stochastic Learning. In *Advances in Neural Information Processing Systems 27: Annual Conference on Neural Information Processing Systems 2014, December 8-13 2014, Montreal, Quebec, Canada*, pages 1116–1124.
- Paleologu, C., Benesty, J., and Ciochină, S. (2008). A robust variable forgetting factor recursive least-squares algorithm for system identification. *Signal Processing Letters, IEEE*, 15:597–600.
- Pasquale, G., Carlo, C., Odone, F., Rosasco, L., and Natale, L. (2015). Teaching iCub to recognize objects using deep Convolutional Neural Networks. In *4th Workshop on Machine Learning for Interactive Systems (ICML)*.
- Pattacini, U., Nori, F., Natale, L., Metta, G., and Sandini, G. (2010). An experimental evaluation of a novel minimum-jerk cartesian controller for humanoid robots. In *IROS*, pages 1668–1674.
- Pinkus, A. (1999). Approximation theory of the MLP model in neural networks. *Acta Numerica*, 8:143–195.
- Poggio, T. and Girosi, F. (1989). A theory of networks for approximation and learning. Technical report, DTIC Document.
- Poggio, T. and Girosi, F. (1990). Networks for Approximation and Learning. *Proceedings of the IEEE*.
- Quiñonero-Candela, J. and Rasmussen, C. E. (2005). A unifying view of sparse approximate Gaussian process regression. *Journal of Machine Learning Research*, 6(Dec):1939–1959.
- Raginsky, M. and Lazebnik, S. (2009). Locality-sensitive binary codes from shift-invariant kernels. In *NIPS*.
- Rahimi, A. and Recht, B. (2007). Random Features for Large-Scale Kernel Machines. In *NIPS*, pages 1177–1184. Curran Associates, Inc.
- Rahimi, A. and Recht, B. (2008). Uniform approximation of functions with random bases. In *Communication, Control, and Computing, 2008 46th Annual Allerton Conference on*, pages 555–561. IEEE.
- Rahimi, A. and Recht, B. (2009). Weighted Sums of Random Kitchen Sinks: Replacing minimization with randomization in learning. In *NIPS*.
- Raskutti, G., Wainwright, M. J., and Yu, B. (2014). Early stopping and non-parametric regression: An optimal data-dependent stopping rule. *The Journal of Machine Learning Research*, 15(1):335–366.

- Rasmussen, C. E. and Williams, C. K. I. (2006). *Gaussian Processes for Machine Learning*. MIT Press.
- Rifkin, R., Yeo, G., and Poggio, T. (2003). Regularized least-squares classification. *Nato Science Series Sub Series III Computer and Systems Sciences*, (190):131–154.
- Rifkin, R. M. (2002). *Everything old is new again: a fresh look at historical approaches in machine learning*. PhD thesis, Massachusetts Institute of Technology.
- Romeres, D., Zorzi, M., Camoriano, R., and Chiuso, A. (2016). Online semi-parametric learning for inverse dynamics modeling. In *Decision and Control (CDC), 2016 IEEE 55th Conference on*, pages 2945–2950. IEEE.
- Rosasco, L. and Villa, S. (2015). Learning with Incremental Iterative Regularization. In *Advances in Neural Information Processing Systems*, pages 1621–1629.
- Rosenblatt, F. (1958). The perceptron: a probabilistic model for information storage and organization in the brain. *Psychological review*, 65(6):386.
- Rudi, A., Camoriano, R., and Rosasco, L. (2015). Less is More: Nyström Computational Regularization. In Cortes, C., Lawrence, N. D., Lee, D. D., Sugiyama, M., and Garnett, R., editors, *Advances in Neural Information Processing Systems 28*, pages 1657–1665. Curran Associates, Inc.
- Rudi, A., Camoriano, R., and Rosasco, L. (2016). Generalization Properties of Learning with Random Features. *ArXiv e-prints*.
- Rudi, A., Canas, G. D., and Rosasco, L. (2013). On the Sample Complexity of Subspace Learning. In *NIPS*, pages 2067–2075.
- Russakovsky, O., Deng, J., Su, H., Krause, J., Satheesh, S., Ma, S., Huang, Z., Karpathy, A., Khosla, A., Bernstein, M., Berg, A. C., and Fei-Fei, L. (2015). ImageNet Large Scale Visual Recognition Challenge. *International Journal of Computer Vision (IJCV)*.
- Russell, S. J., Norvig, P., Canny, J. F., Malik, J. M., and Edwards, D. D. (2003). *Artificial intelligence: a modern approach*, volume 2. Prentice hall Upper Saddle River.
- Saunders, C., Gammerman, A., and Vovk, V. (1998). Ridge Regression Learning Algorithm in Dual Variables. In Shavlik, J. W., editor, *ICML*, pages 515–521. Morgan Kaufmann.
- Sayed, A. H. (2008). *Adaptive Filters*. Wiley-IEEE Press.

- Schmidt, M., Roux, N. L., and Bach, F. (2013). Minimizing finite sums with the stochastic average gradient. *arXiv preprint arXiv:1309.2388*.
- Schölkopf, B., Herbrich, R., and Smola, A. J. (2001). A generalized representer theorem. In *Computational learning theory*, pages 416–426. Springer.
- Schölkopf, B., Smola, A., and Müller, K.-R. (1998). Nonlinear component analysis as a kernel eigenvalue problem. *Neural computation*, 10(5):1299–1319.
- Schölkopf, B. and Smola, A. J. (2002). *Learning with Kernels: Support Vector Machines, Regularization, Optimization, and Beyond (Adaptive Computation and Machine Learning)*. MIT Press.
- Schwarz, M., Schulz, H., and Behnke, S. (2015). RGB-D object recognition and pose estimation based on pre-trained convolutional neural network features. In *International Conference on Robotics and Automation (ICRA)*. IEEE.
- Shamir, O. and Zhang, T. (2013). Stochastic Gradient Descent for Non-smooth Optimization: Convergence Results and Optimal Averaging Schemes. In *Proceedings of the 30th International Conference on Machine Learning*, pages 71–79.
- Shawe-Taylor, J. and Cristianini, N. (2004). *Kernel Methods for Pattern Analysis*.
- Si, S., Hsieh, C.-J., and Dhillon, I. S. (2014). Memory Efficient Kernel Approximation. In *ICML*, volume 32 of *JMLR Proceedings*, pages 701–709. JMLR.org.
- Simonyan, K. and Zisserman, A. (2014). Very deep convolutional networks for large-scale image recognition. *arXiv preprint 1409.1556*.
- Smale, S. and Zhou, D. (2007). Learning theory estimates via integral operators and their approximations. *Constructive approximation*, 26(2):153–172.
- Smola, A. and Vapnik, V. (1997). Support vector regression machines. *Advances in neural information processing systems*, 9:155–161.
- Smola, A. J. and Schölkopf, B. (2000). Sparse Greedy Matrix Approximation for Machine Learning. In *ICML*, pages 911–918. Morgan Kaufmann.
- Sriperumbudur, B. and Szabó, Z. (2015). Optimal rates for random Fourier features. In *NIPS*.
- Srivastava, R. K., Masci, J., Kazerounian, S., Gomez, F., and Schmidhuber, J. (2013). Compete to compute. In *Advances in neural information processing systems*.

- Steinwart, I. and Christmann, A. (2008). *Support Vector Machines*. Springer Science Business Media.
- Steinwart, I., Hush, D. R., and Scovel, C. (2009). Optimal Rates for Regularized Least Squares Regression. In *COLT*.
- Sun, Y. and Fox, D. (2016). NEOL: Toward Never-Ending Object Learning for Robots. In *International Conference on Robotics and Automation (ICRA)*.
- Sun de la Cruz, J., Kulic, D., Owen, W., Calisgan, E., and Croft, E. (2012). On-Line Dynamic Model Learning for Manipulator Control. In *IFAC Symposium on Robot Control*, volume 10, pages 869–874.
- Tacchetti, A., Mallapragada, P. K., Santoro, M., and Rosasco, L. (2013). GURLS: a least squares library for supervised learning. *The Journal of Machine Learning Research*, 14(1):3201–3205.
- Tarres, P. and Yao, Y. (2014). Online Learning as Stochastic Approximation of Regularization Paths: Optimality and Almost-Sure Convergence. *IEEE Transactions on Information Theory*, 60(9):5716–5735.
- Thrun, S. (1996). Is learning the n-th thing any easier than learning the first? *Advances in neural information processing systems*.
- Thrun, S. and Mitchell, T. M. (1995). *Lifelong robot learning*. Springer.
- Tikhonov, A. N. (1963). On the solution of ill-posed problems and the method of regularization. *Dokl. Akad. Nauk SSSR*, 151:501–504.
- Tommasi, T., Orabona, F., and Caputo, B. (2010). Safety in numbers: Learning categories from few examples with multi model knowledge transfer. In *Computer Vision and Pattern Recognition (CVPR)*. IEEE.
- Traversaro, S., Del Prete, A., Ivaldi, S., and Nori, F. (2015). Inertial parameters identification and joint torques estimation with proximal force/torque sensing. In *ICRA*.
- Traversaro, S., Prete, A. D., Muradore, R., Natale, L., and Nori, F. (2013). Inertial parameter identification including friction and motor dynamics. In *Humanoids*, pages 68–73. IEEE.
- Turing, A. M. (1950). Computing machinery and intelligence. *Mind*, 59(236):433–460.
- Um, T. T., Park, M. S., and Park, J.-M. (2014). Independent Joint Learning: A novel task-to-task transfer learning scheme for robot models. In *ICRA*, pages 5679–5684. IEEE.
- Vapnik, V. (1998). *Statistical learning theory*, volume 1. Wiley New York.

- Vapnik, V. N. and Kotz, S. (1982). *Estimation of dependences based on empirical data*, volume 40. Springer-Verlag New York.
- Vijayakumar, S. and Schaal, S. (2000). Locally Weighted Projection Regression: Incremental Real Time Learning in High Dimensional Space. In Langley, P., editor, *ICML*, pages 1079–1086. Morgan Kaufmann.
- Wahba, G. (1990). *Spline Models for Observational Data*, volume 59 of *CBMS-NSF Regional Conference Series in Applied Mathematics*. SIAM, Philadelphia.
- Wang, S. and Zhang, Z. (2013). Improving CUR Matrix Decomposition and the Nyström Approximation via Adaptive Sampling. *JMLR*, 14(1):2729–2769.
- Wang, S. and Zhang, Z. (2014). Efficient Algorithms and Error Analysis for the Modified Nystrom Method. In *AISTATS*, volume 33 of *JMLR Proceedings*, pages 996–1004. JMLR.org.
- Williams, C. and Seeger, M. (2000). Using the Nyström Method to Speed Up Kernel Machines. In *NIPS*, pages 682–688. MIT Press.
- Wu, T. and Movellan, J. (2012). Semi-parametric Gaussian process for robot system identification. In *IROS*, pages 725–731.
- Xiao, T., Zhang, J., Yang, K., Peng, Y., and Zhang, Z. (2014). Error-driven incremental learning in deep convolutional neural network for large-scale image classification. In *Proceedings of the 22nd ACM international conference on Multimedia*. ACM.
- Yamane, K. (2011). Practical kinematic and dynamic calibration methods for force-controlled humanoid robots. In *Humanoids*, pages 269–275. IEEE.
- Yang, J., Sindhvani, V., Avron, H., and Mahoney, M. W. (2014). Quasi-Monte Carlo Feature Maps for Shift-Invariant Kernels. In *ICML*, volume 32 of *JMLR Proceedings*, pages 485–493. JMLR.org.
- Yang, T., Li, Y.-F., Mahdavi, M., Jin, R., and Zhou, Z.-H. (2012). Nyström Method vs Random Fourier Features: A Theoretical and Empirical Comparison. In *NIPS*, pages 485–493.
- Yao, Y., Rosasco, L., and Caponnetto, A. (2007). On Early Stopping in Gradient Descent Learning. *Constructive Approximation*, 26(2):289–315.
- Ying, Y. and Pontil, M. (2008). Online gradient descent learning algorithms. *Foundations of Computational Mathematics*, 8(5):561–596.

- Zhang, K., Tsang, I. W., and Kwok, J. T. (2008). Improved Nyström Low-rank Approximation and Error Analysis. *ICML*, pages 1232–1239. ACM.
- Zhang, T. and Yu, B. (2005). Boosting with early stopping: convergence and consistency. *Annals of Statistics*, pages 1538–1579.
- Zhang, Y., Duchi, J. C., and Wainwright, M. J. (2013). Divide and Conquer Kernel Ridge Regression. In *COLT*, volume 30 of *JMLR Proceedings*, pages 592–617. JMLR.org.

Appendices

Appendix A

Different Loss Functions Yield Different Target Functions

The choice of the loss function reflects itself on the target function resulting from the associated minimization of the expected risk. We show this in practice by a simple binary classification example, first with the square loss and then with the logistic loss.

Example 3 (Square loss). Recall that the square loss is defined as $\ell(a, b) = (a - b)^2$, with $a, b \in \mathbb{R}$. Thus, the minimization of the expected error takes the form

$$\begin{aligned}\mathcal{E}(f) &= \int \rho(x, y) \ell(y, f(x)) dx dy \\ &= \int \rho(y|x) \rho_{\mathcal{X}}(x) dx dy (y - f(x))^2 \\ &= \int \rho_{\mathcal{X}}(x) dx \int \rho(y|x) dy (y - f(x))^2.\end{aligned}\tag{A.1}$$

To simplify the computation, it can be shown that it is possible to disregard the first term and write the target function as

$$f^*(x) = \arg \min_{a \in \mathbb{R}} \int \rho(y|x) dy (y - a)^2 \quad \forall x \in \mathcal{X},$$

which corresponds to

$$f^*(x) = a \quad \text{s. t.} \quad \frac{d}{da} \left[\int \rho(y|x) dy (y - a)^2 \right] = 0 \quad \forall x \in \mathcal{X}.$$

Therefore,

$$\begin{aligned} \frac{d}{da} \left[\int \rho(y|x) dy (y-a)^2 \right] &= 0 \\ \int \rho(y|x) \frac{d}{da} [(y-a)^2] dy &= 0 \\ \int \rho(y|x) 2(a-y) dy &= 0 \\ 2a \underbrace{\int \rho(y|x) dy}_1 - 2 \int \rho(y|x) y dy &= 0 \\ a &= \int \rho(y|x) y dy \end{aligned}$$

Thus, the target function is

$$f^*(x) = \int \rho(y|x) y dy.$$

Since we are considering the binary classification setting, we can further decompose $f^*(x)$ as

$$f^*(x) = (+1)p + (-1)(1-p) = 2p - 1,$$

with $p = p(1|x)$, $1-p = p(-1|x)$. Thus, if $p(1|x) = 1$ then $f^*(x) = 1$ while if $p(-1|x) = 1$ then $f^*(x) = -1$, which justifies taking the sign of the learned estimator f to obtain the output class label.

Example 4 (Logistic loss). Consider the logistic loss

$$\ell(a, b) \log(1 + e^{-ab})$$

with $a, b \in \mathbb{R}$. The target function can be written as

$$\begin{aligned} f^*(x) &= \arg \min_{a \in \mathbb{R}} \int \rho(y|x) \log(1 + e^{-ya}) dy = \\ &= \arg \min_{a \in \mathbb{R}} p \log(1 + e^{-a}) + (1-p) \log(1 + e^a). \end{aligned} \tag{A.2}$$

By performing similar calculations to the ones of the previous example, we obtain that $f^*(x) = a$ such that

$$\begin{aligned} p \frac{-e^{-a}}{(1 + e^{-a})} + (1-p) \frac{e^a}{(1 + e^a)} &= 0 \\ -p \frac{1}{(1 + e^a)} + (1-p) \frac{e^a}{(1 + e^a)} &= 0 \\ p &= \frac{e^a}{(1 + e^a)} \\ a &= \log \frac{p}{1-p}. \end{aligned}$$

Appendix B

Linear Systems

Consider the problem

$$Ma = b,$$

where M is a $d \times d$ matrix and a, b vectors in \mathbb{R}^d . We are interested in determining a satisfying the above equation given M, b . If M is invertible, the solution to the problem is

$$a = M^{-1}b.$$

- If M is a diagonal $M = \text{diag}(\sigma_1, \dots, \sigma_d)$ where $\sigma_i \in (0, \infty)$ for all $i = 1, \dots, d$, then

$$M^{-1} = \text{diag}(1/\sigma_1, \dots, 1/\sigma_d), \quad (M + \lambda I)^{-1} = \text{diag}(1/(\sigma_1 + \lambda), \dots, 1/(\sigma_d + \lambda))$$

- If M is symmetric and positive definite, then considering the eigen-decomposition

$$M = V\Sigma V^\top, \quad \Sigma = \text{diag}(\sigma_1, \dots, \sigma_d), \quad VV^\top = I,$$

then

$$M^{-1} = V\Sigma^{-1}V^\top, \quad \Sigma^{-1} = \text{diag}(1/\sigma_1, \dots, 1/\sigma_d),$$

and

$$(M + \lambda I)^{-1} = V\Sigma_\lambda V^\top, \quad \Sigma_\lambda = \text{diag}(1/(\sigma_1 + \lambda), \dots, 1/(\sigma_d + \lambda))$$

The ratio σ_d/σ_1 is called the *condition number* of M .

Appendix C

Incremental Algorithm for Random Features Regularization

The algorithm below was used in Section 5.4 and is a variation of the incremental algorithm introduced in [Rudi et al., 2015] for KRLS with Nyström approximation. It computes the regularized least squares solution for random features (see (5.6)) incrementally in the number of random features, by means of Cholesky updates. In this way, for a given regularization parameter λ and a number of random features m_{\max} , the algorithm computes all the possible estimators $\tilde{f}_{1,\lambda}, \dots, \tilde{f}_{m_{\max},\lambda}$ at the cost of computing only $\tilde{f}_{m_{\max},\lambda}$. Thus it is possible to explore the whole regularization path in the number of random features with computational cost $O(nm_{\max}^2 + m_{\max}^3)$, instead of $O(nm_{\max}^3 + Lm_{\max}^4)$.

Input: Dataset $(x_i, y_i)_{i=1}^n$, Feature mappings $(\psi(\omega_j, \cdot))_{j=1}^m$, Regularization Parameter λ .

Output: coefficients $\{\tilde{\alpha}_{1,\lambda}, \dots, \tilde{\alpha}_{m,\lambda}\}$, see (5.6).

$A_0 \leftarrow ()$; $R_1 \leftarrow ()$;

for $t \in \{1, \dots, m\}$ **do**

$a_t = (\psi(\omega_t, x_1), \dots, \psi(\omega_t, x_n))$; $A_t = (A_{t-1} \ a_t)$;

$\gamma_t = a_t^\top a_t + \lambda n$; $c_t = A_{t-1}^\top a_t$; $g_t = (\sqrt{3} - 1)\gamma_t$;

$u_t \leftarrow (2c_t/g_t, \sqrt{3\gamma_t/4})$; $v_t \leftarrow (-2c_t/g_t, \sqrt{\gamma_t/4})$;

$R_t \leftarrow \begin{pmatrix} R_{t-1} & 0 \\ 0 & 0 \end{pmatrix}$;

$R_t \leftarrow \text{choleskyupdate}(R_t, u_t, ' + ')$;

$R_t \leftarrow \text{choleskyupdate}(R_t, v_t, ' + ')$;

$\tilde{\alpha}_{t,\lambda} \leftarrow R_t^{-1}(R_t^{-\top}(A_t^\top y))$;

end

Appendix D

Incremental Algorithm for Nyström Computational Regularization

Let $(x_i, y_i)_{i=1}^n$ be the dataset and $(\tilde{x}_i)_{i=1}^m$ be the selected Nyström points. We want to compute $\tilde{\alpha}$ of (4.6), incrementally in m . Towards this goal we compute an incremental Cholesky decomposition R_t for $t \in \{1, \dots, m\}$ of the matrix $G_t = K_{nt}^\top K_{nt} + \lambda n K_{tt}$, and the coefficients $\tilde{\alpha}_t$ by $\tilde{\alpha}_t = R_t^{-1} R_t^{-\top} K_{nt}^\top Y$. Note that, for any $1 \leq t \leq m - 1$, by assuming $G_t = R_t^\top R_t$ for an upper triangular matrix R_t , we have

$$G_{t+1} = \begin{pmatrix} G_t & c_{t+1} \\ c_{t+1}^\top & \gamma_{t+1} \end{pmatrix} = \begin{pmatrix} R_t & 0 \\ 0 & 0 \end{pmatrix}^\top \begin{pmatrix} R_t & 0 \\ 0 & 0 \end{pmatrix} + C_{t+1},$$

with

$$C_{t+1} = \begin{pmatrix} 0 & c_{t+1} \\ c_{t+1}^\top & \gamma_{t+1} \end{pmatrix},$$

and c_{t+1}, γ_{t+1} as in Subsection 4.2.4. Note moreover that $G_1 = \gamma_1$. Thus if we decompose the matrix C_{t+1} in the form $C_{t+1} = u_{t+1} u_{t+1}^\top - v_{t+1} v_{t+1}^\top$ we are able to compute R_{t+1} , the Cholesky matrix of G_{t+1} , by updating a bordered version of R_t with two rank-one Cholesky updates. This is exactly Algorithm 4.1 with u_{t+1} and v_{t+1} as in Subsection 4.2.4. Note that the rank-one Cholesky update requires $O(t^2)$ at each call, while the computation of c_t requires $O(nt)$ and the ones of $\tilde{\alpha}_t$ requires to solve two triangular linear systems, that is $O(t^2 + nt)$. Therefore the total cost for computing $\tilde{\alpha}_2, \dots, \tilde{\alpha}_m$ is $O(nm^2 + m^3)$.